IntechOpen

Rice

Technology and Production

Edited by Amanullah and Shah Fahad

RICE - TECHNOLOGY AND PRODUCTION

Edited by **Amanullah** and **Shah Fahad**

Rice - Technology and Production
http://dx.doi.org/10.5772/64480
Edited by Amanullah and Shah Fahad

Contributors

Norinsan Kamil Othman, Denni Asra Awizar, Zulhusni Dasuki, Kok Yeow You, Li Ling You, Chen Son Yue, Hou Kit Mun, Chia Yew Lee, Leonardo Behak, Muna Ilowefah, Jamilah Bakar, Hasanah Ghazali, Kharidah Muhammad, Mercedes Salazar-Hernández, Carmen Salazar-Hernández, Rocio Lona-Ramos, Enrique Elorza, Agustín H. Rocha-Ramírez, Dr. Amanullah, Shah Fahad

Notice

First published in Croatia, 2017 by INTECH d.o.o.
eBook (PDF) Published by IN TECH d.o.o.
Place and year of publication of eBook (PDF): Rijeka, 2019.
IntechOpen is the global imprint of IN TECH d.o.o.
Printed in Croatia

Legal deposit, Croatia: National and University Library in Zagreb

Additional hard and PDF copies can be obtained from orders@intechopen.com

Rice - Technology and Production
Edited by Amanullah and Shah Fahad
p. cm.
Print ISBN 978-953-51-3029-1
Online ISBN 978-953-51-3030-7
eBook (PDF) ISBN 978-953-51-5480-8

Meet the editors

Editor, Dr. Amanullah is currently working as an associate professor in the Department of Agronomy, University of Agriculture, Peshawar, Pakistan. He did his PhD degree in Agronomy from the University of Agriculture, Peshawar, and his postdoctorate from Dryland Agriculture Institute, WTAMU, Canyon, Texas, USA. Dr. Amanullah has published more than 100 papers in impact factor journals. He has published many books including a recent book by FAO (2016): *Soil and Pulses: Symbiosis for Life*. Dr. Amanullah has been awarded with two Research Productivity Awards by the Pakistan Council for Science and Technology (PCST), Islamabad, in 2011–2012 and 2012–2013.

Co-Editor, Dr. Shah Fahad was born in Dargai (Malakand Division), Pakistan. He studied in Pakistan at Agricultural University Khyber Pakhtunkhwa and Quaid-I-Azam University, Islamabad, where he successfully completed two degrees: a BSC (Hons) in Agronomy and MPhil. in Plant Physiology. As a scholar, he continued for another degree, in graduate studies at Huazhong Agricultural University pursuing PhD degree in Agronomy, which was achieved with honors in 2015. Dr. Shah Fahad is now doing his postdoctorate studies at Huazhong Agricultural University. He is a contributor to many international journals with focuses on global warming and their influences on rice crop attributes in his articles. He is a member of the editorial board and a critic of seven international journals.

Contents

Preface

Rice is life, for most people living in Asia. Rice has shaped the cultures, diets, and economies of thousands of millions of people. Products of the rice plant are used for a number of different purposes, such as fuel, thatching, industrial starch, and artwork. Rice is the most important human food crop in the world, and more than 3.5 billion people depend on rice for more than 20% of their daily calories. Asia accounts for 90% of global rice consumption, exceeding 100 kg per capita annually in many Asian countries.

The purpose of the book *Rice: Technology and Production* is an attempt to present a comprehensive picture of the importance of rice crop globally. This book is intended to satisfy the needs of students, researchers, technologists, and policy makers. The book comprises six chapters. The first chapter of the book deals with the impact of global warming on rice growth and quality. The first chapter addresses (1) rice crop history and plant characteristics, (2) empirical reduction of rice yield and its area of production, and (3) highlights of the key significant mechanisms that influence grain quality attributes. The book goes on to approve the fermented brown rice flour as a valuable ingredient to modify technological and nutritional properties of rice bread in the second chapter. In this chapter, the prefermentation of brown rice flour was found to be an appropriate way to relief the negative effects of the bran fraction and reduce some of the gluten-free bread drawbacks. The importance of nanosilicate corrosion inhibitors from the rice husk ash that has good inhibition properties, which reduce the corrosion rate of carbon steel, was discussed in the third chapter. In the fourth chapter, a review on silica materials (mesoporous or nanoparticle silica) in comparison to rice silica is presented in detail. This leads to a discussion to introduce the application of microwave technology during rice processing, such as rice dying process, rice moisture detection, broken rice measurement, and rice insect control in the fifth chapter. Microwave technology suggested a rapid and accurate measurement to test the quality of the rice in this chapter. In the sixth and last chapter, improvement of sandy soils with rice husk ash, which was found to have environmental, social, and economic benefits, is discussed. We are thankful to all authors who contributed their valuable chapters to this book.

We are also extremely grateful to Romina Rovan of InTech for helping us to publish the book in an excellent form in the shortest possible time. We owe our sincere thanks and irreparable gratitude to our families whose consistent encouragement and love have been a tremendous impetus for the completion of this book.

Dr. Amanullah
University of Agriculture, Peshawar, Pakistan

Dr. Shah Fahad
Department of Plant Science and Technology
Huazhong Agricultural University, Wuhan, China

Chapter 1

Rice Crop Responses to Global Warming: An Overview

Amanullah, Shah Fahad, Sumera Anwar,
Shahbaz Khan Baloch, Shah Saud, Hesham Alharby,
Fahad Alghabari and Muhammad Zahid Ihsan

Additional information is available at the end of the chapter

http://dx.doi.org/10.5772/68035

Abstract

The mean temperature might rise up to range of 2.0–4.5 °C worldwide by the end of this century. Beside from this, a prediction has been made that rise in minimum night temperature will be at a quicker rate as compare to the maximum day temperature. Rising temperatures not only affect the crop growth process, but also lead to direct changes in other environmental factors and pose indirect effect on yield and quality of rice has been observed, so at the present stage, it aroused public attention. Breeds, including through breeding and biotechnology to improve high temperature tolerance of rice help to mitigate the negative effects of high temperature, however, progress in this area have been slow. By adopting different methods like sowing, water and nutrient management can also to some extent mitigate the effects of high temperature on rice performance, but in most cases, these techniques are influenced by many factors, such as crop rotation, irrigation and other constraints like their applications are hard to applied to large area. Therefore, this chapter addresses (1) empirical reduction of rice yield (2) highlights the key significant mechanisms that influence main grain quality attributes under high temperature stress (3) inducing stress resistance and adopting mitigation strategies for high performance of rice.

Keywords: high temperature, rice, yield, area, production and grain quality

1. Introduction

1.1. Rice crop future

Rice (*Oryza sativa*) is one of the significant cereals grown world widely. Globally, it is consumed mostly as a staple food crop to feed greater portion of the world's human population,

particularly in Asia. According to FAOSTAT data [1], it ranks third world wide on production basis, after sugarcane and maize crops. Regarding to human nutrition and caloric intake, it is considered the most significant cereal crop supplying over one-fifth of the calories consumed by humans globally [2]. Though for many years used as a model plant, however, in the last decades, the unprecedented increase in temperature extremities exposed a wide series of variances related with heat stress. In different regions of the world, its harsh influences on different crops have been noticeably apparent. Currently, rice production is facing multiple challenges such as water stress, insect pest infestation, disease attack, which delay its planting and as a result barricade its sustainable production its sustainable production. Forthcoming major challenge will be heat stress and its consequences on grain development. An increase of 1.4–5.8°C in surface air temperature is estimated by the end of twenty-first century as a result of global climate change events [3]. Risk of variability to this mean temperature even poses more severe threats to rice grain development. Experimental evidences have repeatedly repressed that a short episode of high temperature (owing to climatic fluctuations) had greater negative impacts on grain than continuous mild stress [4]. A 25-year weather data report from International Rice Research Institute, Philippines has indicated greater increase in night time temperature (1.13°C) over day time temperature (0.35°C) [5].

Like most of the other regions of the world, high temperature stress has raised in majority parts of China particularly in the northern parts for the last 50 years or so. In most parts of China, especially Xinjiang and mid lower reaches of Yangtze River, both hot days and heat waves have augmented [6]. The main rice-growing area of China i.e., Yangtze River Valley (YRV) faced severe problem of heat stress, causing heavy loss of mid-season rice [7]. According to Tian et al. [7], the extended heat stress in heat vulnerable rice varieties and hybrids in the provinces of Hubei and Sichuan China, resulting in greater reduction in yield of rice because of poor seed set (up to 10% only). In most rice-growing areas, the existing temperatures are almost touching the range of optimum temperatures; if further increases in temperature occur, there will be a chance of finishing the rice crop in such areas. Hence, during sensitive stages, any supplementary raises in mean temperatures or occurrences of high temperatures for shorter time, may lead heavy losses in grain yield. Due to the disastrous heat stress episode of 2003 in China, enormous amount of 5.18 million tons losses in rice yield was accounted from an area of 3 million ha [7, 8]. Likewise, in South-East Asia, Lobell et al. [9] noted a reduction of 4–14% in rice yield because of 1°C enhance in temperature.

By the end of the twenty-first century, 41% of reductions have been estimated in rice yields [10]. There is enough confirmation that, rising nighttime temperature since in the middle of the twentieth century has been the major reason of enhances in worldwide mean temperatures and is thus the major aspect contributing to the yield decrease [11, 12]. At the vegetative stage, rice with comparatively higher tolerance is tremendously susceptible during their reproductive stage against high temperature, mainly at flowering [13–17]. From the *Rice almanac*, using cropping pattern data [18], spatial analysis demonstrated rice susceptible stages from flowering to early grain-filling stages matching with high temperature situations in Bangladesh, southern Myanmar, northern Thailand, and eastern India [19]. Rice, with its extensively miscellaneous genetic traits, flees the influence of higher temperature during the morning later hours because of its early morning flowering (EMF) [20], while through transpiration cooling, avoidance of

elevated temperature is better equipped to resist high day temperature, provided that adequate water is accessible [21]. Conversely, at night time, the limited stomatal activity makes rice enormously susceptible to promptly mounting night temperature. Taking into consideration, the present and envisaged speeds of enhance in night temperature, the harmful effect is likely to be considered on a much larger range on rice production, with major losses in yield.

According to Mohammed and Tarpley [22], enhanced respiration rates are generally related with high night temperatures (HNTs), resulting to a lessening in yield. However, in response to both high day and night temperature, connection of physiological processes up to some extent (e.g., effect of the pollination process, reduced germinated pollen number on the stigma, and augmented spikelet sterility) has been recognized [17, 23]. According to Nakagawa et al. [24], High temperatures induced floret sterility and therefore, decreased rice yield and therefore, decreased rice yield. In response to a temperature more than 35°C, spikelet sterility was significantly augmented [25, 26]. Jagadish et al. [15] conducted an experiment in greenhouse condition using both genotypes (*Indica* and *Japonica*), observed that plants exposure to temperatures above 33.7°C for less than 1 h was enough to induce sterility. This problem may further aggravate by enhanced levels of CO_2, probably because of decreased transpirational cooling [26–29].

1.2. Global warming influences rice crop production

Rice production significantly gets affected by diurnal temperature changes. Beyond the critical level, day temperatures can severely affect the activity of photosynthesis, by altering the thylakoids structural organization and upsetting the photosynthetic system II [30, 31]. As a result of this modification, it will enhance the production of reactive oxygen species (ROS) and thus cause damage to integrity of cell membrane, cell content leakage, and eventually decease of cells [32]. Recently, high night temperature (HNT) stress has gained the attention in rice examine region. In the region of tropics and subtropics, critical ranges of an extremely narrow 2–3°C have caused severe reduction in grain yield [11, 33]. Although the reduced yield caused by HNT may be attributed to higher respiration rates [23], the percentage yield decline was much higher than the percentage increase in respiration rate [11]. Comprehensive attempts are needed to facilitate rice plants to survive under high temperature stress, just by utilizing the present existing variation of the accessible genetic resources; rice plants can target by researchers with increased tolerance to high temperature stress. Besides, to avoid these losses of crop production by the imminent global warming, researches relating to physiological outcomes of high temperature on grain-filling stage are also highly critical [34]. Time of cultivation and their adjustment, for instance flowering and booting stages, which are the most vulnerable stages, do not hit the highest point of temperature stress is a valuable approach for crop management; therefore, this approach will assist the plants to flee the adverse effect of heat stress [35].

1.3. Rising temperature influences rice grain quality attributes

During kernel development, environmental temperature plays a fundamental part in producing the observed, impenetrable variations in the quality of rice grain [36]. Rice quality traits encompass milling, physical manifestation, cooking, and sensory characteristics and also

their eating and nutritional worth [37]. The assessment criteria for milling quality generally include percentage of brown rice, milled rice, and head rice, which reflect the ratio of entire kernels (head rice or head milled rice) and broken kernels produced throughout the milling of rough rice. According to Koutroubas et al. [38] observed that with the market demand, the above mentioned criteria are intimately related because broken milled rice is less than half of the price of head milled rice. Quality of appearance is mostly decided by grain size, translucency, chalky grain percentage, chalky area, and chalky degree. An opaque mark has present in the endosperm of chalky grains that range in size, either found on the grain dorsal side (white belly) or in the middle (white center) [39]. Contents of amylase, gelatinization temperature, and also gel consistency of the grain starch determine the cooking and eating characteristics of rice [40].

Fahad et al. [28] observed that at a period of kernel development, a relationship of decrease in yield of head rice with enhance in nighttime temperature. Likewise, chalkiness formation in grain, small amount of amylose content, and reduction in grain size are assisted by high temperature stress during grain ripening phase [34, 36, 41]. Moreover, during grain-filling stage, high temperatures can vary physico-chemical characteristics, breading, and flour qualities of grain crops [42], together with alterations in flour protein contents [43]. Proficient utilization of the already accessible genotypic deviation in rice [44] and use of different chemical application can alleviate the pessimistic influence of high temperatures on yield of crops. However the potential role of these two approaches concerning on the qualitative features of rice there is a literature scarcity which limits our understanding. Furthermore, in the view of the predicted global warming, understanding the molecular basis of these traits is essential to allow breeders to develop new genotypes, which can withstand across a wide range of environmental conditions and locations.

2. Inducing stress resistance and mitigation strategies

For the study of heat tolerance, rice is considered an excellent model plant among all cereal crops because of the accessibility of high-density genetic and physical maps, expressed sequence tags (ESTs), genomic sequences, and mutant stocks such as T-DNA insertional mutants [45]. Due to the greater level of synteny and homology within the Poaceae family will help to recognize perfect QTLs and transfer of candidate genes from rice to other cereals [46]. Various approaches that may enable rice plant to perform better against coming threats of changing climate are outlined below.

2.1. Breeding strategy

Because of the accessibility to the full rice genome sequence [47] and rigorous QTL mapping efforts for a greater range of traits [48], breeders have achieved a lot of success in rice-breeding program to combat the high temperature. Therefore, various options of the breeding program,

if we utilized, will assist to alleviate the issue of mounting temperature to large extents. Some of the approaches are briefly summarized below.

During the reproductive stage, spikelets fertility is considered an important trait for rice yield and it can be utilized as a screening tool for high temperature tolerance. Plant selection should be done for heat tolerance from those breeding materials, which can perform well even at temperatures more than 38°C [49]. While some cultivars such as N22 have already been well known for their tolerance to comparatively higher temperatures, they should be used as "genetic donors" in the case of breeding for high temperature stress. Visible markers are needed of the high temperature tolerance for the effective assortment in a breeding program. Especially in flowering time (mainly the wild type), investigating the existing genotypic alteration assists as an important alleviation choice for mounting temperature as it is a comparatively simple attribute that needs to be a focal point in breeding programs. According to Ishimaru et al. [50], positive influence has been recorded on reducing the spikelet fertility by the introgression of the early morning flowering gene from Oryza officinalis into *Oryza sativa*. QTL mapping, together with allied genetic studies concentrating on the association between the phenotypic quality and its genetic markers, would afford an opportunity to relate specific alleles to trait variant and consequently to recognize candidate genes [51].

Investigating the alteration in both genotypic and morphological attributes, future studies should be focused at identification and breeding of heat tolerant germplasms. Numerous strategies should be vigorously identified in order to enhance tolerance in existing cultivars against heat stress, comprising discovery and utilization of novel genes and alleles, enhanced breeding efficacy, marker-assisted selection and genetic variation.

2.2. Agronomic strategy

In the present, rice genetic reserve existence of large unpredictability exists against temperature. To achieve high production of rice globally, sensitive cultivars should be replaced with tolerant ones in the fields. Timely sowing of varieties is also very critical to avoid peak stress periods from the management point of view. And for this determination, varieties development along with appropriate growth periods and tolerance of altered sowing times can perform a key part. To cope with the climatic severities that vary within the region, adjustments of site specific in cropping systems may be required. Therefore, aerobic and flooded rice systems may be relatively helpful for this targeted adaptation. Likewise, in nearby future shifting from flooded to aerobic rice is expected in the cropping pattern. According to Yu et al. [52], maintain the field wet but not flooded along with the addition of organic matter decreases the global warming potential from rice fields without any reduction in the yield. So, management approaches such as saturated soil culture (SSC), alternate wetting and drying (AWD), and aerobic rice cultivation under drought stress, while cultivating advanced varieties comprising the sub1 gene in flooded soils, provide certain adaptive choices for the indirect stresses connected to high temperature. Alternate wetting and drying strategy in the irrigated rice fields may also assist indirectly, as it decreases methane emission (an important contributor to global warming).

3. Conclusion

For attaining high yield production under more imperfect circumstances is one of the main challenges of this century. It is now clear that the emphasis on stress tolerance in plants has to be readdressed from the vegetative to reproductive stages because of greater sensitivity to environmental variations and also their direct connection with fruit and seed production. Current constraints caused by high temperature related to yield losses and to overcome these issues have gained much attention among the researchers, though investigating the multifaceted concerns connecting with grain quality losses continue to be a main task. Further challenges that might arise with the shift from entirely flooded rice conditions to water-saving technologies require more concentration to confirm that the benefit attained under fully flooded situations assists the alteration with lowest harm under a future warmer and drier climate.

Author details

Amanullah[1], Shah Fahad[2]*, Sumera Anwar[2], Shahbaz Khan Baloch[2], Shah Saud[3], Hesham Alharby[4], Fahad Alghabari[5] and Muhammad Zahid Ihsan[5]

*Address all correspondence to: shah.fahad@mail.hzau.edu.cn

1 Department of Agronomy, Faculty of Crop Production Sciences, The University of Agriculture, Peshawar, Pakistan

2 College of Plant Science and Technology, Huazhong Agricultural University, Wuhan, P.R. China

3 Department of Horticultural and Forestry, Northeast Agricultural University, Harbin, P.R. China

4 Department of Biological Sciences, Faculty of Science, King Abdulaziz University, Jeddah, Saudi Arabia

5 Department of Arid Land Agriculture, Faculty of Meteorology, Environment and Arid Land Agriculture, King Abdul Aziz University, Jeddah, Saudi Arabia

References

[1] Faostat. 2011. at the Wayback Machine. Faostat.fao.org (October 23, 2014). Retrieved on September 4, 2015.

[2] Smith, Bruce D. The Emergence of Agriculture. Scientific American Library, A Division of HPHLP, New York, ISBN 0-7167-6030-4.

[3] IPCC (Intergovernmental Panel on Climate Change) 2007. Climate change and its impacts in the near and long term under different scenarios. In Climate Change 2007:

Synthesis Report (Eds The Core Writing Team, Pachauri R.K. and Reisinger A.), pp. 43–54. Geneva, Switzerland: IPCC.

[4] Reidsma, P., Ewert F., Lansink A.O., and Leemans R. 2010. Adaptation to climate change and climate variability in European agriculture: The importance of farm level responses. Eur J Agron. 32:91–102

[5] Peng, S., Huang J., Sheehy J.E., Laza R.C., Visperas R.M., Zhong X., Centeno G.S., Khush G.S. and Cassman K.G. 2004. Rice yields decline with higher night temperature from global warming. Proc Natl Acad Sci U S A. 101:9971–9975.

[6] Ding, T., Qian W. and Yan Z. 2009. Changes in hot days and heat waves in china during 1961–2007. Int J Climatol. 30:1452–1462.

[7] Tian, X., Luo H., Zhou H. and Wu C. 2009. Research on heat stress of rice in China: Progress and prospect. Chin Agri Sci Bull. 25:166–168.

[8] Li, X., Qian Q., Fu Z., Wang Y., Xiong G., Zeng D., Wang X., Liu X., Tang S., Hiroshi F., Yuan M., Luo D., Han B. and Li J. 2003. Control of tillering in rice. Nature. 422:618–621.

[9] Lobell, D.B., Burke M.B., Tebaldi C., Mastrandrea M.D., Falcon W.P. and Naylor R.L. 2008. Prioritizing climate change adaptation needs for food security in 2030. Science. 319:607–610.

[10] Ceccarelli, S., Grando S., Maatougui M., Michael Slash M., Haghparast R., Rahmanian M., Taheri A., Al-yassin A., Benbelkacem A., Labdi M., Mimoun H. and Nachit M. 2010. Plant breeding and climate changes. J Agri Sci Cambridge. 148:627–637.

[11] Watanabe, T., and KUME T. 2009. A general adaptation strategy for climate change impacts on paddy cultivation: Special reference to the Japanese context. Paddy Water Environ. 7:313–320.

[12] Sheehy, J.E., Elmido A., Centeno G. and Pablico P. 2005. Searching for new plants for climate change. J Agri Met. 60:463–468.

[13] Prasad, P.V.V., Boote K.J., Allen L.H., Sheehy J.E. and Thomas J.M.G. 2006. Species, ecotype and cultivar differences in spikelet fertility and harvest index of rice in response to high temperature stress. Field Crops Res. 95:398–411.

[14] Jagadish, S.V.K., Cairns J., Lafitte R., Wheeler T.R., Price A.H. and Craufurd P.Q. 2010. Genetic analysis of heat tolerance at anthesis in rice (*Oryza sativa* L.). Crop Sci. 50:1–9 (doi: 10.2135/cropsci2009.09.0516).

[15] Jagadish, S.V.K., Craufurd P.Q. and Wheeler T.R. 2007. High temperature stress and spikelet fertility in rice (*Oryza sativa* L.). J Exp Bot. 58:1627–1635.

[16] Jagadish, S.V.K., Craufurd P.Q. and Wheeler T.R. 2008. Phenotyping parents of mapping populations of rice (*Oryza sativa* L.) for heat tolerance during anthesis. Crop Sci. 48:1140–1146.

[17] Jagadish, S.V.K., Muthurajan R., Oane R., Wheeler T.R., Heuer S., Bennett J. and Craufurd P.Q. 2010. Physiological and proteomic approaches to dissect reproductive stage heat tolerance in rice (*Oryza sativa* L.). J Exp Bot. 61:143–156.

[18] Maclean, J.L., Dawe D.C., Hardy B. and Hettel G.P. 2002. Rice Almanac. Source Book for the Most Important Activity on Earth. Los Baños (Philippines): International Rice Research Institute, West Africa Rice Development Association, International Center for Tropical Agriculture, and Food and Agriculture Organization.

[19] Wassmann, R., Jagadish S.V.K., Sumfleth K., Pathak H., Howell G., Ismail A., Serraj R., Redoña E., Singh R.K. and Heuer S. 2009. Regional vulnerability of rice production in Asia to climate change impacts and scope for adaptation. Adv Agron. 102:91–133.

[20] Ishimaru, T., Hirabayashi H., Ida M., Takai T., San-Oh Y.A., Yoshinaga S., Ando I., Ogawa T. and Kondo M. 2010. A genetic resource for early-morning flowering trait of wild rice *Oryza officinalis* to mitigate high temperature-induced spikelet sterility at anthesis. Ann Bot. 106 (3): 515–520. doi:10.1093/aob/mcq124.

[21] Weerakoon, W.M.W., Maruyama A. and Ohba K. 2008. Impact of humidity on temperature-induced grain sterility in rice (*Oryza sativa* L). J Agron Crop Sci. 194:135–140.

[22] Mohammed A.R. and Tarpley L. 2009. Impact of high night time temperature on respiration, membrane stability, antioxidant capacity and yield of rice plants. Crop Sci. 49:313–322.

[23] Mohammed A.R. and Tarpley L. 2009. High night time temperatures affect rice productivity through altered pollen germination and spikelet fertility. Agric For Meteorol. 149:999–1008.

[24] Nakagawa, H., Horie T. and Matsui T. 2003. Effects of climate change on rice production and adaptive technologies. In Rice Science: Innovations and Impact for Livelihood. Proceedings of the International Rice Research Conference, Beijing, China, 16–19 September 2002 (Eds Mew T.W., Brar D.S., Peng S., Dawe D., Hardy B.), pp. 635–658. Manila, The Philippines: IRRI.

[25] Fahad, S., Hussain S., Saud S., Tanveer M., Bajwa A.A., Hassan S., Shah A.N., Ullah A. Wu C., Khan F.A., Shah F., Ullah S., Chen Y. and Huang J. 2015. A biochar application protects rice pollen from high-temperature stress. Plant Physiol Biochem. 96:281–287

[26] Fahad, S., Hussain S., Saud S., Khan F., Hassan S., Jr A., Nasim W., Arif M., Wang F., Huang J. 2016a.Exogenously applied plant growth regulators affect heat-stressed rice pollens. J Agron Crop Sci 202:139–150.

[27] Fahad, S., Hussain S., Saud S., Hassan S., Tanveer M., Ihsan Z., Shah A.N., Ullah A., Nasrullah, S., Ullah, H. Alharby, W., Nasim W., Wu C. and Huang J. 2016b. A combined application of biochar and phosphorus alleviates heat-induced adversities on physiological, agronomical and quality attributes of rice. Plant Physiol Biochem. 103:191–198.

[28] Fahad, S., Hussain S., Saud S., Hassan S., Chauhan B.S. and Khan F., et al. 2016c. Responses of rapid Viscoanalyzer profile and other Rice grain qualities to exogenously applied plant growth regulators under high day and high night temperatures. PLoS One. 11(7):e0159590. doi:10.1371/journal.pone.0159590

[29] Fahad, S., Hussain S., Saud S., Hassan S., Ihsan Z., Shah A.N., Wu C., Yousaf M., Nasim W., Alharby H., Alghabari F. and Huang J. 2016. Exogenously applied plant growth regulators enhance the morphophysiological growth and yield of Rice under high temperature. Front Plant Sci. 7:1250. doi:10.3389/fpls.2016.01250

[30] Karim, M.A., Fracheboud, Y. and Stamp P. 1997. Heat tolerance of maize with reference of some physiological characteristics. Ann Bangladesh Agri. 7:27–33.

[31] Zhang, J.H., Huang W.D., Liu Y.P. and Pan Q.H. 2005. Effects of temperature acclimation pretreatment on the ultrastructure of mesophyll cells in young grape plants (*Vitis vinifera* L. cv. Jingxiu) under cross temperature stresses. J Integr Plant Biol. 47:959–970.

[32] Schöffl, F., Prandl R. and Reindl A. 1999. Molecular responses to heat stress. In: Shinozaki K., Yamaguchi-Shinozaki K., editors. Molecular responses to cold, drought, heat and salt stress in higher plants. R.G. Landes Co: Austin, Texas. pp 81–98.

[33] Nagarajan, S., Jagadish S.V.K., Hari Prasad A.S., Thomar A.K., Anand A., Pal M. and Agarwal P.K. 2010. Local climate affects growth, yield and grain quality of aromatic and non-aromatic rice in northwestern India. Agric Ecosyst Environ. 138:274–281.

[34] Yamakawa, H., Hirose T., Kuroda M. and Yamaguchi T. 2007. Comprehensive expression profiling of rice grain filling-related genes under high temperature using DNA microarray. Plant Physiol. 144:258–277.

[35] Shah, F., Huang J., Cui K.H., Nie L.X., Shah T., Wu W., Wang K., Khan Z.H., Zhu L. and Chen C. 2011. Physiological and biochemical changes in rice associated with high night temperature stress and their amelioration by exogenous application of ascorbic acid (vitamin C). Aust J Crop Sci. 5:1810–1816.

[36] Cooper N.T.W., Siebenmorgen T.J., Counce P.A. 2008. Effects of nighttime temperature during kernel development on rice physicochemical properties. Cereal Chem. 85:276–282.

[37] Zhang, H., Zhang S., Zhang, J., Yang J. and Z. Wang. 2008. Postanthesis moderate wetting drying improves both quality and quantity of rice yield. Agro J. 100:726–734.

[38] Koutroubas, S.D., Mazzini F., Pons B. and Ntanos D.A. 2004. Grain quality variation and relationships with morphophysiological traits in rice (*Oryza Sativa* L.) genetic resources in Europe. Field Crop Res. 86:115–130.

[39] Khush, G.S., Paule C.M. and de la Cruz N.M. 1979. Rice grain quality evaluation and improvement at IRRI. In. Proceedings of the Workshop on Chemical Aspects of Rice Grain Quality. pp. 21–31. (International Rice Research Institute: Los Baños, Philippines).

[40] Bao, J.S., Sun M. and Corke H. 2002. Analysis of genetic behavior of some starch properties in Indica rice (*Oryza sativa* L.): thermal properties, gel texture, swelling volume. Theor Appl Genet. 104:408–413.

[41] Ishimaru, T., Horigane A.K., Ida M., Iwasawa N., San-OH Y.A., NakazonoM., Nishizawa N.K., Masumura T., Kondo M. and Yoshida M. 2009. Formation of grain chalkiness and changes in water distribution in developing rice caryopses grown under high-temperature stress. J Cereal Sci. 50:166–174.

[42] Perrotta, C., Treglia A.S., Mita G., Giangrande E., Rampino P., Ronga G., Spano G. and Marmiroli N. 1998. Analysis of mRNAs from ripening wheat seeds: the effect of high temperature. J Cereal Sci. 27:127–132.

[43] Wardlaw, I.F., Blumenthal C., Larroque O. and Wrigley C.W. 2002. Contrasting effects of chronic heat stress and heat shock on kernel weight and flour quality in wheat. Funct Plant Biol. 29:25–34.

[44] Krishnan, P., Swain D.K., Bhaskar B.C., Nayak S.K. and Dash R.N. 2007. Impact of elevated CO_2 and temperature on rice yield and methods of adaptation as evaluated by crop simulation studies. Agr Ecosyst Environ. 122:233–242.

[45] Jeon, J. S., Lee S., Jung K. H., Jun S.H., Jeong D. H., Lee J., et al. 2000. Technical advance: T-DNA insertional mutagenesis for functional genomics in rice. Plant J. 22:561– 570.

[46] Maestri, E., Klueva N., Perrota C., Gulli M., Nguyen H.T., and Marmiroli N. 2002. Molecular genetics of heat tolerance and heat shock proteins in cereals. Plant Mol Biol. 48:667–681.

[47] IRGSP (International Rice Genome Sequencing Project) (2005). The map-based sequence of the rice genome. Nature 436:793–800.

[48] Ismail, A.M., Heuer S., Thomson M.J. and Wissuwa M. 2007. Genetic and genomic approaches to develop rice germplasm for problem soils. Plant Mol Biol. 65:547–570.

[49] Satake, T. and Yoshida S. 1978. High temperature-induced sterility in indica rices at flowering. Jap J Crop Sci. 47:6–17.

[50] Ishimaru, T., Hirabayashi H., IDA M., Takai T., San-oh Y.A., Yoshinaga S., Ando I., Ogawa T. and Kondo M. 2010. A genetic resource for early-morning flowering trait of wild rice Oryza officinalis to mitigate high temperature-induced spikelet sterility at anthesis. Ann Bot. 106:515–520.

[51] Cardon, L.R., and Bell J.I. 2001. Association study designs for complex diseases. Nat Rev Genet. 2:91–99.

[52] Yu, K., Chen G. and Patrick W.H. JR. 2004. Reduction of global warming potential contribution from a rice field by irrigation, organic matter, and fertilizer management. Global Biogeochem Cycles. 18: 1-10 doi: 10.1029/2004GB002251

Chapter 2

Effect of Yeast Fermented Brown Rice Flour Substitution on Nutritional, Rheological and Textural Properties of Steamed Brown Rice Bread

Muna Ilowefah, Jamilah Bakar,
Hasanah Mohd Ghazali and Kharidah Muhammad

Additional information is available at the end of the chapter

http://dx.doi.org/10.5772/66880

Abstract

The current study investigated effect of fermented brown rice (*Oryza sativa*) flour (FBRF) at moderate acidity (pH 5.5) on the nutritional, rheological and textural properties of steamed brown rice bread (SBRB). Brown rice flour was substituted with 40% FBRF and its batter and steamed bread characteristics were evaluated. The results revealed that incorporation of 40% FBRF decreased breakdown, setback and final viscosity of brown rice flour, while its peak viscosity significantly increased. The batter system containing 40% FBRF had softer structure than the control, which was reflected by lower storage module (G′) and loss module (G″). Furthermore, the crumb texture of its bread was also significantly ($p < 0.05$) improved, since it had higher chewiness, cohesiveness and springiness, as well as higher specific volume than the control. Incorporation of 40% FBRF significantly increased protein, zinc, nicotinic acid and pyridoxine contents of SBRB. However, its content of antioxidant activity, total γ-oryzanol and phytic acid significantly decreased. This investigation approved that FBRF can be used as a valuable ingredient to modify technological and nutritional properties of steamed brown rice bread.

Keywords: fermented brown rice flour, steamed brown rice bread, nutritional value, rheological properties, textural properties

1. Introduction

Regular consumption of whole grain cereals was approved to have several health benefits since, whole grain cereals are cereals are the appropriate source of fiber and many bioactive components. The bioactive components, which were reported to have positive health influ-

ences, include fiber, phenolics and vitamins [1]. Moreover, recent researches have pointed out that cereal fiber could be a functional constituent that helps to deliver antioxidant substances to the gut [2, 3]. Brown rice (*Oryza sativa*) is one of the most important whole grain cereals and a rich source of several bioactive substances, such as vitamin E, vitamin B, fiber, phenolics and γ-oryzanol. Its consumption as a whole grain (brown rice) is not popular due to its hard texture and dark color. Thus, it can be ground into flour and utilized to produce numerous kinds of gluten-free foods, such as cakes and breads [4, 5].

Brown rice bread is one of the most common non-gluten products, which are suitable for celiac patients, where the demand is increasing. Currently, the only effective way to deal with celiac disease is to avoid consumption of gluten-containing cereals such as wheat, barley and rye [6]. Indeed, development of gluten-free products is a difficult task for food technologists. They are nutritionally poor and are subjected to short shelf life and poor texture [7]. The gluten-free dough show lesser cohesive and elastic cake batter-like compared to wheat dough due to the absence of gluten, which makes them greatly sticky and challenging to handle. In addition, their gluten-like protein network is extremely weak, when untreated non-gluten flours are used as a major constituent of the mixture [8]. As a result, the volume of their end product is relatively low with dense crumb, because of low ability to hold CO_2 released through proofing [9, 10]. For that reason, some food additives or biotechnological pretreatments of the flour would be taken into consideration to improve its baked product qualities [11].

A variety of additives and different nutritive ingredients were investigated in order to improve their technological and nutritional characteristics [12]. Utilization of whole grain flour such as millet, brown rice and sorghum to produce these kinds of formulations could enhance their nutritional value [13, 14]. On the other hand, the incorporated amount of cereal bran or the usage of whole flour in which their health benefits can be predictable causes several detrimental effects on product quality due to the bran fraction [15]. Addition of enzymes and usage of gelatinized starch and sourdough are also attempts which have been investigated to overcome gluten-free product disadvantages and to relief the negative effects of the bran [4, 5].

Technologically, pre-fermented flour or sourdough was pointed to significantly modify rheological properties of non-gluten batters. In our previous investigation, incorporation of yeast fermented brown rice flour significantly improved texture and volume of steamed white rice bread [16]. A study also indicated that addition of amaranth sourdough to amaranth batters positively affected their viscoelastic properties [17]. Sorghum bread quality significantly improved with addition of sorghum sourdough compared to that supplemented with hydroxypropyl methyl cellulose (HPMC) [18]. A number of suggestions have been reported to explain the influence of sourdough on batter and bread qualities including the direct impact of pH on batter structure, in addition to enzymatic and microorganism activities [19].

Pre-fermented flour or sourdough could also modulate the nutritional properties of gluten-free and whole grain products in several ways, like increasing content or bioavailability of

http://dx.doi.org/10.5772/66880

bioactive substances, hindering starch digestibility and reducing anti-nutritional factors [19, 20]. However, there is a noticeable gap between the fundamental basis for gluten-free bread building up structure and their nutritional significance. Investigations regarding non-gluten-free foods, specifically bread, have been focused on improving technological parameters that include volume and crumb hardness, as well as sensorial aspects. However, their nutritional concept has not been well addressed.

Cereal-based fermented foods are attracting both technologists and consumers because of higher content of phytochemicals, minerals and dietary fiber, in addition to low fat content [19, 20]. Certainly, fermentation is an ancient, inexpensive and simple technique that can be applied at home and an important technique in the third world countries for enrichment and preservation of a food material [21]. However, investigations concerning influence of food processes, such as fermentation on the fate of nutritive components and the rheological properties of steamed brown rice bread as an important non-gluten product, are still limited. These knowledge is required when development of whole grain functional foods is considered. Accordingly, the objective of this study was to investigate the effect of yeast fermented brown rice flour substitution on flour, batter and steamed brown rice bread qualities. The obtained outcomes may allow development of gluten-free functional foods with high qualities.

2. Materials and methods

2.1. Materials

Baker's yeast (Eagle, CY 1266, China) and Eco-brown rice grains (MR219) were purchased from a local supermarket in Selangor, Malaysia. Brown rice flour (BRF) was prepared by grinding brown rice grains in a FOSS Tecator (Cyclotech™ 1093, Hoganas, Sweden) to attain a particle size of 500 μm, whereas fermented brown rice flour (FBRF) with moderate acidity (pH 5.5) was prepared as described in our previous study [20]. Flour samples were packaged in polyethylene plastic and stored at 4°C till further analysis. The used chemicals for analysis were of analytical or HPLC grade and were supplied by Merck (Darmstadt, Germany) and Sigma-Aldrich (USA).

2.2. Methods

2.2.1. Bread making process

A preliminary study was firstly conducted, where BRF was substituted with 0, 10, 20, 30, 40 and 50% of FBRF to evaluate the sensory properties and the volume of their steamed brown rice bread (SBRB). According to the results, SBRB with 40% FBRF recorded the highest overall acceptability and bread volume among the others (data not presented). Therefore, SBRB with 40% FBRF was selected for further analysis to be compared with the control sample (SBRB without FBRF). Bread samples were prepared based on batter formula of 100 g of BRF, which consisted of 2% sugar, 2% salt, 3% baker's yeast and 93% volume of water based on the flour weight. During preparation of the batter, instant yeast was dissolved in a solution of water and

sugar and then pre-fermented in a fermenting chamber (Binder 10-01536, Germany) at 32°C for 10 min. Afterwards, dry ingredients, which consisted of BRF, salt and FBRF were thoroughly mixed, then all the ingredients were mixed manually in a beaker for 3 min. After mixing, the batter samples were located in bread pans and fermented in the fermenting chamber at 32°C for 30 min. After fermentation, the samples were steamed for 15 min, cooled at room temperature (25°C) for 1 h before further analysis. Bread samples were made in five replicates.

2.2.2. Determination of batter acidity

Titratable acidity of brown rice batter and brown rice batter with 40% FBRF was determined following the method described by Kati et al. [22], whereas, a pH meter (DELTA 320, shanghai, China) was utilized to measure the pH values.

2.2.3. Determination of pasting properties

Pasting properties of BRF and BRF with 40% FBRF were determined using Rapid Visco Analyser (RVA) (Newport Scientific Pty. Ltd., Warriewood NSW 2102, Australia) according to AACC [23].

2.2.4. Determination of dynamic rheological properties

The rheostress (HAAKE Rheowin 600, Germany) at 30°C using parallel plate geometry (35 mm diameter and 1 mm gap) was utilized to measure the dynamic rheological properties of batter samples as detailed in the early study [16].

2.2.5. Bread volume measurement

Bread volume was determined according to the seed displacement method described by Hallén et al. [24] using sago pearls after 1 h from steaming as reported in our previous study [16].

2.2.6. Texture profile analysis

Crumb texture properties of bread samples were measured using Texture analyser (TA-XT2, UK) equipped with a 30 N load cell and compression plate with a diameter of 75 mm as previously performed [16].

2.2.7. Microscopic analysis

Microstructure of bread samples was examined using scanning electron microscope (JEOL-JSM-6400 SEM, Japan). Bread samples were freeze-dried, ground and then attached on circular aluminum stubs, coated with gold and scanned at an accelerating potential of 15 KV.

2.2.8. Determination of proximate composition and nutritional value

Proximate composition of SBRBs, which included moisture, crude protein, total lipid, total fiber, soluble fiber and insoluble fiber contents, was determined according to the methods of AOAC [25]. Concerning total ash, it was measured according to ISO method [26]. Mineral contents, which include calcium, magnesium, iron and zinc contents, were estimated following the method of AOAC [25]. Phosphorus content quantification was carried out subsequent to

the yellow method with the ammonium-vanadomolybdate reagent according to AOAC [25]. The concentration of phytic acid was determined following the method described by Wu et al. [27] with some modifications [20].

Total phenolic content (TPC) was evaluated using Folin-ciocalteau method according to Beta et al. [28] with certain modifications [20]. The extraction procedure used to determine TPC was employed to measure the ferric reducing ability power of the bread sample as performed in the previous research [20].

The extraction of tocopherols, tocotrienols and total γ-oryzanol were carried out according to the described method by Aguilar-Garcia et al. [29]. Their quantification was conducted by high-performance liquid chromatography (HPLC) fitted with fluorescence detector (Agilent Technologies 1200 Series, Germany). Vitamin E standards were prepared according to Ye et al. [30]. Determination of vitamin B2, B3 and B6 contents was conducted using HPLC fitted with UV detector (Waters 2489 UV/visible Detector and Empower software, USA) following the method of AACC [31] with some modifications [20].

2.2.9. Statically analysis

One-way analysis of variance (ANOVA) and Tukey's multiple range tests with p-value >0.05 were used to report the significant differences between data obtained.

3. Results and discussion

3.1. Batter acidity

The initial pH of FBRF (5.7) was in the acidity range of sourdough prepared with yeast (4.7–5.8) that was previously reported [19]. Substitution of BRF with 40% FBRF resulted in a moderate acidification of brown rice batter. The pH value of the treated batter (6.13) was significantly ($p < 0.05$) lower than the control (6.50), and the same trend was observed for TTA values (**Table 1**). A possible explanation for this result could be related to the effect of the initial pH of FBRF. Additionally, the reached pH (5.5) of FBRF is close to the optimum pH of some enzymes, such as α-amylase, protease, phytase, β-glucanase and pentosanase [19], that could activated and allowed them to breakdown the macro-components of FBRF and produce some organic acids like lactic and acetic acids that led to a reduction in the pH value of the batter, in addition to the effect of microbial metabolism products.

Batter	pH	TTA (mL)
BRB	6.50 ± 0.00[a]	2.23 ± 0.10[a]
BRB + 40% FBRF	6.13 ± 0.02[b]	3.78 ± 0.46[b]

[a] Represented values are the means ± standard deviations of three replicates.

[b] Values with the same superscript letter in a column are not significantly different ($p > 0.05$).

Table 1. The pH and TTA values of brown rice batters (BRBs).

3.2. Rheological properties

The rheological measurements of cereal flour are a significant indication to the bakery industry, where they assist to predict dough handling and processing characteristics as well as final backed product quality [32, 33]. The variation in storage modulus (G′ elastic component) and loss modulus (G″ viscous component) with frequency sweep of brown rice batters is presented in **Figure 1**. The moduli were greater for control batter than the batter containing FBRF. This may be an indication that control batter had more rigid structure than the batter containing FBRF, since it had higher G′ and G″. The G′ and G″ of the batter containing FBRF became less independent of frequency compared to the control. Thus, the structure of the batter having FBRF became softer and stronger than the control as indicated by lower (G′) and (G″). Complex modulus (G^*) was also lower for the batter containing FBRF (**Figure 1**), which indicates a decrease in resistance to deformation. These changes may be related to the effect of protease supplemented by FBRF, where it was reported that addition of protease to brown rice batter reduced resistance to deformation [5]. It also indicated that the elastic (G′) and viscous (G″) moduli values of white rice batter having 40% FBRF were lower than the control at all the tested frequency ranges, and they were independent of the frequency [16]. The increase in protein content of bread containing FBRF [20] might also have an effect on the rheological properties of the batter [15]. From the current results, there was no significant change in tan delta (δ) between the samples (**Figure 1**). The tan δ is an indication of liquid to solid state, and this may demonstrate that water absorption of the batter was not significantly affected by FBRF. Thus, it can be suggested that substitution of BRF with 40% FBRF did not affect water holding capacity of the flour, but could alter protein interactions and functionality, such as changes in sulfhydryls (-SH) and disulphides (-S-S-) bonds, which play an essential role in developing protein network as reported by Elkalifa et al. [34]. It could be expected that, these observed alterations in the viscoelastic properties of the treated batter would be also attributed to the degradation of macro-components (starch, protein and fiber) as affected by the active enzymes supplemented by FBRF. According to Rieder et al. [35], pre-fermented barley flour degraded β-glucan in composite wheat bread as indicated by a reduction in its molecular weight.

The pasting parameters of BRF were also significantly ($p < 0.05$) influenced by its substitution with 40% FBRF (**Figure 2**). It caused significant increase in hot paste viscosity, while cold paste viscosity, breakdown and setback were significantly reduced. Chinma et al. [36] also indicated a decline in pasting parameters of wheat flour when it was substituted by 15% of natural and yeast fermented rice bran protein concentrations. According to Renzetti and Arendt [4], addition of protease to BRF during bread making decreased peak viscosity, final viscosity and breakdown without a significant effect on setback. Similarly, another study reported that addition of α-amylase to wheat dough decreased setback [12]. As mentioned earlier fermented brown rice flour could be a source of these enzymes that caused a reduction in pasting parameters of BRF. These observations might give indication about the modification of starch and/or protein interactions due to enzyme actions [7]. Moreover, the decrease in carbohydrate and the variation in protein content might lead to a reduction in pasting parameters [37]. During RVA determinations, starch granules could not swell

http://dx.doi.org/10.5772/66880

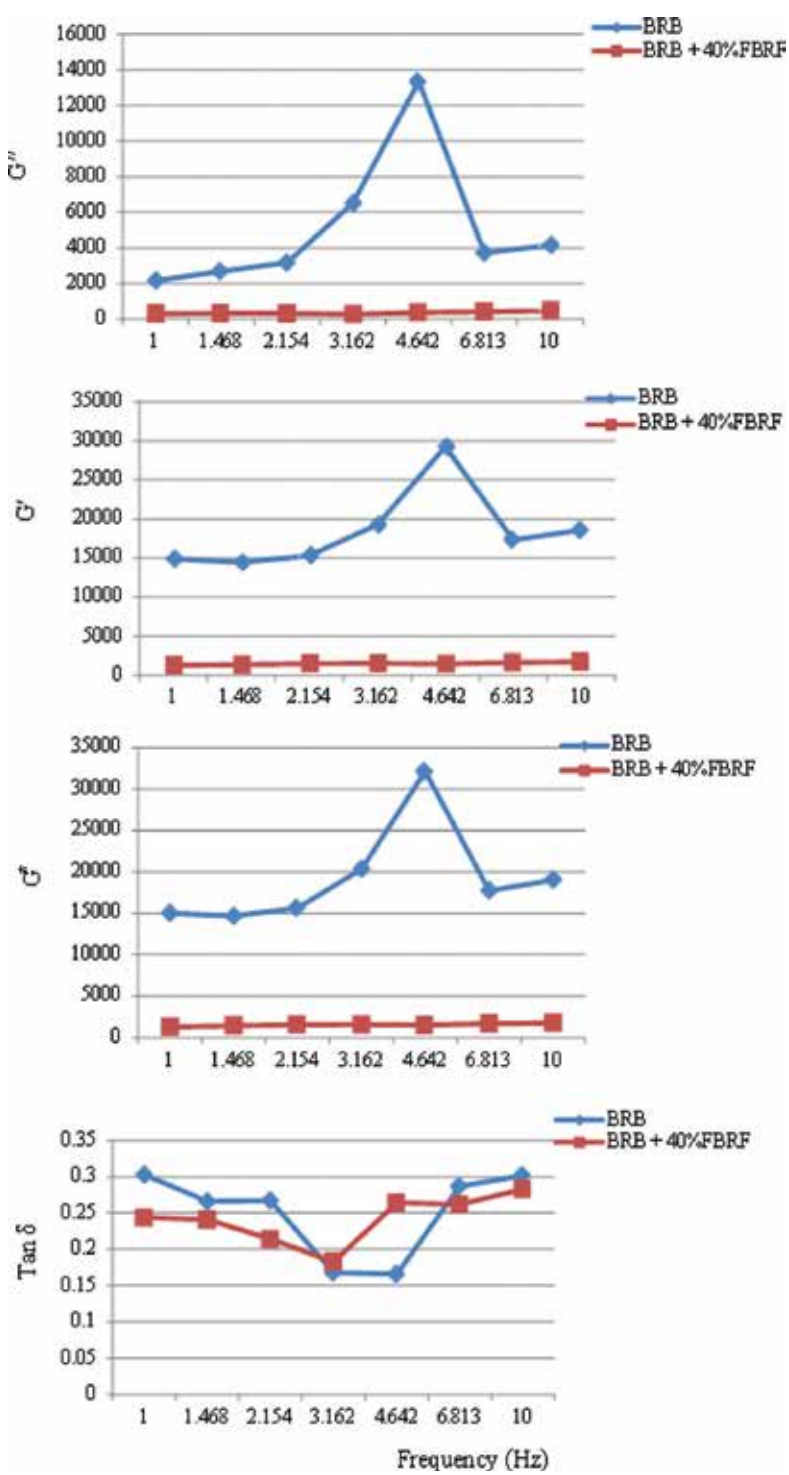

Figure 1. Viscoelastic properties of brown rice batters (BRBs).

to their maximum size due to the limited amount of water. In such environment, protein structure surrounded starch granules causing rigid paste [38] and elevated viscosity as observed for the control flour. Protein and starch hydrolysis, which occurred during pre-fermentation process to produce FBRF could disrupt the rigidity of the paste, as a result, reduced viscosity of the treated flour [39]. The decrease in breakdown value might explain the increase in resistance to deformation and higher stability of the paste. A study reported that the positive effect of sourdough on sorghum bread quality was due to formation of strong starch paste during baking [18]. Furthermore, the decrease in setback delays the retrogradation process (lower degree of amylose polymerization) in the final product and increased its shelf life.

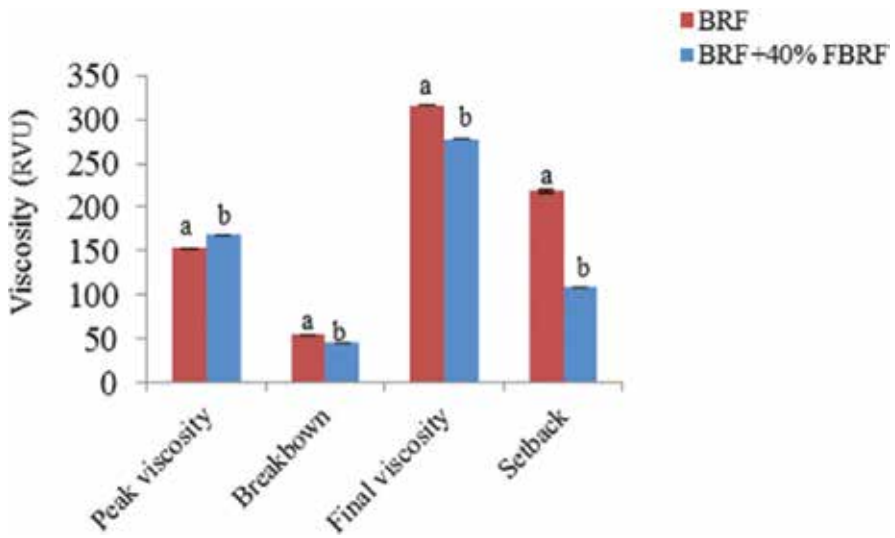

Figure 2. Pasting properties of brown rice flours (BRFs). Error bars: standard deviations of three replicates. Each different small letters above columns means statistically significant ($p > 0.05$) difference.

3.3. Steamed bread volume

Specific volume of bread is a significant quality consideration as it is associated with ability of dough-inflating and oven spring and could not be too large or too small as it influences the crumb structure and determine the overall bread quality [40]. **Figure 3** shows that specific volume of bread significantly increased from 2.2 to 2.75 cm^3/g with usage of FBRF. Also, our previous study indicated that steamed white rice bread containing 40% FBRF had higher specific volume (2.46 cm^3/g) compared to the control sample (2.06 cm^3/g) [16]. In this study, the increase in specific volume of the bread could be due to the reduction in viscoelastic properties and the viscosity of its batter and improve protein network that could make it softer and enhanced its ability to hold more CO_2 [41, 42]. Furthermore,

http://dx.doi.org/10.5772/66880

FBRF could have more damaged starch due to pre-fermentation which perhaps increased the yeast activity leading to higher gas production.

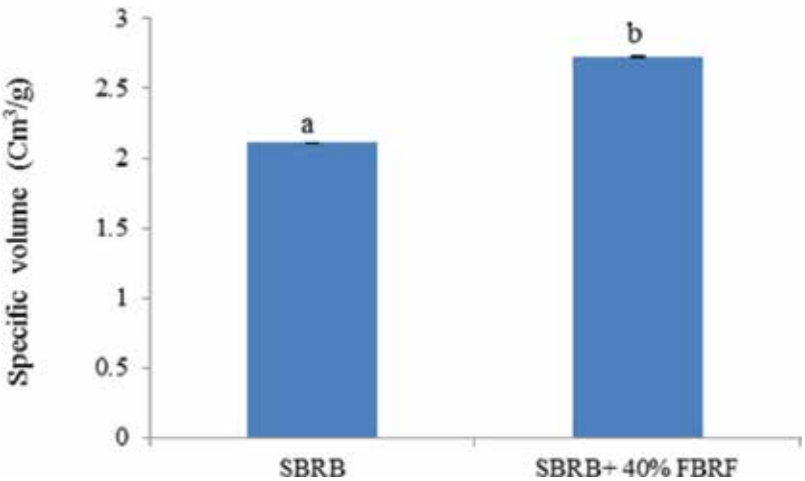

Figure 3. Specific volume of steamed brown rice breads (SBRBs). Error bars: standard deviations of three replicates. Each different small letters above columns means statistically significant ($p > 0.05$) difference.

3.4. Steamed bread texture

The textural characteristics of a food were described as group of physical properties, which are sensed through the feeling of touch [43]. **Figure 4** revealed that FBRF had significant effect on the textural properties of the bread. The springiness, cohesiveness and chewiness were significantly increased due to addition of FBRF, whereas there was no significant impact on the hardness of bread. The increase in springiness indicated higher recovery in the bread height during the first and second bite and also an indication on the increase in the elasticity and softness. Cohesiveness is a measure of fracturability, an increase in its value means higher ability of the bread structure to resists a second deformation in relation to its withstand in the first deformation. Chewiness is an indication of the time required to chew a solid food to be ready for swallowing. Its value was higher in the bread containing FBRF, which reflects higher time needed to masticate it and less breakable in the mouth which is an important attribute of bread. An early study reported that substitution of white rice bread with FBRF significantly decreased the hardness of white rice bread (6398.61 g) compared to the control (6948.13 g). In addition, its chewiness, cohesiveness and resilience were also significantly improved [20]. Moreover, crumb texture properties of wheat bread supplemented with bran were significantly improved due to addition of pre-fermented wheat bran [44]. Meanwhile, it is reported that natural and yeast fermented rice bran protein concentrates, which were used for wheat bread making significantly increased hardness, springiness, chewiness and gumminess of the bread; however, its cohesiveness value was reduced [32]. It was stated that usage of pre-fermented bran with yeast and lactic acid bacteria enhanced retention of CO_2 during dough proofing and as a result increased the bread volume and softness of crumb texture [19, 44].

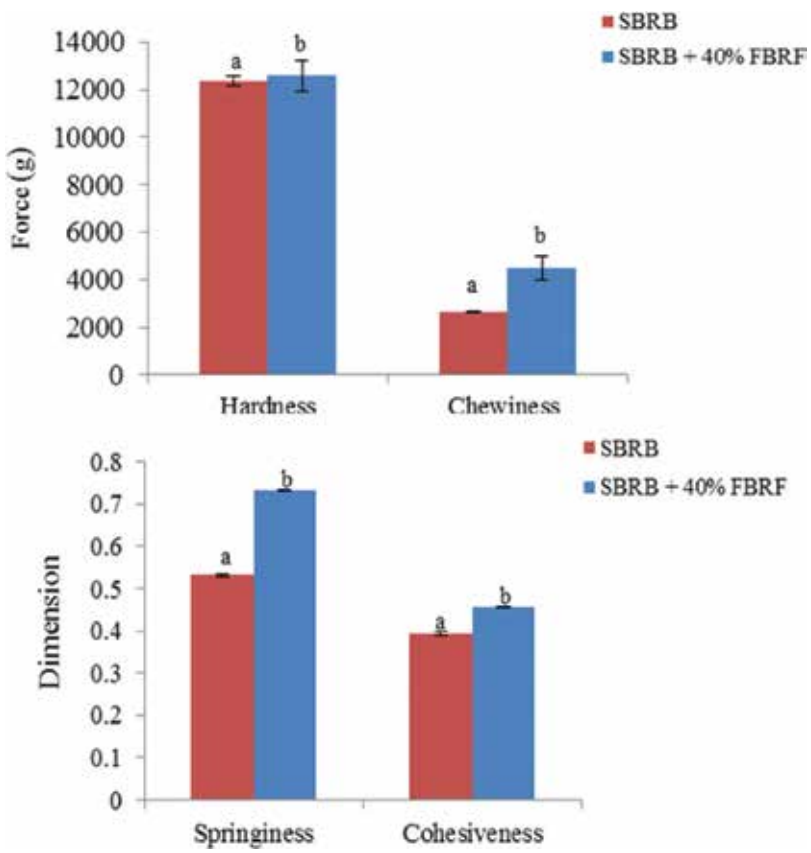

Figure 4. Textural properties of steamed brown rice breads (SBRBs). Error bars: standard deviations of three replicates. Each different small letters above columns means statistically significant ($p > 0.05$) difference.

3.5. Morphological structure of steamed bread

The microstructure organization of SBRBs was investigated using scanning electron microscopy (SEM) at different magnifications (**Figure 5**). As presented in **Figure 5B** and **D**, SBRBs with FBRF demonstrated a smooth structure and the underneath compounds were not simply visualized. The control bread illustrated a compact structure and more continuous surface, coupled with the fact that the underneath substances were not revealed (**Figure 5A** and **C**). Usage of FBRF probably caused a disruption in the protein-starch matrix of the bread that causes these differences in the microstructure between samples.

3.6. Proximate composition and nutritional value

The chemical composition of steamed bread samples is presented in **Table 2**. The protein content of the bread prepared using FBRF (8.67%) was significantly ($p < 0.05$) higher than its content in reference bread (8.29%). The reason could be due to amount of protein added by FBRF, where it possesses greater protein content after fermentation [20]. This is in line with the findings reported by Chinma et al. [36] where wheat bread substituted with natural and yeast fermented

http://dx.doi.org/10.5772/66880

rice bran protein concentrates had higher values of protein content than the control, whereas lipid content of bread containing 40% FBRF was significantly lower than the control and ash content was not significantly affected. Total and insoluble fibers in both bread samples were greater than their levels in the original flour with bread containing FBRF having higher values. However, the difference was not significant. It can be suggested that the increase in total fiber might be due to formation of resistance starch because of retrograding process after steaming. A similar study indicated that protein content of wheat bread supplemented with sourdough was higher than the control, without significant difference in ash and fiber contents [45]. Another study also demonstrated that sourdough treatment had no significant impact on chemical composition of whole wheat bread, except the increase in water soluble arabinoxylans [46].

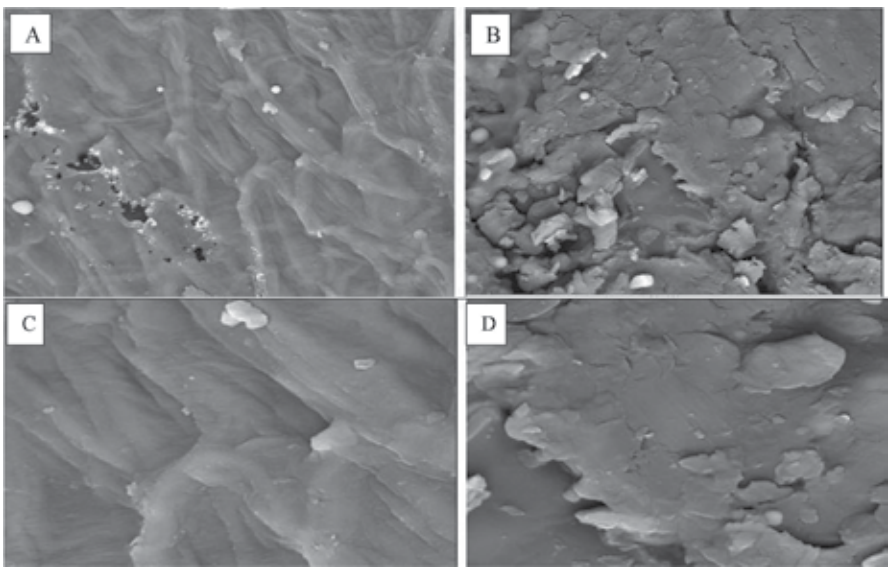

Figure 5. Microstructures of steamed brown rice bread (A and C) and steamed brown rice bread with 40% fermented brown rice flour (B and D).

Phytic acid is the most important anti-nutritive component in cereals, including brown rice due to its ability to bind divalent and trivalent minerals. It is also considered the main storage form of phosphorus and plays a part as an antioxidant factor [47]. Phytic acid content significantly decreased in both SBRBs compared to its content in the flour. Addition of FBRF significantly ($p < 0.05$) reduced phytic acid level in the treated bread (39.34 μg/g) compared to the reference bread (43.23 μg/g) (**Table 2**). Several factors are affecting phytic acid content during bread making such as, fermentation time and the pH that activate phytase enzyme, in addition to baking temperature [48]. Accordingly, the difference in phytic acid content in the SBRBs could be attributed to the supplemented phytase by FBRF. These results agreed with the reports of previous study that indicated application of sourdough with or without yeast significantly decreased phytic acid content compared to conventional yeast fermentation [48]. They also reported that sourdough increased mineral solubility in the whole wheat bread. Fermentation process of the batter may create the optimal pH for endogenous phytase, in addition to that secreted by the yeast, which helps

to breakdown phytic acid and increase the mineral content of the produced bread [7]. This fact might be approved in the current study, since the concentration of calcium, zinc, iron, magnesium and phosphorus significantly increased in both breads. It is noticeable that the increase in their contents was more pronounced in the treated bread, particularly calcium, phosphorus, magnesium and zinc contents. However, the increment was only significant in the zinc content (**Table 2**).

	BRF	SBRB	SBRB with 40% FBRF
Proximate composition			
Moisture (%)	9.77 ± 0.01	44.33 ± 0.11	44.41 ± 0.03
Protein (%)	7.70 ± 0.00[a]	8.29 ± 0.02[b]	8.67 ± 0.01[c]
Ash (%)	1.13 ± 0.01[a]	2.10 ± 0.00[b]	2.03 ± 0.03[b]
Lipid (%)	2.58 ± 0.02[a]	1.57 ± 0.01[b]	1.26 ± 0.03[c]
Nutritional value			
Soluble fibre (%)	1.12 ± 0.01[a]	0.15 ± 0.04[b]	0.13 ± 0.01[b]
Insoluble fibre (%)	1.35 ± 0.04[a]	3.46 ± 0.35[b]	3.85 ± 0.79[b]
Total fibre (%)	2.47 ± 0.01[a]	3.61 ± 0.32[b]	3.98 ± 0.80[b]
Phosphorus (%)	18.90 ± 0.13[a]	20.57 ± 0.04[b]	20.85 ± 0.54[b]
Phytic acid (μg/g)	128.71 ± 0.43[a]	43.23 ± 0.60[b]	39.34 ± 0.58[c]
Magnesium (μg/g)	19.70 ± 0.12[a]	22.38 ± 0.11[b]	22.49 ± 0.13[b]
Zinc (μg/g)	14.21 ± 0.35[a]	18.88 ± 0.16[b]	21.48 ± 2.07[c]
Calcium (μg/g)	105.75 ± 1.48[a]	136.95 ± 0.78[b]	135.30 ± 0.28[b]
Iron (μg/g)	5.09 ± 0.12[a]	6.64 ± 0.23[a]	6.57 ± 0.57[a]
Riboflavin (μg/g)	0.24 ± 0.00[a]	3.28 ± 0.34[b]	2.25 ± 0.35[b]
Nicotinic acid (μg/g)	6.87 ± 0.01[a]	2.76 ± 0.91[b]	4.02 ± 0.74[c]
Pyridoxine (μg/g)	0.12 ± 0.00[a]	0.05 ± 0.01[b]	0.07 ± 0.00[c]
γ-Oryzanol (μg/g)	262.40 ± 2.82[a]	96.10 ± 3.87[b]	76.55 ± 2.18[c]
α-Tocopherol (μg/g)	4.03 ± 0.01[a]	2.45 ± 0.08[b]	2.70 ± 0.05[b]
γ-Tocopherol (μg/g)	2.95 ± 0.02[a]	2.02 ± 0.04[b]	1.99 ± 0.07[b]
δ-Tocopherol (μg/g)	0.76 ± 0.00[a]	0.81 ± 0.04[b]	0.75 ± 0.01[a]
α-Tocotrienol (μg/g)	2.52 ± 0.05	ND	ND
γ-Tocotrienol (μg/g)	10.31 ± 0.16[a]	4.78 ± 0.01[b]	4.75 ± 0.35[b]
δ-Tocotrienol (μg/g)	1.22 ± 0.02[a]	0.81 ± 0.01[b]	0.83 ± 0.01[b]
Antioxidant activity			
TPC (mg GAE/g)	1.10 ± 0.01[a]	1.18 ± 0.00[b]	1.20 ± 0.01[b]
FRAP (mmol TE/g)	1.03 ± 0.01[a]	0.53 ± 0.01[b]	0.43 ± 0.01[c]

[a] Represented values are the means ± standard deviations of three replicates.
[b] Values with the same superscript letter in a row are not significantly different ($p > 0.05$).
[c] ND, not detected; GAE, gallic acid equivalent; TE, trolox equivalent.

Table 2. Proximate compositions, nutritional values and antioxidant activities of steamed brown rice breads (SBRBs).

http://dx.doi.org/10.5772/66880

The effect of FBRF on total phenolic content of SBRB is presented in **Table 2**. The substitution of BRF with 40% FBRF slightly increased TPC. This may be attributed to the difference between control bread and bread containing FBRF in their acidity, where the batter containing FBRF was more acidic than the control. This result is in line with reports of Liukkonen et al. [1] who reported that formation of acidity during sourdough process can increase phenolic substances, or due to the effect of enzymes supplemented by FBRF, which breakdown the cell wall and increased the extractable phenolic compounds. Also, Katina et al. [19] reported an increase in the extractable phenolic compounds with addition of sourdough. Even though, total phenolic content was higher in treated bread, its antioxidant activity (FRAP value) (0.43 mmol TE/g) was significantly ($p < 0.05$) lower than the control bread (0.53 mmol TE/g) (**Table 2**). This is in contrast with another study that reported substitution of natural and yeast fermented rice bran protein concentrates to wheat flour elevated its ferric reducing ability power and radical scavenging activity [36]. In fact, antioxidants in foods play a critical role in the prevention and regulation degenerative maladies in which oxidative destruction has been involved [49].

Brown rice is a good source of vitamin B and E as well as γ-oryzanol. The present study provided new facts on the effects of steaming process and the addition of fermented flour on vitamins and total γ-oryzanol contents in BRF (**Table 2**). Tocopherols and tocotrienols were reduced in SBRBs compared to their levels in the flour that could be due to the heat effect during steaming. Pascual et al. [50] reported that cooking of brown rice caused significant decrease in tocols. It has been reported that sourdough might change the levels of tocopherols and tocotrienols and that depends on sourdough process and the raw material [1, 19]. However, in this study, incorporation of FBRF did not have any significant ($p > 0.05$) change on their concentrations. Total γ-oryzanol content significantly decreased in control bread (96.10 μg/g) and bread containing 40% FBRF (76.55 μg/g) compared to its initial level in the flour (262.40 μg/g) (**Table 2**). This is in contrary to the reports of Pascual et al. [50] that heat treatment of brown rice such as parboiling and cooking did not decrease oryzanol content. Substitution with FBRF caused higher reduction in its concentration. From the obtained results, this compound is sensitive to heat and acidity, where the reduction was higher in the bread containing FBRF, which its batter was more acidic.

Riboflavin content significantly ($p < 0.05$) increased in steamed breads compared to flour. SBRB without FBRF had higher riboflavin content but was not significant. Pyridoxine and nicotinic acid contents significantly decreased in the bread samples and the reduction was greater in the control bread (**Table 2**). Previous study indicated that sourdough fermentation had no influence on riboflavin and pyridoxine contents [51]. It is well known that fermentation increases vitamin B group. Nevertheless, these compounds are sensitive to heat, which may explain their reduction in the bread samples. An early study reported that riboflavin is more stable to heat than the others [51]. Thus, the current investigation supported that where their concentrations in the breads were greater than in the flour (**Table 2**).

4. Conclusions

The results of the present study indicated that pre-fermentation of BRF is an appropriate way to relief the negative effects of the bran fraction and reduce some of the gluten-free bread

drawbacks. As the brown rice batter having 40% pre-fermented brown rice flour had a softer system, as indicated by lower viscoelastic properties and pasting parameters, The softer system could be stronger and more stable during proofing and steaming, which had greater ability to retain more air bubbles and as a result higher specific volume and improved texture of its bread were obtained. Besides, pre-fermented whole flour enhanced the nutritional value of the steamed bread. These improvements might relate to the enzyme actions activated during pre-fermentation, in addition to the acidification rate and microbial metabolism products. The differences in the SBRBs microstructures might explain the whole changes that occurred in the rheological, textural and nutritional properties of the treated bread, which still need to be investigated.

Author details

Muna Ilowefah, Jamilah Bakar, Hasanah Mohd Ghazali and Kharidah Muhammad*

*Address all correspondence to: kharidah@upm.edu.my

Faculty of Food Science and Technology, Universiti Putra Malaysia, Selangor, Malaysia

References

[1] Liukkonen K., Katina K., Wilhelmsson A., Myllymaki O., Lampi A., Kariluoto S., Piironen V., Heinonen S., Nurmi T., Adlercreutz H., Peltoketo A., Pihlava J., Hietaniemi V., Poutanen K. Process-induced changes on bioactive compounds in whole grain rye. Proceedings of the Nutrition Society. 2003;**62**:117–122. doi:10.1079/PNS2002218

[2] Chen L., Hu J.Y., Wang S.Q. The role of antioxidants in photoprotection: a critical review. Journal of the American Academy of Dermatology. 2012;**67**:1013–1024. doi:10.1016/j.jaad.2012.02.009

[3] Vitaglione P., Napolitano A., Fogliano V. Cereal dietary fibre: a natural functional ingredient to deliver phenolic compounds into the gut. Trends in Food Science & Technology. 2008;**19**:451–463. doi:10.1016/j.tifs.2008.02.005

[4] Renzetti S., Arendt E. Effect of protease treatment on the baking quality of brown rice bread: From textural and rheological properties to biochemistry and microstructure. Journal of Cereal Science. 2009;**50**:22–28. doi:10.1016/j.jcs.2009.02.002

[5] Schober T.J., Messerschmidt M., Bean S.R., Park S.H., Arendt E.K. Gluten-free bread from sorghum: quality differences among hybrids. Cereal Chemistry. 2005;**82**:394–404. doi:10.1094/CC-82-0394

[6] Ciclitira P.J., Ellis H.J., Lundin K.E. Gluten-free diet—what is toxic? Best Practice & Research Clinical Gastroenterology. 2005;**19**:359–371. doi:10.1016/j.bpg.2005.01.003

[7] Moroni A.V., Dal Bello F., Arendt E.K. Sourdough in gluten-free bread-making: an ancient technology to solve a novel issue? Food Microbiology. 2009;**26**:676–684. doi:10.1016/j.fm.2009.07.001

[8] Marti A., Pagani M.A. What can play the role of gluten in gluten free pasta? Trends in Food Science and Technology. 2013;**31**:63–71. doi:10.1016/j.tifs.2013.03.001

[9] Moore M.M., Juga B., Schober T.J., Arendt E.K. Effect of lactic acid bacteria on properties of gluten-free sourdoughs, batters, and quality and ultrastructure of gluten-free bread. Cereal Chemistry. 2007;**84**:357–364. doi:10.1094/CCHEM-84-4-0357

[10] Demirkesen I., Mert B., Sumnu G., Sahin S. Quality of gluten-free bread formulations baked in different ovens. Food Bioprocess Technology. 2013;**6**:746–753. doi:10.1007/s11947-011-0712-6

[11] Marengo M., Bonomi F., Marti A., Pagani M.A., Abd Elmoneim O.E., Iametti S. Molecular features of fermented and sprouted sorghum flours relate to their suitability as components of enriched gluten-free pasta. LWT-Food Science and Technology. 2015;**63**:511–518. doi:10.1016/j.lwt.2015.03.070

[12] NovieAlviola J.N., Waniska R.D. Determining the role of starch in flour tortilla staling using α-amylase. Cereal Chemistry. 2008;**85**:391–396. doi:10.1094/CCHEM-85-3-0391

[13] Alvarez-Jubete L., Arendt E.K., Gallagher E. Nutritive value and chemical composition of pseudocereals as gluten-free ingredients. International Journal of Food Sciences and Nutrition. 2009;**60**:240–257. doi:10.1080/09637480902950597

[14] Repo-Carrasco-Valencia R., Peña J., Kallio H., Salminen S. Dietary fiber and other functional components in two varieties of crude and extruded kiwicha (Amaranthuscaudatus). Journal of Cereal Science. 2009;**49**:219–224. doi:10.1016/j.jcs.2008.10.003

[15] Schmiele M., Jaekel L.Z., Patricio S.M.C., Steel C.J., Chang Y.K. Rheological properties of wheat flour and quality characteristics of pan bread as modified by partial additions of wheat bran or whole grain wheat flour. International Journal of Food Science & Technology. 2012;**47**:2141–2150. doi:10.1111/j.1362621.2012.03081

[16] Ilowefah M., Chinma C., Bakar J., Ghazali H.M., Muhammad K., Makeri M. Fermented brown rice flour as functional food ingredient. Foods. 2014;3:149–159. doi:10.3390/foods3010149

[17] Houben A., Götz H., Mitzscherling M., Becker T. Modification of the rheological behavior of amaranth *Amaranthus hypochondriacus*) dough. Journal of Cereal Science. 2010;**51**:350–356. doi:10.1016/j.jcs.2010.02.003

[18] Schober T.J., Bean S.R., Boyle D.L. Gluten-free sorghum bread improved by sourdough fermentation: Biochemical, rheological, and microstructural background. Journal of Agricultural and Food Chemistry. 2007;55:5137–5146. doi:10.1021/jf0704155

[19] Katina K., Arendt E., Liukkonen K.H., Autio K., Flander L., Poutanen K. Potential of Sourdough for Healthier Cereal Products. Trends in Food Science & Technology. 2005;**16**:104–112. doi:10.1016/j.tifs.2004.03.008

[20] Ilowefah M., Bakar J., Ghazali H.M., Mediani A., Muhammad K. Physicochemical and functional properties of yeast fermented brown rice flour. Journal of Food Science and Technology. 2015;**52**:5534–5545. doi:10.1007/s13197-014-1661-7

[21] Shekib L.A. Nutritional improvement of lentils, chick pea, rice and wheat by natural fermentation. Plant Foods for Human Nutrition. 1994;**46**:201–205. doi:10.1007/BF01088991

[22] Kati K., Kaisa P., Karin A. Influence and interactions of processing conditions and starter culture on formation of acids, volatile compounds, and amino acids in wheat sourdoughs. Cereal Chemistry. 2004;**81**:598–610. doi:10.1094/CCHEM.2004.81.5.598

[23] AACC International. Approved Methods of Analysis, 9th Ed. Method 61-02. Determination of the pasting properties of rice with Rapid Visco-Analyser. First Approval 10-26-94, 2000. AACC International, St. Paul, MN, USA

[24] Hallén E., İbanoğlu S., Ainsworth P. Effect of fermented/germinated cowpea flour addition on the rheological and baking properties of wheat flour. Journal of Food Engineering. 2004;**63**:177–184. doi:10.1016/S0260-8774(03)00298-X

[25] AOAC (2005). Official Methods of Analysis, 18th ed, Method 934.01, 920.87, 923.05 and 993.19, 985.35, 995.11. Association of Official Analytical Chemists. Washington, DC

[26] ISO 2171: 1993 International Standard, Cereals and milled cereal products—determination of total ash.

[27] Wu P., Zhao T., Tian J. Phytic acid contents of wheat flours from different mill streams. Agricultural Sciences in China. 2010;**9**:1684–1688. doi:10.1016/0144-8617(89)90041-6

[28] Beta T., Nam S., Dexter J.E., Sapirstein H.D. Phenolic content and antioxidant activity of pearled wheat and roller-milled fractions. Cereal Chemistry. 2005;**82**:390–393. doi:10.1094/CC-82-0390

[29] Aguilar-Garcia C., Gavino G., Baragaño-Mosqueda M., Hevia P., Gavino V.C. Correlation of tocopherol, tocotrienol, γ-oryzanol and total polyphenol content in rice bran with different antioxidant capacity assays. Food Chemistry. 2007;**102**:1228–1232. doi:10.1016/j.foodchem.2006.07.012

[30] Ye L., Landen Jr W., Lee J., Eitenmiller R. Vitamin E content of margarine and reduced fat products using a simplified extraction procedure and HPLC determination. Journal of Liquid Chromatography & Related Technologies. 1998;**21**:1227–1238. doi:10.1080/10826079808006596

[31] AACC International. Approved Methods of Analysis, 11th Ed. Method 86-90.01. B-Vitamin in Vitamin Concentrates by HPLC. Approved November 3, 1999. AACC International, St. Paul, MN, USA.

[32] Haros M., Ferrer A., Rosell C.M. Rheological behaviour of whole wheat flour. 13th World Congress of Food Science and Technology. 2006. doi:10.1051/IUFoST:20060681

[33] Song Y., Zheng Q. Dynamic rheological properties of wheat flour dough and proteins. Trends in Food Science & Technology. 2007;**18**:132–138. doi:10.1016/j.tifs.2006.11.003

[34] Elkalifa O.A., Schiffler B., Bernhardt R. Effect of fermentation on the functional properties of sorghum flour. Food Chemistry. 2005;**92**:1–5. doi:10.1016/j.foodchem.2004.05.058

[35] Rieder A., Holtekjølen A.K., Sahlstrøm S., Moldestad A. Effect of barley and oat flour types and sourdoughs on dough rheology and bread quality of composite wheat bread. Journal of Cereal Science. 2012;**55**:44–52. doi:10.1016/j.jcs.2011.10.003

[36] Chinma C., Ilowefah M., Shammugasamy B., Mohammed M., Muhammad K. Effect of addition of protein concentrates from natural and yeast fermented rice bran on the rheological and technological properties of wheat bread. International Journal of Food Science and Technology. 2015;**50**:190–197. doi:10.1111/ijfs.12619.

[37] Gómez M., Oliete B., Rosell C.M., Pando V., Fernández E. Studies on cake quality made of wheat-chickpea flour blends. LWT-Food Science and Technology. 2008;**41**:1701–1709. doi:10.1016/j.lwt.2007.11.024

[38] Steeneken P. Rheological properties of aqueous suspensions of swollen starch granules. Carbohydrate Polymers. 1989;**11**:23–42. doi:10.1016/0144-8617(89)90041-6

[39] Derycke V., Veraverbeke W., Vandeputte G., De Man W., Hoseney R., Delcour J. Impact of proteins on pasting and cooking properties of nonparboiled and parboiled rice. Cereal Chemistry. 2005;**82**:468–474. doi:10.1094/CC-82-0468

[40] Bhol S., John Don Bosco S. Influence of malted finger millet and red kidney bean flour on quality characteristics of developed bread. LWT-Food Science and Technology. 2014;**55**:294–300. doi:10.1016/j.lwt.2013.08.012

[41] Corsetti A., Gobbetti M., Rossi J., Damiani P. Antimould activity of sourdough lactic acid bacteria: identification of a mixture of organic acids produced by Lactobacillus San francisco CB1. Applied Microbiology and Biotechnology. 1998;**50**:253–256. doi:10.1007/s002530051285

[42] Di Cagno R., De Angelis M., Auricchio S., Greco L., Clarke C., De Vincenzi M., Giovannini C., D'Archivio M., Landolfo F., Parrilli G. Sourdough bread made from wheat and nontoxic flours and started with selected lactobacilli is tolerated in celiac sprue patients. Applied and Environmental Microbiology. 2004;**70**:1088–1096. doi:10.1128/AEM.70.2.1088-1096.2004

[43] Arendt E.K., Ryan L.A.M., Dal Bello F. Impact of sourdough on the texture of bread. Food Microbiology. 2007;**24**:165–174. doi:10.1016/j.fm.2006.07.011

[44] Salmenkallio-Marttila M., Katina K., Autio K. Effects of bran fermentation on quality and microstructure of high-fiber wheat bread. Cereal Chemistry. 2001;**78**:429–435. doi:10.1094/CCHEM.2001.78.4.429

[45] Kopeć A., Pysz M., Borczak B., Sikora E., Rosell C., Collar C., Sikora M. Effects of sourdough and dietary fibers on the nutritional quality of breads produced by bake-off technology. Journal of Cereal Science. 2011;**54**: 499–505. doi:10.1016/j.jcs.2011.07.008

[46] Lappi J., Selinheimo E., Schwab U., Katina K., Lehtinen P., Mykkänen H., Kolehmainen M., Poutanen K. Sourdough fermentation of wholemeal wheat bread increases solubility

of arabinoxylan and protein and decreases postprandial glucose and insulin responses. Journal of Cereal Science 2010;**51**:152–158. doi:10.1016/j.jcs.2009.11.006

[47] Kumar V., Sinha A.K., Makkar H.P.S., Becker K. Dietary roles of phytate and phytase in human nutrition: a review. Food Chemistry. 2010;**120**:945–959. doi:10.1016/j.foodchem.2009.11.052

[48] Lopez H.W., Krespine V., Guy G., Messager A., Demigne C., Remesy C. Prolonged fermentation of whole wheat sourdough reduces phytate level and increases soluble magnesium. Journal of Agricultural and Food Chemistry 2001;**49**:2657–2662. doi:10.1021/jf001255z

[49] Lim Y.Y., Lim T.T., Tee J.J. Antioxidant properties of several tropical fruits: a comparative study. Food Chemistry. 2007;**103**:1003–1008. doi:10.1016/j.foodchem.2006.08.038

[50] Pascual C.S.C.I., Massaretto I.L., Kawassaki F., Barros R.M.C., Noldin J.A., Marquez U.M.L. Effects of parboiling, storage and cooking on the levels of tocopherols, tocotrienols and γ-oryzanol in brown rice (*Oryza sativa* L.). Food Research International. 2011;**115**:389–404. doi:10.1016/j.foodres.2011.07.013

[51] Batifoulier F., Verny M., Chanliaud E., Rémésy C., Demigné C. Effect of different breadmaking methods on thiamine, riboflavin and pyridoxine contents of wheat bread. Journal of Cereal Science. 2005;**42**:101–108. doi:10.1016/j.jcs.2005.03.003

Chapter 3

Soil Stabilization with Rice Husk Ash

Leonardo Behak

Additional information is available at the end of the chapter

http://dx.doi.org/10.5772/66311

Abstract

Rice husk ash (RHA) is a by-product of rice milling. Its use as a soil stabilizer is an alternative to the final disposition with environmental benefit. Because RHA is not self-cementitious, a hydraulic binder such a lime must be added to form cements to improve the soil strength. Researches on stabilization by applying RHA and lime combinations were conducted in sandy soils. RHA of no-controlled rice husk incineration in conventional ovens and of laboratory burning at controlled temperatures were used. The alkaline reactivity of the RHA was studied through X-ray diffractometry analysis and loss on ignition tests. The formation of cementitious compounds was observed in mixtures of soil with different RHA and lime contents. Unconfined compression strength tests were conducted on soils treated with RHA and lime. Results show strength improvements for all RHA and lime contents and time periods studied, and all materials produced can be defined as modified rather than stabilized. Improvement of sandy soils with RHA is an alternative to the final disposition with environmental, social and economic benefits.

Keywords: rice husk ash, waste valuation, soil stabilization, alkaline reactivity, mechanical behaviour

1. Introduction

Rice husk is a by-product of the rice milling. About 100 millions of tons of husk per year are produced worldwide [1]. The husk is not suitable as animal feed because of its abrasive character and almost negligible digestible protein content [2], its high ash and lignin contents make it unsuitable as a raw material for paper manufacturing [3].

In order to reduce such volume of waste, rice husk is burned either in open heaps or as a fuel in ovens for rice drying, power generation, etc. The burning volatilizes the organic compounds and water of the rice husk, and about 20% of the mass remains as rice husk ash (RHA)

[2, 4–9]. If all rice husks had been burned, it would annually produce about 20 millions of tons of RHA worldwide. To value this residue is an alternative to its final disposition with environmental benefit.

Pozzolanas are siliceous and/or aluminous materials, which in themselves possess little or no cementing properties, but chemically react with calcium hydroxide, such as lime, to form compounds possessing cementitious properties [10]. The RHA contains around 90% of silica [4, 5], which is the highest concentration of all plant residues [2]. Based upon this, RHA has been used to improve properties of soil either when added alone or when mixed with a hydraulic activator such as the cement and lime [1, 6–8, 11–16]. Soil stabilization by the addition of RHA and lime is particularly attractive for road pavements because it leads to cheaper construction and lesser disposal costs, reduces environmental damage and preserves the most highly qualified materials for priority uses [7, 8].

The effect of the addition of RHA alone on the plasticity, unconfined compression strength (UCS) and California Bearing Ratio (CBR) of a lateritic soil with 45% passing the #200 sieve (75 μm), was studied by Rahman [11]. Results showed increases of UCS and CBR in 1 day with increase in RHA up to 20 and 18%, respectively, after which they started to decrease. Similarly, Alhassan [14] observed increasing of CBR with 6-day and 1-day soaking and without soaking when a clayey soil was stabilized with RHA up to 6 and 12%, respectively.

Generally, RHA cannot be used alone in soil stabilization because of its lack of cementitious properties [7, 8]. Development of UCS has been observed when clayey, clayey sandy, silty clayey and silty sandy soils were treated with RHA and lime or cement [1, 7, 8, 12, 13]. In the case of cement, it was observed that little or insignificant increases of UCS in lateritic and clayey soils stabilized with RHA and cement with respect to its increase when they were treated with cement alone [6, 12]. For a given lime or cement content there is an optimum value of RHA content which corresponds to the maximum UCS, which varies depending on the type of soil, ash characteristics, hydraulic activator and curing time [1, 7, 8]. Alhassan [15] attributes the UCS decreasing after this optimum value to the excess RHA that could not be utilized for the alkaline reactions. Also, he shows that addition of RHA in clayey soil-lime specimens further increased the UCS at specified lime content. This increment was rapid between 0 and 4% RHA content but decreased in rate from 6 to 8% RHA content at specified curing period.

Basha et al. [8] found that a lesser amount of cement is required to achieve a given strength as compared to cement-stabilized silty sandy soil when RHA is added. Since cement is more costly than RHA, this results in lower construction cost. Ali et al. [7], evaluating the effectiveness in the improvement of a clayey sandy soil with RHA, showing that lime is a more effective stabilizing agent than cement.

The aim of this chapter is to summarize experiences conducted in Uruguay to use soils improved with RHA and lime as pavement materials of low-volume roads [17–20]. First, a background of the state of the art of soil stabilization and, particularly, with RHA is performed. It is presented as results of mineralogical and reactivity characterizations of RHA with different burning processes, and unconfined compression strength improvement of different soils

http://dx.doi.org/10.5772/66311

treated with mixtures of these ashes and lime. The results are analysed taking into account the accumulated worldwide experience, from which general conclusions are drawn.

2. Background

2.1. Soil improvement

Soils are the most widely used materials in civil engineering works, particularly in pavements. However, the properties of local soils are not suitable for the requirements of particular structures. In these cases, improving soil properties is an attractive alternative. There are essentially two forms of improvement: modification and stabilization [1, 21]. When physical properties of soil, such as plasticity, texture, volumetric stability, hydraulic conductivity and workability are improved, it is named modification, and stabilization when a significant level of long-term strength gain and durability are developed. Modification can produce important strength improvement.

Different criteria have been proposed to define whether the soil treated is modified or stabilized. Thompson [22, 23] established an optimum content of lime to stabilize the soil one which produces a UCS of 345 kPa with 28-day cured at room temperature or 48 h at 49.5°C. The criterion has been extended to soil stabilization with ashes and lime. The National Association of Australian State Road Authorities (NAASRA) divides lime-treated materials as modified and stabilized according to their fundamental behaviour under applied loadings [24]. Modified materials are used and evaluated in the same manner as conventional unbound flexible pavement while stabilized materials have a sufficiently enhanced elastic modulus and tensile strength to have a practical application in stiffening the pavement. Austroads suggests for lime modification of pavement layers 28-day UCS values between 0.5 MPa and 1.5 MPa, and for lime stabilization UCS greater than 1.5 MPa [24]. For lime stabilization, the use of pH testing together with 28-day UCS testing is recommended to establish the optimum lime content of a material, however, no mention is made on the strength to produce a lime-modified material.

The strength requirements for using lime-stabilized materials as structural layers in pavement systems vary considerably from agency to agency [21]. Thompson [23] defined a lime-soil mixture as acceptable for a structural base if the UCS exceeded about 1050 kPa while some transport agencies of USA require minimal UCS values for sub-base and base layers between 700 kPa and 1400 kPa [21].

The soil stabilization using ashes is explained by the pozzolanic reactions. When the lime ($Ca(OH)_2$) is mixed with RHA, in the presence of water, it releases calcium ions (Ca^{++}) and the pH of the medium increases above 12.4 [25]. In this high basic environment, the silicates and aluminates dissolve from the ash and react with the Ca^{++} to form calcium silicate hydrate (CSH) [2, 7, 8, 26]. In the case of mixture of cement and RHA, the silica reacts with the extra lime in the cement which in some cases can be as high as 60% [2]. Following James and Rao [27] the silicates formed are of the kind CSHI and CSHII, according to Eq. (1).

$$Ca(OH)_2 + SiO_2 \Rightarrow CSHI + CSHII \quad (1)$$

Where

CSHI = $CaO_{0.8\text{-}1.5}SiO_2.(H_2O)_{1.0\text{-}2.5}$

CSHII = $CaO_{1.5\text{-}2.0}SiO_2.2(H_2O)$

These products of the pozzolanic reactions are primarily gels that cover and bond the soil grains causing the strength gain [7, 27, 28]. The gels slowly crystallize turning into well-defined CHS, which results in a further enhancement in strength. Pozzolanic reactions begin quickly, a few hours after adding the water to the mixture, and can continue for a very long period of time, even many years, as long as enough lime, silica and water are present and the pH remains high [21]. Ali et al. [7] show X-ray diffractograms (XRD) of mixtures of clayey sandy soil with RHA and lime cured for 7, 28 and 90 days. New peaks of calcium aluminate hydrate (CAH) and CSH appear after 7 days and continue to form after 28 and 90 days, while peaks of lime disappear at 28 days. These slow reactions cause a long-term strength gain of soils.

Ali et al. [7] showed that addition of RHA-lime to a clayey sandy soil produces higher initial rate of UCS development. 6 and 9% RHA contents give an average increase in strength of 35 and 49% as the curing time increased from 7 to 28 days at 30°C. The rate of UCS development reduces at the later stages. The dependence of strength development on curing provides a considerable factor of safety for designs based on say 7-, 28- or 56-day strength [7]. UCS increases can be observed between 1 day and 7 day when both lime and cement were used to improve lateritic soil treated with RHA [11] and up to 28 days in a clayey soil stabilized with RHA and cement [12].

The enhancement of UCS development by adding RHA is influenced by the temperature [7]. As the temperature increases, the rate of strength development is intensified, due to the crystallization of cementing minerals is accelerated. Ali et al. [7] observed a significantly higher rate of UCS development in specimens of clayey sandy soil stabilized with 612 and 18% RHA and 6 and 9% lime cured during 28 days at 60°C with respect to similar specimens cured with the same time but at 30°C.

2.2. Rice husk ash reactivity

The properties of RHA depend greatly on whether the husks have undergone complete destructive combustion or have only been partially burnt [4]. Houston [4] classified RHA into high-carbon char (black), low-carbon (grey) ash and (3) carbon-free (pink or white) ash. Colour changes are associated with the completeness of the combustion process as well as structural transformation of the silica in the ash [2]. XRD studies have shown that pink ash consists essentially of tridymite and cristobalite [4], the high-temperature crystalline forms of silica. There is little if any quartz, the low-temperature crystalline form of silica. At low-combustion temperatures considerable amorphous silica remains, giving black and grey ash. Also, white colour is an indication of complete oxidation of the carbon in the ash [2].

The characteristic of the ash depends on temperature, burning time, cooling time and burning type [3, 8]. The type of ash suitable for pozzolanic activity is amorphous rather than crystallized [2]. The structural transformations of the silica affect the ash reactivity since the larger surface area of the silica the greater the extent of the chemical reactions with the

$Ca(OH)_2$ [2, 6]. Incineration of rice husk in the temperature range of 550–700°C is generally found to produce amorphous silica in the ash while temperatures in excess of 900°C produce unwanted crystallized forms [2]. However, Smith and Kamwanja [29] have reported that temperatures of about 800°C maintained for 12 h give small proportions of crystallized silica. Mehta [3] established that a highly reactive ash can be produced by maintaining the combustion temperature below 500°C under oxidizing conditions for relatively prolonged period or up to 680°C provided the high temperature exposure was less than one minute. Prolonged heating above this temperature may cause the material to convert (at least in part) to crystalline silica. Yeoh et al. [30] report that silica in RHA can remain in amorphous form at combustion temperatures of up to 900°C if the combustion time is less than 1 h, whereas crystalline silica is produced at 1000°C with combustion time more than 5 min. Other reports claim that crystallization of silica can take place at temperatures as low as 600, 500 or even at 350°C with 15 h of exposure [31].

Technologies of ash production vary from open-heap burning to specially designed incinerators. When the rice husk is burned in open-heap or conventional oven, crystalline ash with low reactivity produced, while when it is incinerated in an oven with controlled temperatures, the residue is a highly reactive white ash [3]. The rice husk incinerated in oven at controlled temperature conditions between 800–900°C verified a high reactivity of the ash in comparison with the ash resulting of the open-heap burning. RHA from burning in heaps and oven-dried at 60°C showed a much scattered XRD with peaks of quartz and tridymite [7].

The carbon content of RHA influences the stabilization process, retarding the reactions and producing low increases of strength. The avidity of carbon by calcium ions interfere the reactions between Ca^{++} and silica [32]. According to these authors, lime stabilization of soils with 6% of carbon is economically impracticable. Remaining carbon content less than 3% have been measured in a RHA obtained by burning in a simple combustion chamber at 800°C [11] and in heaps and oven-dried at 60°C [7].

3. Materials and methods

3.1. Rice husk ash

Four RHA from no-controlled burning were studied (RHAU). Three RHA from rice husk burned in conventional ovens to rice drying were collected in the rice mills of Arrozur (RHAA) in Villa Sara, Arrozal 33 (RHA33) in Vergara, both in Eastern Uruguay, and Demelfor (RHAD) in Artigas, northern Uruguay. The remaining no-controlled RHA is a result of the incineration in the furnaces of the power-generation plant of Galofer (RHAG), situated in Villa Sara.

RHA produced in laboratory at controlled temperature and time (RHAC) was also studied. Rice husk taken from Arrozur was incinerated in an oven at 500, 650, 800 and 900°C (RHA500, RHA650, RHA800 and RHA900) for 4 h and cooled at room temperature.

3.2. Soils

Four different sandy soils were used in the researches. The soil, classified according to the Unified Soil Classification System (USCS) as well-graded silty sand (SW-SM), collected in the Perez Bustos quarry, near Montevideo (PBS). The silty sand (SM) from a quarry located in Vergara (VS) and a poorly graded sand (SP) taken from Villa Passano (VPS), both in eastern Uruguay. The reddish poorly graded silty sand (SW-SM) from the Sandstone quarry, near Artigas (SS), northern Uruguay. **Table 1** shows the properties and classification of the soils. The fine content (grain-size passing the #200 sieve) is similar in PBS, VS and SS (less than 7%), while VPS has about 17% of fines. All the soils have plasticity index equal to zero (IP = 0), that is the soils are not plastic.

3.3. Lime

A commercial hydrated lime (L), mark Bulldog, produced by the Oriental de Minerales Company of Uruguay was used in the stabilization of PBS and SS. It is a calcium lime with 66% of calcium oxide (CaO), 5% of magnesium oxide (MgO) and other elements like silica and ferric oxide. The lime is fine with 100% passing the #10 sieve and 93% passing the #200 sieve, whereas 91% was greater than 2 mm.

The VPS and VS were treated with a residual quicklime (RL) from Cementos del Plata Plant. This lime does not accomplish the requirements for its use as chimney filter and it is a calcium lime with CaO varying between 70 and 93%, a maximum MgO of 8% and ferric oxide (Fe_2O_3) between 0.5 and 4.5%.

3.4. X-ray diffraction

X-ray diffraction analyses were performed on the residual RHA from the no-controlled burning in the Arrozur Mill (RHAA), RHA of controlled incineration (RHA500, RHA650, RHA800 and RHA900), PBS, mixtures of PBS with 15 and 20% RHAA and 5 and 10% lime cured for 28 days (PBS-15RHAA-5L, PBS-20RHAA-5L, PBS-20RHAA-10L), and mixtures of PBS with 15% RHA650 or RHA800 and 5% lime with 28 days (PBS-15RHA650-5L, PBS-15RHA800-5L). A dusty diffractometer with CuKα radiation and wavelength of 1.5418 Å was used. The samples were obtained from the specimens for the UCS tests once these were completed and they were milled in mortar before analysis to have a grain size less than 0.075 mm.

Property	Perez Bustos (PBS)	Vergara (VS)	Villa Passano (VPS)	Sandstone (SS)
Passing #4 (4.76 mm)	98.6	100.0	99.8	99.8
Passing #10 (2 mm)	89.6	99.9	91.6	99.6
Passing #40 (0.42 mm)	26.1	41.0	13.8	77.6
Passing #200 (0.074 mm)	6.5	16.9	3.6	6.2
USCS Classification	SW-SM	SM	SP	SP-SM

Table 1. Physical properties and classification of soils.

3.5. Loss on ignition

The organic matter content of all RHAU and RHAC was evaluated by loss on ignition tests, following the ASTM standard D7348. Samples of the RHAU were initially weighed and then subjected to a controlled temperature of 550°C during 3 h into a muffle. Because the RHAU were produced with temperatures similar or greater than 550°C, a temperature of 1000°C was adopted for tests. Thereafter, the samples were weighed after cooling at room temperature. The carbon content is the ratio between the final and initial weights of the samples.

3.6. Compaction tests

Standard Proctor compaction tests according to AASHTO Standard T99 were carried out to determine the maximum dry unit weight (MDUW) and the optimum moisture content (OMC) of the PBS and materials of PBS treated with 20% of RHAA (PBS-20RHAA-10L) by dry weight of soil and 10% of lime by dry weight of soil. Modified Proctor compaction tests were conducted in accordance to AASHTO T180 on soils and soil-RHA-lime materials.

The soils, RHA and lime were previously manually mixed in dry and thereafter various moisture contents were added and homogenized by manual mixing. The compaction was carried out immediately or 1 h after water mixing.

3.7. Unconfined compression strength tests

UCS tests of the soils and the soils stabilized with different RHA and lime contents and for different time periods were carried out following the AASHTO Standard T208. Cylindrical specimens, 3.72 cm in diameter and 7.65 cm in high were compacted into a metallic mould by kneading system at MDD and OMC of the corresponding standard or modified Proctor compaction test. The soil-RHA-lime specimens were compacted immediately or 1 h after water mixing and thereafter they were enveloped in polyvinyl film and stored in a moisture chamber at room temperature for the corresponding curing time. Finally, the specimens were tested in a triaxial load press up to failure.

4. Results and discussion

4.1. Mineralogical composition of rice husk ash

XRD analyses of RHA from Arrozur (RHAA) and RHA from laboratory-controlled incineration (RHA500, RHA650, RHA800, RHA900) are given in **Figure 1**, where they have been dislocated in the intensity axle for better viewing. Peaks in the diffraction angles (2θ) of 21.96, 31.42, and 36.35° are observed in the XRD of the RHAA, which are characteristics of cristobalite, a high-temperature crystalline form of silica [4]. The rice husk is burned in conventional ovens in the Arrozur Mill producing a crystalline ash with low reactivity [3]. Peak of carbon is also identified in RHAA at 2θ of 26,62°, which is indication of crystallization of part of the organic of the husk during the burning.

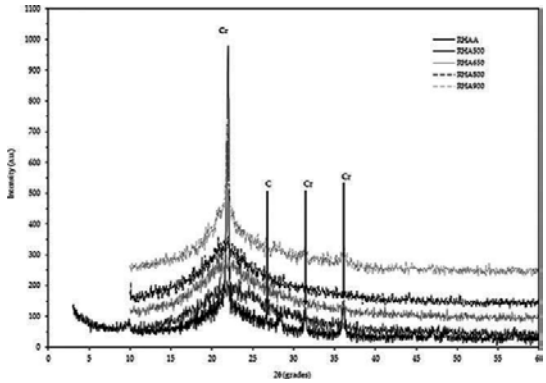

Figure 1. X-ray diffractograms of residual RHA from Arrozur and laboratory-controlled incinerating RHA. Cr: cristobalite; C: carbon.

XRD of RHA500, RHA650, and RHA800 are similar and show amorphous shape, without well-defined peaks, indicating that the silica in these ashes is amorphous rather than crystalline. The XRD of RHA900 presents peaks of cristobalite similar to that of the no-controlled burning ash. An upper limit of controlled temperature to secure RHA with considerable amorphous silica would be about 800°C, if it is maintained for 4 h, beyond which they would lead to ashes with silica mostly crystallized.

DRX of materials of PBS treated with residual RHA from Arrozur (RHAU) and lime and with RHA burned at controlled temperatures of 650 and 800°C (RHAC) and lime are depicted in **Figure 2**. Peaks of quartz, corresponding to the sandy soil, remain in all the DRX because it is a crystalline mineral that cannot react with the ash and lime.

The DRX of materials with RHAU (15 and 20%) and lime (5 and 10%) are similar. As was expected, peaks of cristobalite of the RHAU remain in those DRX. New peaks for 2θ of 24.37 and 35.75° of antigonite are present. This is a calcium aluminate silicate hydrate (CASH) which have been produced by the pozzolanic reactions between the Ca^{++} the lime and the silica of the

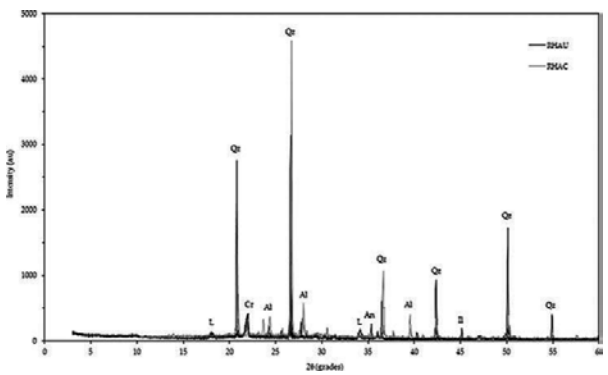

Figure 2. X-ray diffractograms of Perez Bustos soil treated with residual and controlled RHA and lime for 28 days. Qz: quartz; Il: illite; Cr: cristobalite; An: antigonite; L: lime; Al: albite.

ash. Despite the RHAU has mostly crystalline silica, it contains enough amorphous silica to react with the lime and form cementitious products. The peaks of lime mineral could be due to the exceeding lime that has not reacted before 28 days, because the alkaline reactions are slow.

New peaks of albite, a calcium aluminate silicate hydrate (CAH), are observed in both DRX of materials with RHAC, which demonstrates that reactions between the amorphous silica of these ashes and the Ca^{++} of the lime have taken place before 28 days. The similarity among the XDR shows that the pozzolanic reactivity of the RHA is quite independent of controlled incineration temperatures within the range of 650–800°C.

It is more difficult to identify the cementitious products in the DRX of the materials with RHAU than the DRX of the materials with RHAC. This would indicate that the reactivity of the RHAC is much greater than that of the RHAU, particularly within the controlled temperatures from 650 to 800°C. RHA percentages to obtain similar reactions are less in those produced at controlled temperature than in the residual ones. The use of RHA incinerated at controlled temperature within 650–800°C is a more efficient soil improving alternative.

4.2. Carbon content of the rice husk ashes

The mean values of loss on ignition of the four RHAU studied and of the RHA produced in the laboratory at temperatures during 4 h are presented in **Table 2**. All the RHAU are resultant of the husk burning in conventional ovens and are black in colour and remained mainly with this colour with white veining or tended to a grey colour. The carbonized part of the organic during the no-controlled incineration cannot be volatilized when the ash is again incinerated at 550°C for 4 h. However, the RHAU have different organic contents maybe due to the type of oven, temperature gradients inside them and incineration times. The RHAU from the Galofer Power Generation Plant (RHAG) has the least organic content, which coincides with that it is the most fine and free of impurities ash. Slightly higher organic content has the RHAU from the Arrozur Mill (RHAA). This mill and Galofer Plant are located in the same place and the burning process are almost similar. RHA 33 and RHAD present a considerable amount of no burned husk, which influences the greater organic content determined. In any case, the organic content of the RHAU is greater than that considered as suitable for soil stabilization [32]

Material	Temperature (°C)	Time (h)	Loss on ignition (%)
RHAA	550	3	18.6
RHAG	550	3	15.0
RHA33	550	3	34.1
RHAD	550	3	38.8
RHA500	1000	3	7.8
RHA650	1000	3	4.1
RHA800	1000	3	2.3
RHA900	1000	3	0.3

Table 2. Loss on ignition of the RHA.

The organic content of the RHA noticeably decreases when the incineration is temperature-controlled. For a relatively low controlled temperature of 500°C (RHA500), the loss on ignition was 7.8% meanwhile that of RHAA was 18.6%. The organic content almost linearly decreases with the increasing of the controlled temperature. The control of temperature and the incineration method are fundamental when the objective is to produce RHA with high pozzolanic reactivity. The organic content of RHA500 and RHA650 are relatively high for soil stabilization purposes while it can be considered as allowable for RHA800 [32]. A lower limit of controlled temperature to secure a RHA with an allowable organic content would be about above 650°C, if it is maintained for 4 h.

4.3. Compaction characteristics

The dry unit weight-moisture content relationship of PBS, PBS with 20% RHAA and 10% L (PBS-20RHAA-10L), SS, SS with 20% RHAD and 5% L (SS-20RHAD-5L), VPS, and VPS with 20% RHAG and 3% RL and 5% RL (VPS-20RHAG-3RL, VPS-20RHAG-5RL) are depicted in

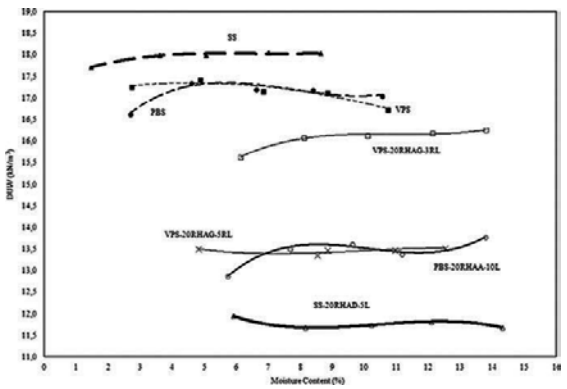

Figure 3. Dry unit weight-moisture content relationship of natural and stabilized Perez Bustos soil, Sandstone soil and Villa Passano soil.

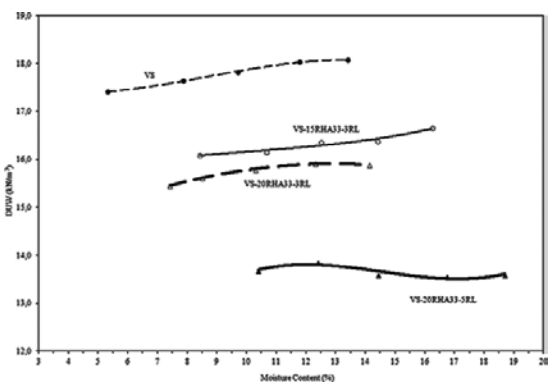

Figure 4. Dry unit weight-moisture content relationship of natural and stabilized Vergara soil.

Figure 3. **Figure 4** shows the compaction curves of VS and VS with 15and 20% RHA33 and 3 and 5% RL (VS-15RHA33-3RL, VS-20RHA33-3RL, VS-20RHA33-5RL).

All the soils have oddly shaped compaction curves without MDD and OMC well defined. This kind of compaction curve is typically obtained in the Proctor tests of sandy soils because the impact effort used in these is not efficient to compact such soils. The most efficient compaction effort for these soils is the vibration. The compaction curves of all treated materials are similar in shape to the respective natural soils. Due to the compactions were performed immediately or 1 h after the mixing, without enough time to the development of the alkaline reactions. The addition of RHA and lime do not produce textural changes in the sandy soil, which results in a similar trend compaction curve for the stabilized material. The vibration is the most recommended compaction method for sandy soils stabilized with RHA and lime independent of the ash and lime characteristics and proportions.

The dry unit weight (DUW) of all soil-RHA-lime materials are less than its corresponding natural soil for all compaction moistures. The RHA and lime have lower specific gravity and finer grain size distribution than those of the soil, so when added to a soil the specific gravity and the grain size distribution of the mixture are reduced resulting in the DUW decreasing [6, 7]. As a result the MDD of soil-RHA-lime materials are less than those of the soils (**Table 3**).

It is observed from the treatment of VPS and VS (**Figures 3** and **4**) that the MDD decreases as the RHA and lime contents increase, which is in agreement with findings in [6, 7, 14, 16]. However, it can be seen from **Figure 4** that the DUW decreases more with the increasing of lime content than that of the RHA.

The OMC is greater with the adding of RHA and lime for all studied cases (**Table 3**). The results are in agreement with the findings given in [6–8, 14, 16]. One portion of the water added to the mixture is absorbed by the RHA due to its porous characteristic [7, 8]. Another part is consumed by the lime hydration, which is required for alkaline reactions. The soil

Soil	RHA (%)	Lime (%)	MDUW (kN/m^3)	OMC (%)
Perez Bustos	0	0	17.4	5.7
	20	10	13.6	8.6
Sandstone	0	0	18.0	5.7
	20	5	11.8	12.4
Villa Passano	0	0	17.4	4.6
	20	3	16.2	10.4
	20	5	13.5	12.4
Vergara	0	0	18.1	13.3
	15	3	16.8	14.4
	20	3	15.9	14.9
	20	5	13.8	15

Table 3. Maximum dry unit weight and optimum moisture content of soils and soil-RHA-lime materials.

improvement with RHA and lime is water consuming, so it is necessary to add a greater moisture content to reduce the suction effect in the pores and to reach the greatest efficiency of compaction. Following the results of the treatment of VPS and VS, the OMC increases with increase in RHA and lime content.

4.4. Unconfined compression strength

Figure 5 shows the 28-day UCS evolution as function of the RHA and lime contents. A general pattern of UCS gain is observed for all RHA and lime contents. The UCS of VS and SS with 5% lime increases with addition of RHA until an optimum is reached, beyond which the strength begins to decrease. The optimum RHA contents found were about 15% for VS-RHA33-5RL and SS-RHAG-5L and about 20% for VS-RHA33-3RL. The maximum UCS were not reached with the studied RHA contents in the other cases, however they were found fitted in parabolic curves, which demonstrates that they also would have an optimum RHA content greater than 20%.

The 28-day UCS of VS and SS treated with 5% lime are greater than those treated with 3% lime for RHA contents up to the optimum, beyond which the strength of soils with 3% lime tends to be greater than those with 5% lime. A similar trend can be observed in the treated VPS, however the difference of UCS for all given RHA contents are practically negligible. When commercial lime is used, the most economical solution would be to adopt the least possible amount of lime even it means using greater amount of RHA since this is a residue.

The maximum 28-day UCS do not achieve the 345 kPa established to consider as optimum to stabilize a soil [22, 23]. From this and following the criteria suggested by different transport agencies [21, 24], all the studied improved soils can be defined as modified materials rather than stabilized. The shear strength of sandy soils mainly depends on the confining pressure so its UCS (confining pressure zero) is very low. In fact, the UCS of the studied soils is 8.2 kPa (PBS), 5.5 kPa (SS), 0 kPa (VPS) and 15.1 kPa (VS). If modified materials are those that behave as the corresponding untreated soil, the shear strength of studied materials would also depends on the confining pressure and therefore its UCS would be relatively low. The UCS method [22, 23] was developed for soil stabilization with lime and it should be adjusted to be adequately used for soil stabilization purpose using ashes.

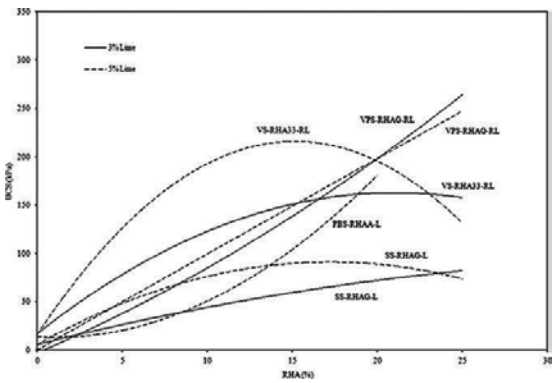

Figure 5. 28-day unconfined compression strength of soils with different RHA and lime contents.

http://dx.doi.org/10.5772/66311

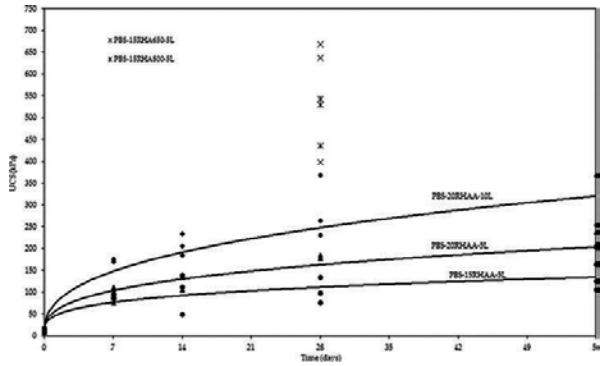

Figure 6. Unconfined compression strength of materials of Perez Bustos soil modified with RHAA and lime as a function of time.

The time dependence of the UCS of sandy soils treated with different residual RHA and lime contents is observed in **Figure 6**. A gain of UCS over time is observed for all studied RHA and lime combinations with a variation rate that reduces with the time. For the same lime content, the initial variation rate is higher when it is added a greater RHA content, 5.6 and 7.6 in the first 7 days for specimens with 15 and 20% RHAA, respectively, and tend to be similar at the later stages, 1.2 and 1.3, respectively, for the same materials from 7 days to 14 days. The initial variation rate is greater when it is increased the lime content maintaining constant the RHA content, 7.6 and 10.8 at 7 days when the lime content varies from 5to 10%, and tend to be similar (1.3) at the later stages. The dependence of strength development on time provides a considerable factor of safety for designs based on say 7- or 28-day strength [7].

A significant increase of UCS results when RHAC are used, as can be seen in **Figure 6**. The UCS of specimens with 15% of these controlled ashes and 5% lime is greater than that of the specimens with RHAU for all stabilizer contents and times. The UCS of PBS-15RHA650-5L and PBS-15RHA800-5L at 28 days are, respectively, 41 and 36 times greater than that of PBS. They are, respectively, 5.1 and 4.5 times the 28-day UCS of PBS-15RHAA-5L, and 1.8 and 1.6 times 56-day UCS of PBS-20RHAA-10L. The RHA from controlled incineration at temperatures from 650 to 800°C are more reactive than the RHA from incineration in conventional ovens, being needed less amounts of RHA and lime to reach greater UCS.

The UCS of tested materials with RHAC is quite similar, which evidences a similar pozzolanic reactivity for both incineration temperatures. The 28-day UCS of soils modified with RHAC and lime cured for 28 days would be independent of the incineration temperature within the range of 650–800°C.

5. Conclusions

The improvement of soils through addition of rice husk ash (RHA) and lime was studied in several researches. Four sandy soils from different locations of Uruguay and four residual RHA (RHAU) produced in conventional ovens were used for this objective. RHA produced

in laboratory with controlled temperature and time (RHAC) were also investigated. Results and analysis of these researches allow to draw the following conclusions:

All the RHAU are black in colour, classifying as high-carbon char, with less or more presence of no burned husk. The RHAU from power-generation oven (RHAG) is the finest and has negligible rice husk content. The X-ray diffractogram (XRD) of the RHA resultant of rice husk incineration in conventional oven of the Arrozur Mill (RHAA) shows peaks of cristobalite, a high-temperature crystalline form of silica and carbon from the crystallization of part of the organic. The organic content of the four RHAU is high to very high, greater than the considered as suitable for soil stabilization. The RHAG has the least loss on ignition, followed by RHAA. The higher loss on ignition is due to the no burned husk presents in these ashes. As the type of ash suitable for pozzolanic activity is amorphous rather than crystallized and with low organic content, the studied RHAU can be defined as low to moderately low ashes.

The RHAC show XRD without clear peaks for incineration temperatures from 500–800°C, indicating that the silica in these ashes is amorphous rather than crystalline. Peak of cristobalite is observed in the RHAC from husk incineration at 900°C. An upper limit of controlled temperature to secure RHA with considerable amorphous silica would be about 800°C, when it is maintained for 4 h. The loss on ignition reduces respect to the RHAU when the incineration is controlled at temperatures between 500 and 900°C, so that is less the greater the temperature. However, the organic content of ashes produced with temperatures until 650°C are still unwanted for soil stabilization purposes, while it is allowable for the ashes incinerated at temperatures equal or greater than 800°C. A lower limit of controlled temperature to secure a RHA with an allowable organic content would be about 650°C, when it is maintained for 4 h. Incineration of rice husk in the temperature range of 650–800°C is found to produce RHA of the highest pozzolanic reactivity.

The DRX of soil treated with RHAU and lime with 28 days show new peaks of antigonite. This is a calcium aluminate silicate hydrate resultant of the reactions between the calcium ions of the lime and the silica of the ash. Despite the RHAU is low reactive, it is still capable to react with the lime to form cementitious products. New peaks of albite, a calcium aluminate silicate hydrate resultants of the reactions between the calcium ions of the lime and the silica of the ash, are observed in the DRX of materials with RHAC and 28 days. When the lime is mixed with RHA, in presence of water, pozzolanic reactions take place to produce cementitious products as calcium silicate hydrate (CSH) and calcium aluminate silicate hydrate (CASH).

The unconfined compression strength (UCS) of soils is improved with adding all RHAU contents. Despite these ashes are low reactive, they can react with the lime to from cementitious products that bond the grains of sandy soils improving their strength. However, the 28-day UCS does not achieve the values established by different transport agencies to consider the soils as stabilized. The materials of soils improved with RHAU and lime can be defined as modified rather than stabilized. Although, modification can produce important strength gain.

The UCS increases with the increase of the RHAU amount until to reach an optimum, beyond which the strength begins to decrease. The optimum RHAU is higher when the lime amount

is less, however it is possible to reach higher UCS when is added the least amount of lime and RHAU contents higher than the optimum corresponding to higher lime contents. When commercial lime is used, it would be a more economical solution since the RHA is a residue.

A gain of UCS over time is observed for all studied RHA and lime combinations. Pozzolanic reactions begin quickly and continue for a very long period of time, even many years, as long as enough free calcium ions and silica are present and the pH remains high. The UCS increase rate is greater at starting and reduces at the later stages.

In countries with high rice production, rice husk and RHA are residues whose final disposition is a big concern, the use of RHA for soil improvement is particularly attractive. It reduces the environmental impact, disposal costs and preserves non-renewable resources such as soils and rocks. It is an economic alternative, particularly in roads, by giving value to a waste material, enabling the use of low-quality materials with reducing transport costs, and improving the pavement performance with reducing maintenance and rehabilitation costs.

Author details

Leonardo Behak

Address all correspondence to: lbehak@fing.edu.uy

Geotechnical Engineering Department, Engineering Faculty, University of the Republic, Montevideo, Uruguay

References

[1] Alhassan M, Mustapha AM. Effect of Rice Husk Ash on Cement Stabilized Laterite. Leonardo Electronic Journal of Practices and Technologies. 2007; **11**: 47–58.

[2] Boateng AA, Skeete DA. Incineration of Rice Hull for Uses as a Cementitious Material. The Guyana Experience. Cement and Concrete Research. 1990; **20(5)**: 795–802.

[3] Mehta PK. The Chemistry and Technology of Cement Made from Rice Husk Ash. In: UNIDO/ESCAP/RCTT Workshop on Rice Husk Ash Cement; 1979, Peshawar. pp. 113–122.

[4] Houston DF. Rice Hulls. In: Rice: Chemistry and Technology. American Association of Cereal Chemists; St. Paul, MN; 1972. pp. 301–340.

[5] Juliano BO, Ed. Rice: Chemistry and Technology. American Association of Cereal Chemists; St. Paul, MN; 1985. 774 p.

[6] Rahman MA. Effects of Cement-Rice Husk Ash Mixtures on Geotechnical Properties of Lateritic Soils. Journal of Soils and Foundations. 1987; **27(2)**: 61–65.

[7] Ali FH, Adnan A, Choy CK. Geotechnical Properties of a Chemically Stabilized Soil from Malaysia with Rice Husk Ash as an Additive. Geotechnical and Geological Engineering. 1992; **10(2)**: 117–134.

[8] Basha EA, Hashim R, Mahmud, HB, Muntohar AS. Stabilization of Residual Soil with Rice Husk Ash and Cement. Construction and Building Materials. 2005; **19**: 448–453.

[9] Brooks RM. Soil Stabilization with Flyash and Rice Husk Ash. International Journal of Research in Applied Sciences. 2009; **1(3):** 209–217. ISSN: 2076-734X.

[10] Malhotra VM, Mehta PK. Pozzolanic and Cementitious Material. Gordon & Breach; Amsterdam; 1996. 191 p.

[11] Rahman MA. The Potential of Some Stabilizers for the Use of Lateritic Soil in Construction**.** Building and Environment Journal. 1986; **21(1)**: 57–61.

[12] Noor M, Abdul Aziz A, Suhadi R. Effects on Cement-Rice Husk Ash Mixtures on Compaction, Strength and Durability of Melaka Series Lateritic Soil. The Professional Journal of the Institution of Surveyors Malaysia. 1993; **28(3)**: 61–67.

[13] Muntohar AS, Hantoro G. Influence of Rice Husk Ash and Lime on Engineering Properties of a Clayey Subgrade. Electronic Journal of Geotechnical Engineering. 2000; 5: 12 p.

[14] Alhassan M. Potentials of Rice Husk Ash for Soil Stabilization. Assumption University Journal of Thailand. 2008; **11(4)**: 246–250.

[15] Alhassan M. Permeability of Lateritic Soil Treated with Lime and Rice Husk Ash. Assumption University Journal of Thailand. 2008; **12(2)**: 115–120.

[16] Choobbasti AJ, Ghodrat H, Vahdatirad MJ, Firouzian S, Barari A, Torabi M, Bagherian, A. Influence of Using Rice Husk Ash in Soil Stabilization Method with Lime. Frontier Earth Science China. 2010; 4(4): 471–480. DOI: 10.1007/s11707-010-0138-x.

[17] Behak L. Stabilization of a Sedimentary Sandy Soil of Uruguay with Rice Husk Ash and Lime [MSc Dissertation]. Porto Alegre: Postgraduation Program in Civil Engineering, Federal University of Rio Grande do Sul; 2007.

[18] Behak L, Núñez WP. Characterization of Material Comprised of Sandy Soil, Rice Husk Ash and Lime potentially Useful in Pavements. Revista de Ingeniería de Construcción. 2008; **23(1)**: 34–41.

[19] Behak L, Núñez WP. Effect of Burning Temperature on Alkaline Reactivity of Rice Husk Ash with Lime. Road Materials and Pavement Design. 2013; **14(3)**: 570–585. DOI:10.108 0/14680629.2013.779305.

[20] Behak L, Musso M. Performance of Low-Volume Roads with Wearing Course Layer of Silty Sandy Soil Modified with Rice Husk Ash and Lime. In: XII Conference on Transport Engineering; 7–9 June 2016; Valencia. DOI: 10.4995/CIT2016.2016.3451. 8 p.

[21] Little DN. Evaluation of Structural Properties of Lime Stabilized Soils and Aggregates. Volume 1: Summary of Findings. National Lime Association; Arlington, VA; 1999. 89 p.

[22] Thompson MR. Lime Reactivity of Illinois Soils. Journal of the Soil Mechanics and Foundation Divisions. 1966; **92**: 67–92.

[23] Thompson MR. Suggested Method of Mixture Design Procedures for Lime-Treated Soils. ASTM Special Technical Publication 1970; **479**:430–440.

[24] Jameson GW. Review of Definition of Modified Granular Materials and Bound Materials. Austroads Research Report AP-R343-13; 2013. 13 p.

[25] Rogers CDF; Glendinning S. Lime Requirement for Stabilization. Transportation Research Record. 2000; **1721**: 9–18. DOI: 10.3141/1721-02.

[26] Eades JL. Reactions of $Ca(OH)_2$ with Clay Minerals in Soil Stabilization [Ph.D. Thesis]. Urbana: University of Illinois; 1962.

[27] James J, Rao MSP. Reaction Product of Lime and Silica from Rice Husk Ash. Cement and Concrete Research. 1986; **16**: 67–73.

[28] Ingles OG, Metcalf JB. Soil Stabilization. Principles and Practice. Butterworths; Melbourne; 1972. 374 p.

[29] Smith, RG, Kamwanja, GA. The Use of Rice Husk for Making a Cementitious Material. In: Joint Symposium on the Use of Vegetable Plants and their Fibers as Building Material, Baghdad, 1986.

[30] Yeoh AK, Bidin R, Chong CN, Tay CY. The Relationship Between Temperature and Duration of Burning of Rice-Husk in the Development of Amorphous Rice-Husk Ash Silica. In: UNIDO/ESCAP/RCTT, Follow-up Meeting on Rice-Husk Ash Cement; Alor Setar, 1979.

[31] Bui DD. Rice Husk Ash a Mineral Admixture for High Performance Concrete [Ph.D. Thesis]. Delft: Civil Engineering and Geosciences, University of Technology; 2001.

[32] Petry TM., Glazier EJ. The Effect of Organic Content on Lime Treatment of Highly Expansive Clay. In: 2nd International Symposium on Treatment and Recycling of Materials for Transport Infrastructure. Paris, 24–24 October 2005; 15 p.

Chapter 4

Nano-Silicate from Paddy Waste as Natural Corrosion Inhibitor

Norinsan Kamil Othman, Denni Asra Awizar and Zulhusni Dasuki

Additional information is available at the end of the chapter

http://dx.doi.org/10.5772/67378

Abstract

The highly advance usage of an agricultural waste of rice husk ash (RHA) from *Oryza sativa* L. was developed by extracting the nanosilicate contained in RHA as a corrosion inhibitor for carbon steel in 0.5 M NaCl media. The corrosion measurement was studied using weight loss, potentiodynamic polarization, electrochemical impedance spectroscopy (EIS), surface analysis, and adsorption isotherm study. The extracted nanosilicate powder from RHA was analyzed using Fourier Transform Infrared Spectroscopy (FTIR) to identify the presence of functional groups (SiO_2), whereas X-ray diffraction (XRD) to identify the phase of silica from RHA. The particle size of nanosilicate was confirmed by transmission electron microscopy (TEM) and Zetasizer analysis, and the results show particle size of nanosilicate in the range of 5–10 nm. The maximum inhibition efficiency (IE%) is up to 88% in NaCl media. On the other hand, the inhibitor adsorption properties follow Temkin isotherm with mixed type of inhibition properties. Surface analysis on specimen that was treated with nanosilicate was smoother with fewer pits and pores than untreated specimen. In future perspectives, nanosilicate from RHA has a promising advantages and imminent applications for industries revolving with composites, biomedicine, and many more.

Keywords: paddy rice husk, nanosilicate, corrosion inhibitor, sodium chloride

1. Introduction

Corrosion inhibitors are a favorable method to prevent corrosion; it can reduce the rate of metal corrosions from corrosive environments. Most of the processing industries, such as water heating system (boiler), seawater cooling system, and pipes, made use of corrosion inhibitor as protective

measurement against corrosion. This is because of corrosion inhibitor is a straightforward use and cost-effective. However, for more than a decade, inorganic and synthetic chemical-based corrosion inhibitor such as chromate and nitrate-based has been widely used in the industries and has led into a serious environmental deterioration and dreadful impact onto marine life as excessive usage of inhibitor has exposed into the environment [1].

These environmental issues regarding the use of the synthetic corrosion inhibitor have led into a rise in environmental warnings, by the authorities and NGOs, such as Environmental Protection Agency (EPA) and Food and Drug Administration (FDA), which has had issued some industrial guidance regarding the use of corrosion inhibitor in the industries. Since then, the urgency to develop environment-friendly corrosion inhibitor has greatly increased the researcher's interest especially in the development of corrosion inhibitor derived from natural sources, i.e. rice husk waste [2].

In general, corrosion inhibitors based on natural sources are environmentally acceptable, less toxic, inexpensive to process and abundant in nature compared to corrosion inhibitor based on synthetic chemical [3, 4]. In this study, corrosion inhibitor based on nanosilicate derived from rice husk waste would be the best candidate in replacing the synthetic corrosion inhibitor. As past study reported, silicate is naturally inorganic corrosion inhibitor that has been used in various applications, such as antifreeze in the engine, which helps prevent corrosion and as an engine coolant and lubricant [5]. Apart from its application as corrosion inhibitor, silicate extracted from rice husk can be manipulated into a lot of applications and fit into today's high technology advancement, for instance, fillers in high durability concrete and structures [6, 7], drug delivery and biomedical applications [8], and many more.

Asia has the largest rice production in tropical regions. By-products of the production of rice are rice husks and rice fingers. In 2007, statistics by the Ministry of Agriculture, Malaysia, has reported that more than 408,000 tons of rice (*Oryza sativa* L.) husks were produced in Malaysia every year. Rice husks contain a high percentage of silica, which is more than 90% [9].

In these times, the study in the field of nanotechnology is growing in parallel with the development of science and technology. Nanotechnology had been applied in various fields, such as biotechnology, medication, sensor, semiconductor, coating materials, and materials industrial uses [10]. Applications of nanotechnology attract interests due to the nanosized structure materials that contained unique properties compared to lump materials.

Based on past studies, commercial silicate corrosion inhibitor delivers good inhibition efficiency for metals and alloys. According to experts, silicate corrosion inhibitors are non-toxic and have been used many years in the industry. Moreover, silicate is a compound that has the ability to be adsorbed on the metal surface to form a thin layer of barrier on the metal surface and protects the metal from corroding [11].

Today, corrosion inhibitors' products in the market were more prone toward selecting corrosion inhibitors derived from natural plant in order to solve corrosion and its problem. Some researchers have been extracting organic and inorganic compounds containing distinctive

http://dx.doi.org/10.5772/67378

corrosion inhibition properties. The source materials of natural corrosion inhibitors are usually inexpensive, readily available and renewable. In other words, natural-based corrosion inhibitors can replace synthetic corrosion inhibitors that are highly toxic, have expensive processing cost, and may cause harm to the environment. In this recent study, the waste from the rice field which is the rice husk will be transformed into a new usable and advance compound which is the nanosilicate compound for the use of solving corrosion problems in heavy industrial usage operation. **Figure 1** shows the summary of what is this study all about.

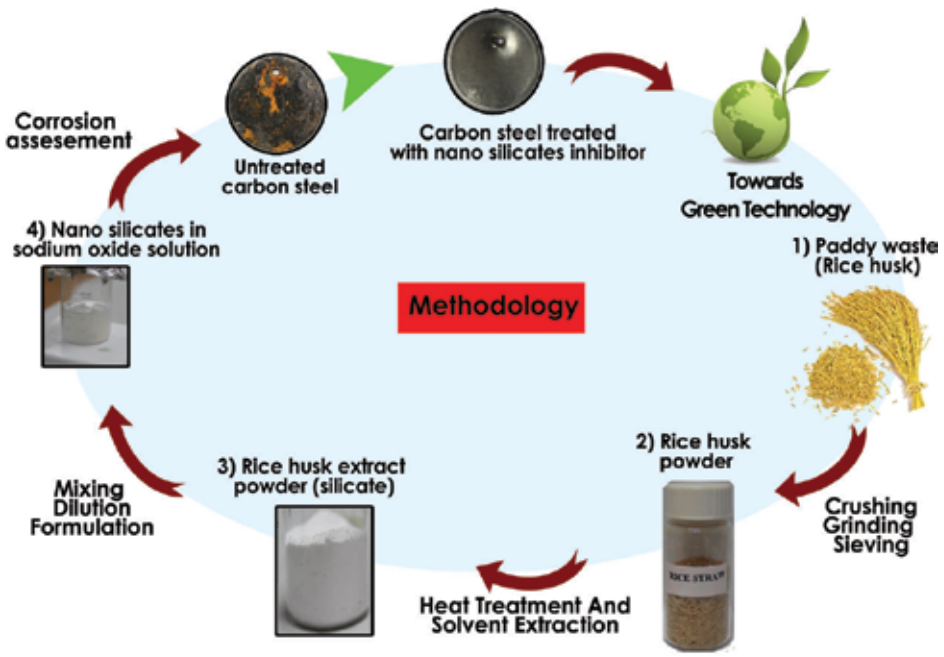

Figure 1. The development of nanosilicate from paddy waste as natural corrosion inhibitors.

As for the future prospect, the availability of abundant raw materials from natural sources can be the prime alternative to solve many industrial problems, i.e. corrosion. By utilizing the waste material and economic resources, such as the rice husk as corrosion inhibitor, the rice husk can produce efficient, harmless, and inexpensive nanosilica. Nanosilica can be extracted from rice husk ash (RHA) and formulated properly in order to act as corrosion inhibitor. Apart from that, the use of nanosilicate can be various and advance in the future. The three major objectives of this research work are the following:

i. To formulate corrosion inhibitor based on nanosilicate from the extract of rice (*O. sativa* L.) husk ash.

ii. To determine the inhibition efficiency of the corrosion inhibitor based on nanosilicate in 0.5 M NaCl.

iii. To determine the surface morphology and type of adsorption isotherm for nanosilicate-based corrosion inhibitor on the surface of carbon steel samples.

2. Materials and methods

Rice (*O. sativa* L.) husk used in this study was obtained from Kedah, Malaysia. The chemicals used in this process were sodium hydroxide (NaOH), sulfuric acid (H_2SO_4), and hydrochloric acid (HCl) from Sigma-Aldrich.

2.1. Preparation and extraction method of nanosilicate from paddy waste for corrosion inhibitor

The collected rice husks were cleaned with distilled water to remove dirt and unwanted material before being dried. The cleaned rice husks were grounded using a blender and filtered with a 500 micron filter. Then, rice husks (50 g) were burnt in a furnace at a temperature of 600°C for 6 h according to the past methods [12, 13].

After a complete combustion, rice husk turned into white-gray ash. Then, 10 g of the ash was dissolved in 2.5 M NaOH (80 ml) to extract out the silica compound. This process carries out at a temperature of 90°C on a heating plate while the mixture was stirred with a magnetic stirrer for 3 h before it was filtered with filter paper. Then, a bright homogeneous and viscous gel of silica was obtained. Reactions that occurred over the rice husk ash containing silica and sodium hydroxide solution are as follows:

$$SiO_{2(s)} + 2NaOH_{(l)} \rightarrow Na_2SiO_{3(l)} + H_2O_{(l)} \quad (1)$$

The next process was the process of neutralization whereby silica gel in alkaline condition was titrated with 2.5 M sulfuric acid until the pH reached to 2, before being stirred with a magnetic stirrer at a temperature of about 90°C. After 3 h of stirring, the agglomerated silica gel was rinsed with distilled water with a temperature of 60°C to remove the sulfuric acid, and the pH would become neutral at around 7.5–8. Lastly, the silica gel was dried in the oven at 70°C for 10 h to obtain a silica powder. This process can be determined using the following equation:

$$Na_2SiO_{3(gel)} + H_2SO_{4(l)} \rightarrow SiO_{2(s)} + H_2O_{(l)} \quad (2)$$

As for the preparation of nanosized silicate powder, reflux system method was followed. The apparatus used in this process is 250 ml round flask, condenser, and a magnetic stirrer system. Pure silica powder was filled in a round flask added with 80 ml of concentrated hydrochloric acid (6 M HCl). This process was carried out for 4 h at a temperature of 90°C. Then, the mixture was filtered using filter paper to obtain the silica gel. Later, 2.5 M NaOH (80 ml) is added in a vessel comprising the sample to dissolve silica and stirred for 10 h. Then the mixture was titrated with sulfuric acid (6 M H_2SO_4) to neutralize the pH of the solution to 7. The mixture was then precipitated, and the nanosilica was filtered with nano-filter paper. Once all the nanosized silica

is collected, it was dried in an oven for 48 h at a temperature of 50°C to obtain the nanosilicate powder. Then, as for preparing the nanosilicate powder for corrosion inhibitor, past method was followed in which the inhibition performance of nanosilicate is influenced by the molar ratio of SiO_2/Na_2O [14].

In this study, the best molar ratio of SiO_2/Na_2O has been determined as 3:1. Corrosion inhibitor based on nanosilicate with molar ratio (SiO_2/Na_2O) 3:1 was prepared by dissolving 6 g nanosilicate powder in a solution of 250 ml of 0.2 M NaOH. This solution was stirred with a magnetic stirrer until the solution appears clear and uniform. Equation was the reaction that occurs on nanosilicate powder and sodium hydroxide solution:

$$SiO_{2(s)} + 2NaOH_{(l)} \rightarrow Na_2SiO_{3(l)} + H_2O_{(l)} \tag{3}$$

2.2. Corrosion test

ASTM G1-03 standard was followed for preparing corrosion test of carbon steel coupon in disc shaped with a diameter of 1.5 cm. Steel used in this study is the SAE 1045 carbon steel which consists of compositions Fe-bal; C, 0.4%; Mn, 0.75%; P, 0.004; and S, 0.5% in weight percentages.

All the carbon steel coupon samples were grinded from 400 to 800 grit using SiC sand paper with running tap water and were polished to produce carbon steel surface that has the same surface roughness. As for weight loss test, the coupon was weighed and its diameter and thickness were measured before and after undergoing weight loss immersion test for 7 days in 25 ml in 0.6 M NaCl solution. After 7 days of immersion, the coupons were removed from the solution and cleaned with distilled water and washed chemically and physically to remove the corrosion product according to the method ASTM G1-03. Based on these data, it can be calculated the lose weight (mg) by the following equation:

$$\Delta B = B_{\text{before}} - B_{\text{after}} \tag{4}$$

where ΔB is the loss of weight (mg) for the coupon, B_{before} is the weight of the coupon prior to immersion (mg) and B_{after} is the weight of the coupons after immersion (mg). The weight loss of data can also be calculated by surface coverage (θ), using the following equation:

$$\theta = \frac{B_{\text{before}} - B_{\text{after}}}{B_{\text{after}}} \tag{5}$$

The percentage of inhibition efficiency (IE%) as well as through the equation, from Ref. [15]:

$$\text{IE}\% = \frac{B_{\text{before}} - B_{\text{after}}}{B_{\text{after}}} \times 100 \tag{6}$$

To calculate the rate of corrosion (mg/cm^2h), follow the following equation (Ref. [13]):

$$\text{CR} = \frac{\Delta B}{\text{LM}} \tag{7}$$

where CR is the corrosion rate (mg/cm^{2}h), ΔB is the weight loss of carbon steel (mg) after immersion, L is the surface area (cm^2) and M is the time (hours).

2.3. Electrochemical test

Potentiodynamic polarization analysis was carried out using the potentiostat K47 Gamry. Potentiostat composed of three-cell electrode which are reference electrode (saturated calomel) with liquid KCl, the working electrode (sample), and the auxiliary electrode (carbon rod). The study was conducted at the potential range between –0.25 and 0.25 V at a scan rate of 1.0 mVs^{-1}. The surface area of the carbon steel corrosion in contact with the medium is 1.0 cm^2. Each experiment was repeated up to three times the reading. The percentage of inhibition efficiency, IE%, is calculated using the following equation:

$$\mathrm{IE}\% = \frac{\mathrm{I_{corr(0)}} - \mathrm{I_{corr(i)}}}{\mathrm{I_{corr(0)}}} \tag{8}$$

where $I_{corr(0)}$ = corrosion current density without the addition of inhibitors (mA cm^2) and $I_{corr(i)}$ = corrosion current density with the addition of inhibitors (mA cm^2).

Impedance studies were carried out using the potentiostat/galvanostat model high frequency response analyzer (FRA Solartron-1260). The initial frequency range used is 1000 kHz–100 Hz frequency end with 10 mV amplitude balance condition. Data were analyzed using the software ZView. Percentage of corrosion inhibition efficiency (IE%) was calculated using the following equation:

$$\mathrm{IE}\% = \frac{\mathrm{R_{ct(i)}} - \mathrm{R_{ct(0)}}}{\mathrm{R_{ct(i)}}} \tag{9}$$

where $R_{ct(0)}$ is the charge transfer resistance without the presence of the inhibitor (Ω cm^2) and $R_{ct(i)}$ is the charge transfer resistance in the presence of inhibitors (Ω cm^2).

2.4. Characterization of nanosilicate from rice husk

Few characterization tests had been performed on the nanosilicate, which are Fourier Transform Infrared Spectroscopy (FTIR), X-ray diffraction (XRD) and TEM. As for FTIR, the equipment used was Perkin Elmer Spectrum GX model. As for XRD, X-ray tube was operated at 60 kV maximum voltage and maximum current of 60 mA. Detection range is from 3 to 80°C. Transmission electron microscopy (TEM) is performed using Phillips CM12 model. The data obtained are in the form of an image or a two-dimensional image of the sample form. The surface of carbon steel coupons that have reacted with corrosive medium and inhibitor solution through weight loss test was scanned through a scanning electron microscope (SEM) ZEISS branded 55VP Supra model. In addition, Energy-dispersive X-ray (EDX) of INCA PENTA FETX3 was also performed on the surface of carbon steel corrosion with corrosion inhibitor and without inhibitors. EDX is used to determine the elements that are present on the surface of carbon steel samples.

http://dx.doi.org/10.5772/67378

3. Results and discussion

3.1. Nanosilicate extraction analysis

About 100 g of rice husk combustion in the furnace at a temperature of 600°C for 6 h resulted in 14.22 g rice husk ash (14–22%). Previous studies [16] have found that the percentage of rice husk ash is 12–20%. X-ray diffraction (XRD) was conducted to determine the phase that has formed from rice husk ash. Later, an analysis of X-ray test fluorescent (XRF) was conducted to determine the elemental composition contained in the rice husk ash.

Rice husk ash was burnt in a furnace at three different temperatures of 600, 700, and 900°C, respectively, for 6 h with a heating rate of 5°C furnace/min. Then, the rice husk ash was analyzed using X-ray diffraction to determine the silica phases formed in husks at three different firing temperatures, which is either amorphous or the crystalline phase. The method is carried out following the studies that have been done by Othman et al. [2].

Figure 2 shows the results of XRD diffraction peak for rice husk ash at different temperatures. Peak formed between the ranges of 22°–25° 2θ is the peak, which confirms the presence of silica [16, 20]. At the sintering temperature of 600°C, the XRD diffraction peak shows peaks formed are broad and wide. A second peak at 700°C has formed a sharp peak, whereas the third is the peak combustion temperature of 900°C that has formed a very sharp peak in the range of 22–25° 2θ. Through the analysis of the results of the XRD, diffraction peak formed demonstrated the formation of an amorphous phase. While the pointed summit has represented the formation of crystalline phases.

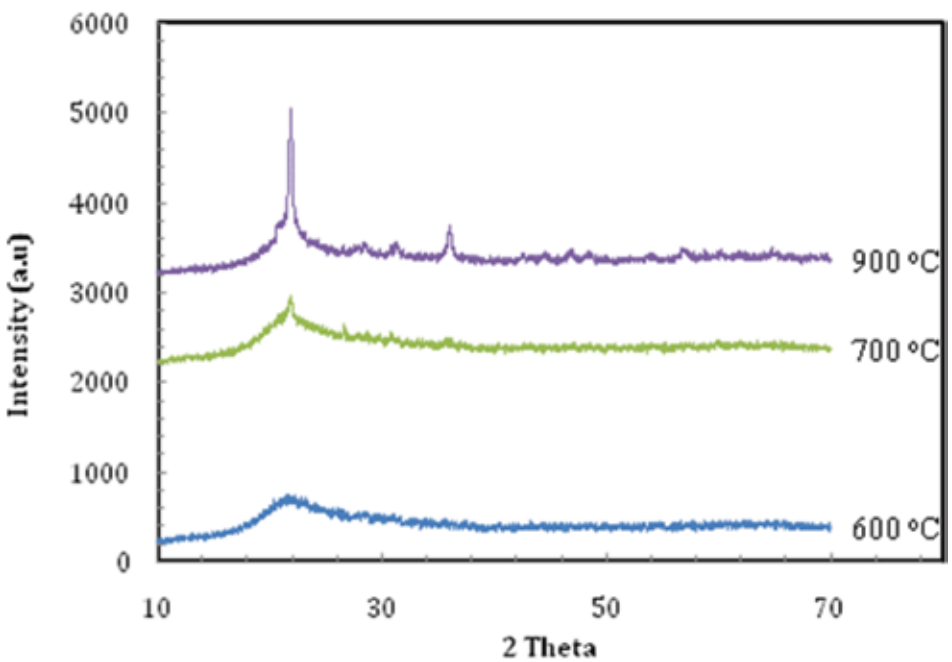

Figure 2. The results of XRD diffraction peak for rice husk ash at different temperatures.

According to previous studies, temperature and time during burning have affected the phases of the rice husk silica, in which combustion temperature below 700C formed an amorphous 3 phase, while temperatures above 700°C showed the formation of crystalline phase [19]. In this study, rice husk ash containing an amorphous phase has been selected as the main material for corrosion inhibitors. Silica particles with amorphous phases have some features that are suitable to act as corrosion inhibitors compared to crystalline phase, such attributes that helps in corrosion inhibition in amorphous silica are high surfaced area, small particle sizes, easily dissolved, irregular shapes, and high reactivity. Thus, the burning of rice husk at a temperature of 600°C is more suitable to be used to produce amorphous silica phases.

At a temperature of 700°C, rice husk ash was burnt, forming a semicrystalline phase and at a temperature of 900°C showed fully formed crystalline silica phases. Crystalline silica phases are unlikely suitable in this study, due to the insoluble crystalline phase [16]. Moreover, crystalline silica particles are harmful to human as it can caused silicosis, which is a respiratory disease caused by inhaling silica haze for long term as stated by the World Health Organization (WHO) in 1999.

The composition of the elements contained in rice husk ash was determined using X-ray instrumentation fluorescent (XRF) as shown in **Table 1**. The main element is oxygen (O) which is at 51.23% and silicon (Si) 42.44% (percentage by weight). In addition to the O and Si, there are also other elements, such as K, P, Mg, Ca, Fe, S, Na, Mn, Al, Zn, and Cl. These results show that rice husk ash contains the elements of O and Si, which represents the compounds of silica (SiO^2). Thus, rice husk ash has a high percentage of silica, which reached 93.67%. Some previous studies have also indicated that the elemental composition of the silica from rice husk ash up to 90% more [16].

Elements	Percentage (%)
Oxygen	51.23
Silica	42.4
Potassium	2.7
Phosphorous	1.0
Magnesium	0.6
Calcium	0.4
Iron	0.4
Sulfur	0.4
Sodium	0.18
Manganese	0.09
Aluminum	0.05

Table 1. The percentage breakdown of the elements contained in the rice husk ash.

Apart from that, the extraction nanosilicate from rice husk ash was analyzed using Infrared Spectroscopy (FTIR) to identify functional groups of the nanosilicate (SiO_2). Then particle size was determined using the transmission electron microscopy (TEM) and particle size instrumentation (Zetasizer) to determine the average size of the particles dispersed in solution.

http://dx.doi.org/10.5772/67378

Based on **Figure 3**, it shows that the spectrum produced two major peaks. A sharp peak and high intensity on adsorption band at 1055 cm^{-1} wave characterize the presence of siloxane groups of Si–O–Si asymmetric, whereas the peak at 791 cm^{-1} adsorption band characterizes the presence of Si–O–Si groups of symmetry at low intensity. The main peak shown in the spectrum is the peak that has been identified as a compound of silica (SiO_2) [13].

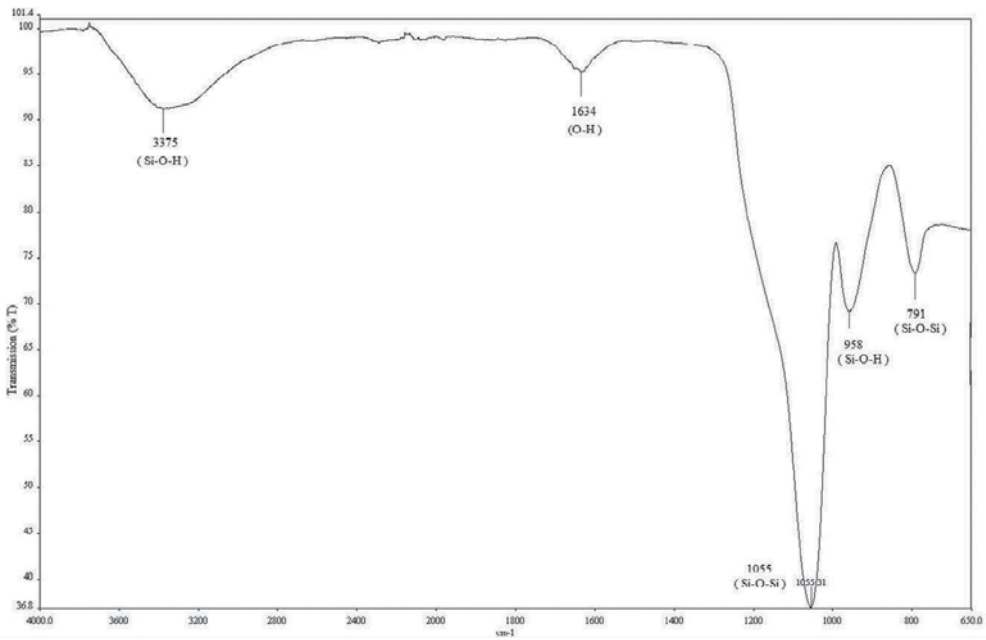

Figure 3. FTIR spectrums of nanosilicate powder.

Additionally, peaks of 3375 and 1634 cm^{-1} indicating the presence of silanol groups, which bind the 7 water group of (Si–O–H) due to the reaction between the silica with a solution of NaOH and 8 water during the extraction process silica from rice husk ash. The peak on the plane stretching vibration (plane) of 958 cm^{-1}, which further indicates silanol group [17].

Other than that, the analysis of transmission electron microscopy (TEM) was used to identify the particle size of the silicate from the rice husk ash extraction. The results of TEM analysis have found that the size of the particles is nanosized silica powder. **Figure 4** represents nanosilicate micrograms of powder extract from rice husk ash. Silica was observed clotted with nanoscale size of approximately 5–10 nm. The silica has a spherical shape similar to previous studies [17].

The concentration of NaOH solution has affected the particle size nanosilicate formed. In the past study, it has been reported that nanosilicate powder particle measurement is influenced by the concentration of NaOH as solvent extraction, i.e. 2.0, 2.5, and 3.0 M NaOH [17]. The results obtained are nanosized silica with different measurements for each concentration of NaOH. NaOH solution with a concentration of 2.5 M produced silica particles having a particle size smaller than the concentration of 2 and 3 M NaOH, which is 5–10 nm.

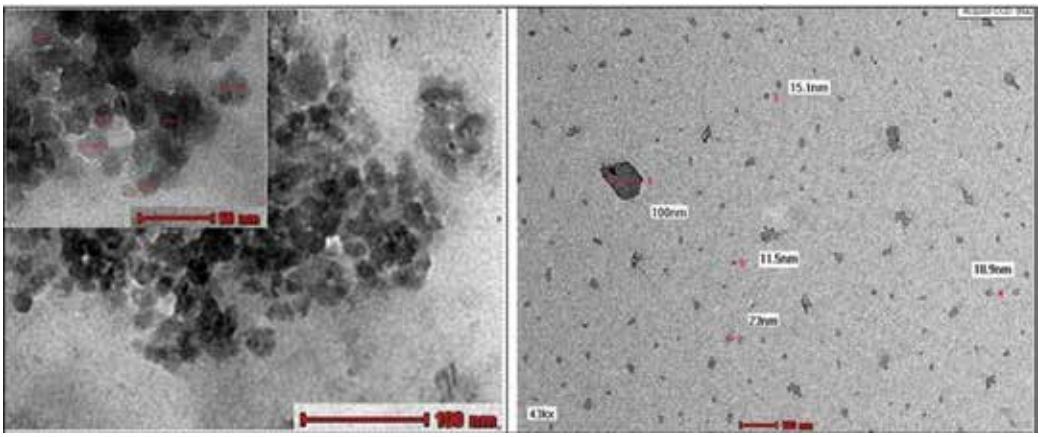

Figure 4. TEM image for nanosilicate powder from the extraction of rice husk and also TEM micrograph of nanosilicate corrosion inhibitor solution.

Figure 4 is a TEM micrograph of a solution of the formulated nanosilicate corrosion inhibitor. **Figure 4** has shown that the solution of the corrosion inhibitor has a fine particle sized of a nanosize between 10 and 100 nm. Characterization of particle size analysis was used to determine the average particle size of nanosilicate corrosion inhibitor. Results of the analysis states that there are three types of peaks indicate the average size of nanosilicate (**Figure 5**). It also shows the size distribution of the silica resulting from the analysis of zeta sizer. The average diameter size of the silica in the first peak is 1.1 nm, which has a share of 5.4%. Wide-sized silica that was featured by this peak was 0.14 nm, whereas the second peak that covers 17.2% indicates the presence of silica that has a diameter of 61.91 nm. The resulting width of silica of this peak is 8.2 nm. The third peak is the highest peak percentage and that is 77.4%.

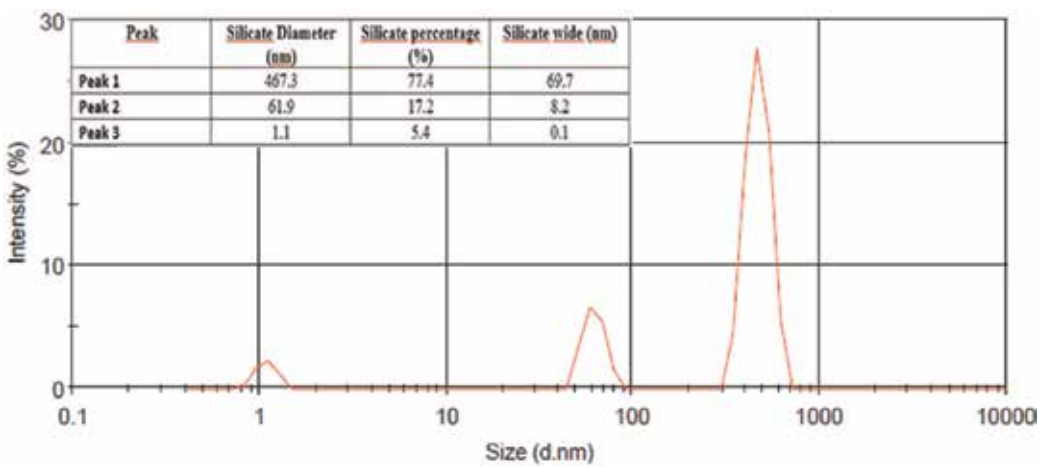

Figure 5. The graph zeta sizer analysis showed three types of particle size peak of nanosilicate.

Size diameter of silica is 467 nm with a width of 69.66 nm. Thus, from this discussion it concluded that the corrosion inhibitor solution of nanosilicate has a nanosized particle of silica.

3.2. Corrosion measurement analysis in 0.5 M NaCl as corrosive media

3.2.1. Inhibition effect through weight loss test

Table 2 shows the results of weight loss test after the addition of nanosilicate corrosion inhibitor in 0.5 M NaCl as corrosive media. The results of the weight loss for carbon steel samples without the presence of nanosilicate were recorded at the value of 4.3 mg. The effect of the inhibitor at concentration of 0.003 M nanosilicate has reduced the weight loss to 3.4 mg. The higher the addition of nanosilicate concentration, which is at 0.008, 0.016, and 0.03 M, the lower the weight loss of carbon steel. Based on these results, it has been found that the weight loss of carbon steel sample is proportional to the increase in the concentration of nanosilicate corrosion inhibitor.

Inhibitor concentration (M)	Weight loss (mg)	Corrosion rate (mg/cm^{2}h)	Inhibition efficiencies (IE%)
0	4.3	0.556	0
0.003	3.4	0.440	20.9
0.008	1.4	0.181	67.4
0.016	1.0	0.129	76.7
0.030	0.5	0.065	88.4

Table 2. Weight loss, inhibition efficiencies %, and the corrosion rate of carbon steel in 0.5 M NaCl aqueous media without and with the presence of rice husk ash nanosilicate.

Table 2 also shows the corrosion rate of carbon steel and IE% in the presence of nanosilicate corrosion inhibitors. **Table 2** shows that the corrosion rate decreased after the addition of the nanosilicate corrosion inhibitor in NaCl media. According to the study of the past discussions which stated that the corrosion rate decreases with increasing concentrations of inhibitors, it has shown that the number of molecule inhibitors can reduce the corrosion reaction of carbon steel [18].

Not to mention, nanosilicate corrosion inhibitor also affects the IE% outcome of carbon steel sample. The highest efficiency percentage was demonstrated by the addition of 0.03 M nanosilicate at an efficiency up to 88.4%. The IE% continues to increase with increasing concentration of inhibitor [19]. This is due to the adsorption of nanosilicate corrosion inhibitor's molecules that managed to cover the surface of carbon steel [20], in which it makes a separation between the surface of carbon steel samples and the corrosive media. Apart from that, previous study has stated that the presence of cations Na^+ and Cl^- ion also has encouraged the inhibition process for carbon steel samples [21].

Equation (10) until Eq. (14) is a reaction between carbon steel (Fe^{2+}) with NaCl as corrosive medium containing decomposing chloride ions. Then, the ions reacted with Fe^{2+} to produce $FeCl_2$:

$$NaCl \rightarrow Na^{+} + Cl \tag{10}$$

$$Fe^{2+} + Cl^{-} \rightarrow FeCl_2 \tag{11}$$

$$Fe \rightarrow Fe^{2+} + 2e\,(\text{release of electrons}) \tag{12}$$

$$Fe^{2+} + 2e \rightarrow Fe\,(\text{accepts electrons}) \tag{13}$$

$$NaSiO_3 \rightarrow Na^{+} + SiO_3{}^{-}\,(\text{nanosilicate}) \tag{14}$$

$$Fe^{2+} + SiO_3{}^{-} \rightarrow (FeSiO_3)_2\,(\text{a complex thin layer compound}) \tag{15}$$

The presence of nanosilicate inhibitor molecules that have functional groups of SiO^{2-} plays an important role as inhibition agents. The reaction between Fe^{2+} with nanosilicate inhibitors has produced a complex compound which forms a thin layer (Eqs. (5) and (6)). In aqueous solution, the functional groups of nanosilicate SiO^{2-} will donate a pair of electrons on the surface of carbon steel whenever Fe^{2+} ions were released into the electrolyte solution. Furthermore, the inhibitor functional group, which is SiO^{2-}, is empty d-orbitals, which can form a thin layer and increase the adsorption and protection on the steel surface.

The thin layer on the surface of carbon steel that was formed is a compound that has high stability compared to Fe only [22]. Moreover, the carbon steel that has been added with nanosilicate corrosion inhibitors has more resistant toward corrosion as the nanosize of the silicate also contributes to the inhibition efficiency. Advantages of nanosilicate inhibitor is shown by the ability of nanosize silicate molecules that have a high surface area that can protect almost all of the active sites on the surface of carbon [12, 13]. Furthermore, the nanosize particle of nanosilicate forms a protective layer with good adhesion on the surface of carbon steel [23].

3.2.2. Potentiodynamic polarization analysis

Figure 6 shows the polarization curves for carbon steel in 0.5 M NaCl media with and without the presence of nanosilicate corrosion inhibitors. The E_{corr} values after the addition of nanosilicate shifted toward more positive for all concentrations than the sample without corrosion inhibitor solution. The apparent shift provides information that nanosilicate from rice husk ash is probably a mix type class of inhibitors. The decline in the value of the current density (I_{corr}) can be observed on the cathodic and anodic reaction after nanosilicate with various concentrations of inhibitor is added to 0.5 M NaCl. This proves that the addition of nanosilicate is able to inhibit both the anodic and cathodic reactions. I_{corr} devaluation that occurred in the anodic and cathodic reactions indicates the presence of molecular nanosilicate preventing current flow carried by ions in the electrolyte solution of NaCl. In the cathodic reaction, nanosilicate molecules adsorbed on the surface of carbon steel in turn can inhibit and prevent the cathodic reaction (decrease). Nanosilicate molecules that are present in a negative charge ($SiO_3{}^{2-}$) are engaged in the solution, which creates competition between the anion chloride (Cl^{-}) to approach the interface steel and bulk solution and then generates resistance to corrosion.

http://dx.doi.org/10.5772/67378

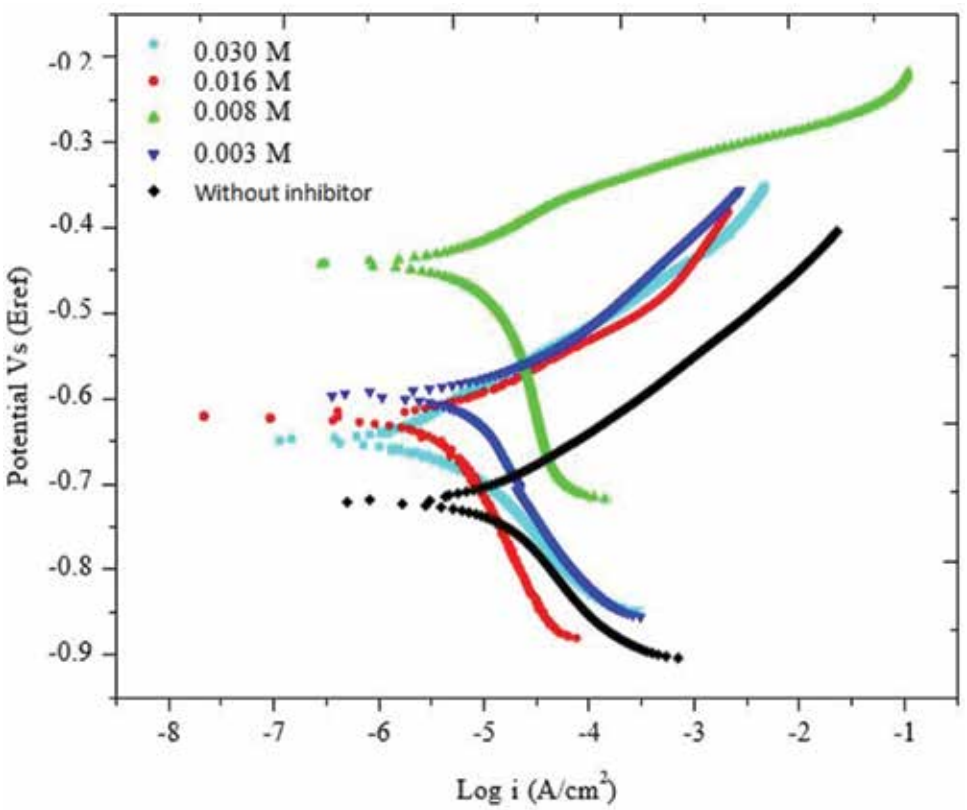

Figure 6. Polarization curves for carbon steel with various concentrations of nanosilicate inhibitor in 0.5 M NaCl as corrosive media.

Based on polarization curves and the data obtained, the inhibition behavior of nanosilicate inhibitor by potentiodynamic polarization test is in term with the results from weight loss analysis. Lower I_{corr} value of polarization curves shows an increase in the IE% for all concentrations of nanosilicate inhibitor, in which higher concentration of nanosilicate inhibitor causes the corrosion rate to decrease, which is from 0.174 to 0.026 millimeters per year (mmpy). These results indicate that nanosilicate molecules have been adsorbed on the surface of the carbon steel and reduced corrosion attack in NaCl medium.

Table 3 explains the changes in the apparent shift of E_{corr} for carbon steel samples with the presence and absence of nanosilicate inhibitor. Corrosion rate of corrosion inhibitors can be identified based on the maximum shift of E_{corr}. When the maximum displacement of E_{corr} value is <85 mV, then the inhibitor showed a mixed type inhibitor. Meanwhile, if the maximum value is $E_{corr} > 85$ mV, it can be classified as cathodic or anodic type of inhibitor. The results of the analysis showed that the nanosilicate inhibitor provides maximum displacement value of E_{corr} which is >85 mV. Thus, nanosilicate inhibitor for carbon steel in NaCl media can be categorized as cathodic or anodic type corrosion inhibitor.

The corrosion potential (E_{corr}) of carbon steel that has been treated with inhibitors has shifted toward more positive values than those untreated with inhibitor. Therefore, the corrosion potential of the reaction shows that the inhibition process is a mix type corrosion inhibitor but more prominently toward anodic type of inhibitor [19]. This is due to the inhibitor molecules that have been adsorbed on the steel surface to form a thin layer, which can prevent corrosion attacks of Cl ions. This is most likely due to the absorption and the formation of a protective film that has been formed between molecule inhibitors of nanosilicate and Fe atoms of carbon steel.

The results in **Table 3** show that the nanosilicate inhibitor has an average value of polarization resistance (R_p), which is more than 20 kΩ. Concentration of nanosilicate inhibitor of 0.030 M has the highest R_p value, which means it has lowest corrosion rate. Since higher R_p value decreases the corrosion rate, it causes IE% to be higher as well.

Concentration (M)	E_{corr} (mV)	I_{corr} (A/cm^2)	B_c (mV/Dec)	B_a (mV/Dec)	R_p (kΩcm^2)	Kadar Kakisan (mmpy)	IE (%)
0	−719.0	1.49×10^{-5}	154.1	95.1	1.714	0.174	0
0.003	−594.8	1.05×10^{-5}	269.2	93.7	2.868	0.123	29.5
0.008	−440.4	0.39×10^{-5}	204.3	53.4	4.697	0.046	73.8
0.016	−620.7	0.41×10^{-5}	241.3	81.2	6.426	0.048	72.5
0.030	−647.9	0.22×10^{-5}	102.4	84.3	8.953	0.026	85.2

Table 3. Results from potentiodynamic polarization analysis of carbon steel with various concentrations of nanosilicate inhibitor in NaCl 0.5 M.

3.2.3. Electrochemical impedance spectroscopy analysis

Figure 7 is a suppress semicircle graph of Nyquist plot showing the carbon steel that has been treated with and without nanosilicate inhibitor at concentrations of 0.003, 0.008, 0.016, and 0.03 M. According to the plot, the size of the overlapping semicircle of carbon steel increased with the development in silicate inhibitor concentration which causes an increase in the corrosion resistance of carbon steel [24]. Besides that, nanosilicate inhibitor that has been added at different concentrations has changed the corrosion mechanism of carbon steel in NaCl media [25].

From the impedance analysis (**Figures 7** and **8**), the IE% of 0.0016 M concentration has reached up to 21.65% only. Furthermore, past studies [26] state that for some situations, corrosion inhibitor effectiveness sometimes gives the declining or negative and inefficient result due to the concentration of the inhibitor, which is probably too low or too high during the impedance test.

In addition, the charge transfer resistance (R_{ct}) has been seen higher after the addition of nanosilicate inhibitor compared with the absence of inhibitor. This matter shows that there has been molecular adsorption of nanosilicate molecule on the surface of carbon steel that forms a protective layer. Without the presence of nanosilicate inhibitors, R_{ct} value is at 0.496 kΩcm^2. While after the addition of nanosilicate at concentration of 0.003, 0.008, 0.016,

http://dx.doi.org/10.5772/67378

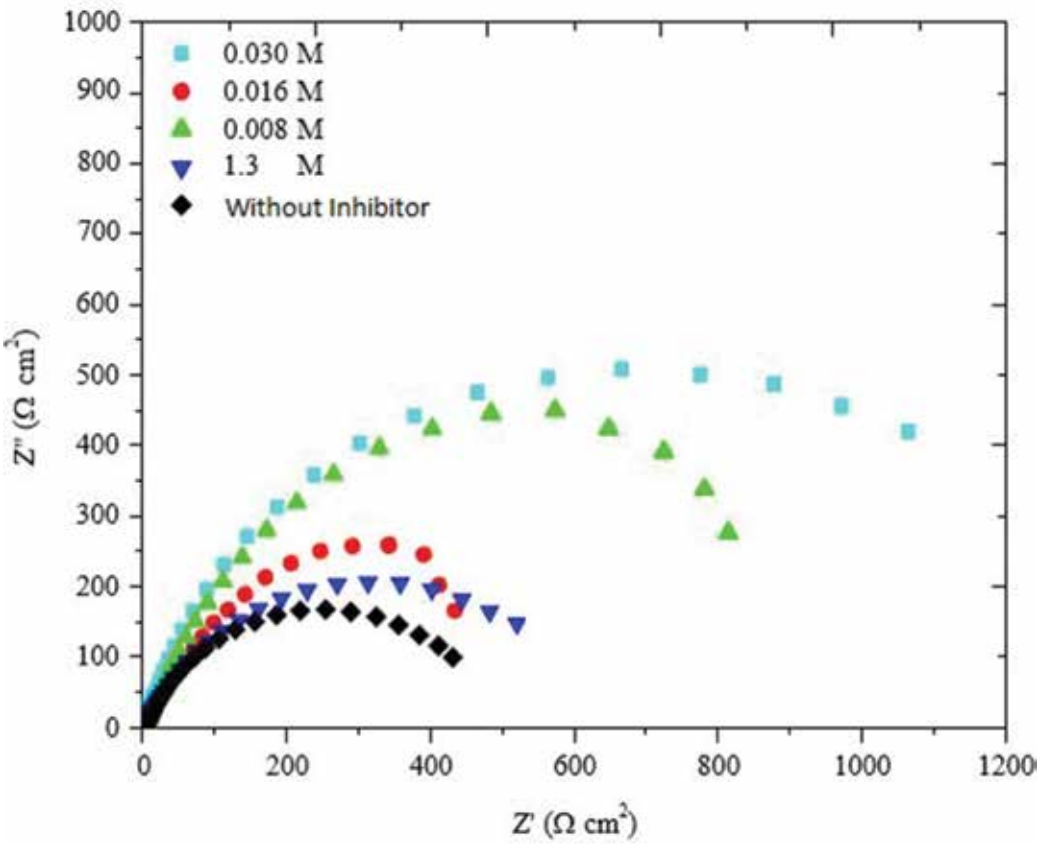

Figure 7. Nyquist plot for carbon steel with various concentrations of nanosilicate in 0.5 M NaCl.

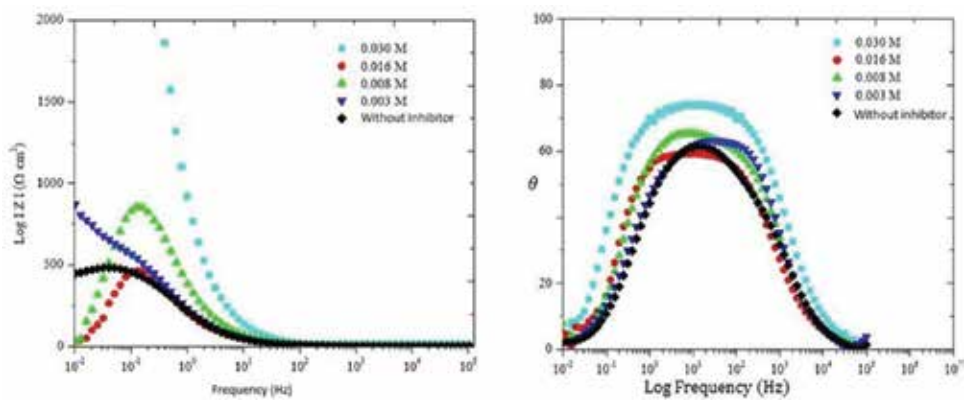

Figure 8. Bode plot for carbon steel with various concentrations of nanosilicate in 0.5 M NaCl.

and 0.03 M, it gave each values of R_{ct} at 0.630, 1.146, 0.634, and 5.426 cm^2 kΩ. Based on these results, it shows that with the addition of nanosilicate inhibitors, the values of IE% and R_{ct} have increased. The highest values of IE% and R_{ct} given are at the concentration of 0.03 M. Thus, it can be stated that the adsorption of molecules on the surface of carbon steel nanosilicate occurs well at a concentration of 0.03 M.

According to **Figure 8**, the overlapping semi-circular suppress can be seen at high frequencies, while the curve of induction is at low frequencies. There is only one time constant that was shown in the Bode plot of carbon steel in 0.5 M NaCl media at various concentrations of nanosilicate. **Figure 8** shows that the phase angle shifted to a higher value when the nanosilicate inhibitor reacts with various concentrations when added to the NaCl medium. This is due to the undergoing process of adsorption molecules on the surface of the metal [27]. Generally, the phase angle shift occurs with increasing concentrations of inhibitors that can further increase the inhibition efficiency percentage.

Moreover, the minimum phase angle is seen at low frequencies with values approaching to 80°. The highest phase shift angle approaching 90° explains good inhibition properties [28]. Other than that, Log Z value increased with the increasing of nanosilicate inhibitor concentration except at a concentration of 0.016 M. The maximum Z value was recorded at concentrations of 0.03 M. The curve of the graph was plotted horizontally at high frequencies for each nanosilicate concentration. According to past studies, it has stated that the formation of the oxide layer occurs at low frequencies, while the adsorption of molecules occurs at a high frequency of mid region with the gradient value of −1 which represents the capacitance value [28].

3.2.4. Surface morphology analysis

Morphology analysis of the carbon steel surface through light microscope with the presence and absence of nanosilicate in the 0.5 M NaCl medium was conducted. Preferred concentrations are 0.03 M. **Figure 9(a)** shows pitting corrosion that happens on the sample surface, while in **Figure 9(b)** there is no indication of pitting corrosion on the carbon steel surface that has been immersed in 0.5 M NaCl with 27 nanosilicate corrosion inhibitors. On the inhibitor-treated carbon steel, it was found to have less pitting corrosion. The surface appears to have more even surface than the surface of untreated carbon steel. These results correspond with the results of the weight loss test, potentiodynamic polarization and impedance. The percentage of inhibition efficiency (IE%) for carbon steel in 0.5 M NaCl medium only reached at 86% in 0.03 M nanosilicate inhibitor.

Based on **Figure 9(c)**, the images show that the surface of carbon steel without corrosion inhibitors appeared to be rough and porous. This is in accordance with a statement by Na and Pyun [29] that corrosion pits occur in a nearly neutral medium and in the presence of Cl^- ion, whereas **Figure 9(d)** shows the carbon steel surface that has been treated with nanosilicate inhibitor, and it shows less pitting compared to **Figure 9(c)**. Thus, it is proven that the nanosilicate inhibitor has the potential as corrosion inhibitor for carbon steel in 0.5 M NaCl medium.

Figure 9(c) and **(d)** also represents the EDX analysis (to provide elemental identification and quantitative compositional information) on carbon steel surfaces that have been immersed in the 0.5 M NaCl medium with the presence and absence of nanosilicate inhibitor. The main

http://dx.doi.org/10.5772/67378

compositions on the surface of carbon steel that has been immersed in 0.5 M NaCl without being treated with nanosilicate inhibitor are Fe (91.34%), O (8.39%), and Cl (0.27%) (**Figure 9 (c)**). However, in **Figure 9(d)**, there are no chloride and oxygen detected. It shows that the corrosion has been retarded by nanosilicate inhibitor.

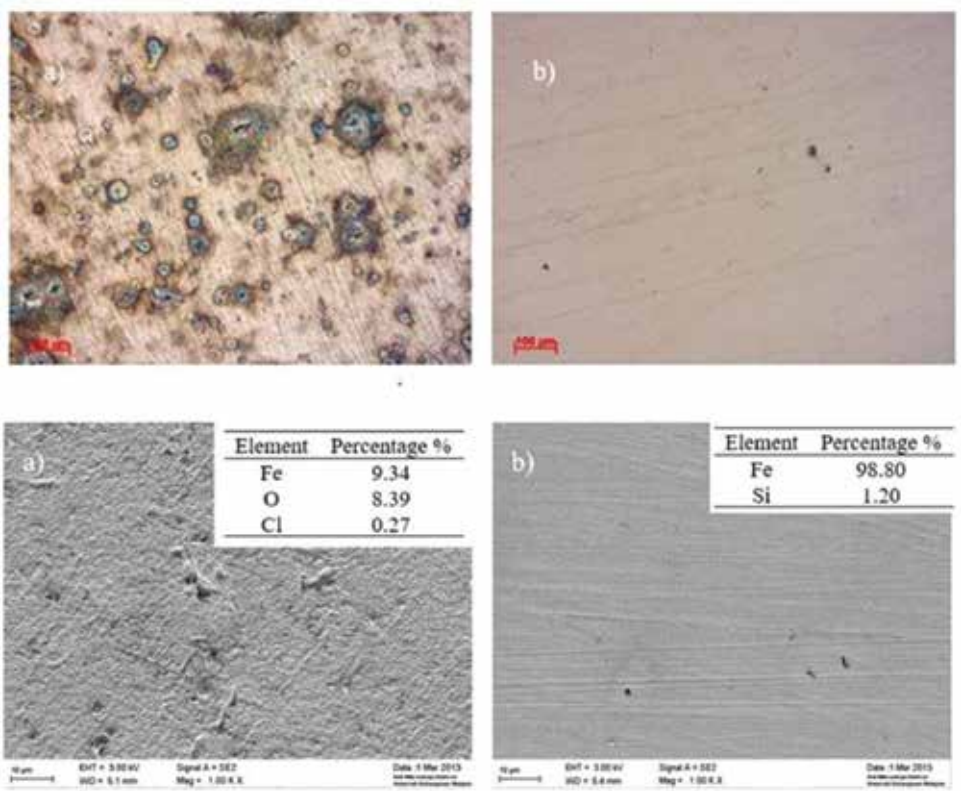

Figure 9. Light microscope and SEM image of carbon steel that has been treated in 0.5 M NaCl (a) without the presence of nanosilicate inhibitors, (b) in the presence of nanosilicate inhibitors and energy dispersive X-ray (EDX) analysis of immersed carbon steel (c) without the presence of nanosilicate inhibitors (d) in the presence of nanosilicate inhibitors.

3.2.5. Adsorption isotherm analysis

The relationship between corrosion inhibitor molecules and carbon steel surface can be explained by adsorption isotherms. To identify adsorption processes occurring in the study, the degree of surface coverage (θ) for each nanosilicate concentration inhibitor at different temperature of 40, 50, and 60°C (313, 323, and 333 K) was calculated. Data from the weight loss analysis of 0.5 NaCl medium were considered to explain the mechanism of adsorption by the adsorption isotherm plot [2]. Generally, the adsorption isotherm reported for the study of corrosion inhibitor is agreement to Langmuir isotherm. However, the type involved isotherm is dependent on many factors such as the type of inhibitor, the concentration of the inhibitor, corrosion medium use, temperature and methods of measurement carried out. Hence, the plot of the Langmuir, Freundlich, and Temkin isotherm is used as a comparison in this study.

In the Langmuir adsorption isotherm equation, Temkin, and Freundlich, respectively, exhibited linear graph with the regression line. The thermodynamic data for the Langmuir, Freundlich, and Temkin isotherm, respectively, are shown in **Table 4**. The results are obtained by comparing the regression (R^2) of the respective adsorption isotherms; it was found that the corresponding plot and regression value are close to 1 which is the Temkin isotherm. In the 0.5 M NaCl medium, the regression at 40°C, 50°C, and 60°C is close to 1, i.e. 0.9989, 0.9950, and 0.9535. This indicates that the temperature is suitable for the adsorption of nanosilicate on carbon steel through Temkin isotherm model [30].

Adsorption isotherm	Temperature (°C)	R^2
Langmuir	40	0.7686
	50	0.9910
	60	0.9389
Freundlich	40	0.9295
	50	0.9753
	60	0.8815
Temkin	40	0.9989
	50	0.9950
	60	0.9535

Table 4. Plots of Langmuir, Freundlich and Temkin adsorption isotherm for nanosilicate inhibitor in NaCl medium at 40, 50, and 60°C.

The results of thermodynamics for nanosilicate adsorption on the surface of carbon steel have produced a negative value for ΔG^{o}_{ads}. This shows that adsorption process has occurred spontaneously [31]. Huge value of K_{ads} characterizes the stability and strength of the interaction of the inhibitor molecules that has been adsorbed on the surface of metal/steel. Results of Temkin isotherm plots indicate the adsorption of nanosilicate molecule inhibitors occurred physically as R^2 regression is approaching to 1. It is clearly shown that the Temkin adsorption isotherm is suitable for nanosilicate corrosion inhibitors on the surface of carbon steel in 0.5 M NaCl medium.

Generally, if the ΔG^{o}_{ads} is about -20 kJ mol^{-1} or lower, it indicates the interaction between the electrostatic interactions of charged molecules and charged metal surface (**Table 5**). This condition is also called physical adsorption. Meanwhile if the ΔG^{o}_{ads} is -40 kJ mol^{-1} or more negative than -40 kJ mol^{-1}, it shows that the charge of the molecule inhibitors is moved to the metal surface to form a coordination bond called chemical adsorption [32]. In this study, the ΔG^{o}_{ads} is obtained between the range of -27 and -30 kJ/mol^{-1}. Therefore, it can be seen that the mechanism for nanosilicate adsorption on the surface of carbon steel is applicable for mixed adsorption (physical and chemical) [15]. Through physical adsorption, inhibition occurs as in electrostatic attraction between the charged molecules of nanosilicate inhibitors and carbon steel surface. Meanwhile, the chemical adsorption of charged nanosilicate inhibitor molecules and the surface of carbon steel molecules can cause better absorption by forming chemical bonds.

Corrosion media	Temperature (°C)	R^2	Ka_{ds} (M^{-1})	ΔGo_{ads} ($kJmol^{-1}$)
0.5 M NaCl	40	0.9989	520.06	−27
	50	0.9950	588.90	−28
	60	0.9535	795.33	−30

Table 5. Thermodynamic results through Temkin isotherm plots for the adsorption of the nanosilicate inhibitor on the surface of carbon steel.

4. Conclusions

Nanosilicate corrosion inhibitors from the rice husk ash have good inhibition properties to reduce the corrosion rate of carbon steel in 0.5 M NaCl. The effectiveness of amorphous nanosilicate corrosion inhibitor with nanosized SiO_2 functional groups with particle sized of 10–100 nm, as corrosion inhibitor, was proven through the weight loss test and electrochemical measurement test. The maximum IE% value reached up to 88.4% in 0.5 M NaCl media. This inhibitor can be classified into a mixed type of corrosion inhibitors. The presence of the protective layer has been contributing to the corrosion resistance reaction on the surface of carbon steel. Through morphology and microstructure analysis on the carbon steel samples, less corroded surface was seen on the samples treated with nanosilicate inhibitor. The adsorption isotherm tests showed that the nanosilicate inhibitor possess Temkin adsorption isotherm and ΔG^{o}_{ads} value obtained between the ranges of −27 and −30 kJ/mol^{-1}. The applications of silica derived from rice husk as corrosion inhibitor have proven its ability to retard corrosion in sodium chloride media. However the usage of rice husk plant waste would not stop on the extracts of nanosilicate only. Apart from nanosilicate, there were other compounds in the rice husk such as lignin and cellulose that would be a major interest for researchers in the future. As research trends nowadays that are more prone toward greener and environmental friendly approach, the waste of rice husk would be the best candidate for source of natural-based products with vast applications in advance.

Author details

Norinsan Kamil Othman*, Denni Asra Awizar and Zulhusni Dasuki

*Address all correspondence to: insan@ukm.edu.my

School of Applied Physics, Faculty of Science and Technology, Universiti Kebangsaan Malaysia (The National University of Malaysia), Bangi Selangor, Malaysia

References

[1] Zhang B.: Synergistic corrosion inhibition of environment-friendly inhibitors on the corrosion of carbon steel in soft water. Corrosion Science. 2015;**94**:6–20.

[2] Othman N.K., S. Yahya and D.A. Awizar: Anticorrosive properties of nanosilicate from paddy husk in salt medium. Sains Malaysiana. 2016;**45**(8):1253–1258.

[3] Sin H.L.Y.: Aquilaria malaccensis as a green corrosion inhibitor for mild steel in HCl solution. International Journal of Electrochemical Science. 2016;**11**(9):7562–7575.

[4] Soltani N., N. Tavakkoli and M. Ghasemi: Corrosion inhibition of low carbon steel by strychnos nux-vomica extract as green corrosion inhibitor in hydrochloric acid solution. International Journal of Electrochemical Science. 2016;**11**(10):8827–8847.

[5] Hamdy A.S.: Corrosion protection of aluminum composites by silicate/cerate conversion coating. Surface and Coatings Technology. 2006;**200**(12):3786–3792.

[6] Kannan C.S.: Investigation on forced vibration response of micro rubber/nanosilica added carbon composite beams for structural applications. 7th International Conference on Mechanical and Aerospace Engineering (ICMAE). 2016.

[7] Supit S.W.M. and F.U.A. Shaikh: Durability properties of high volume fly ash concrete containing nano-silica. Materials and Structures. 2015;**48**(8):2431–2445.

[8] Wang Y.: Mesoporous silica nanoparticles in drug delivery and biomedical applications. Nanomedicine: Nanotechnology, Biology and Medicine. 2015;**11**(2):313–327.

[9] Mohamad N., A. Jalar and Othman N. K.: Surface morphology study on aluminum alloy after treated with silicate-based corrosion inhibitor from paddy residue. Sains Malaysiana. 2014;**43**(6):935–940.

[10] Shchukin D.G.: Active anticorrosion coatings with halloysite nanocontainers. The Journal of Physical Chemistry C. 2008;**112**(4):958–964.

[11] Lin B., J. Lu and G. Kong: Synergistic corrosion protection for galvanized steel by phosphating and sodium silicate post-sealing. Surface and Coatings Technology. 2008;**202**(9):1831–1838.

[12] Awizar D.A.: The performance of nanosilicate from rice husk ash as green corrosion inhibitor for carbon steel in 0.5 M HCl. Materials Science Forum. 2013. Trans Tech Publ.

[13] Awizar D.A.: Nanosilicate extraction from rice husk ash as green corrosion inhibitor. International Journal of Electrochemical Science. 2013;**8**(2):1759–1769.

[14] Yuan M., J. Lu and G. Kong: Effect of SiO_2: Na_2O molar ratio of sodium silicate on the corrosion resistance of silicate conversion coatings. Surface and Coatings Technology. 2010;**204**(8):1229–1235.

[15] Desimone M., G. Gordillo and S. Simison: The effect of temperature and concentration on the corrosion inhibition mechanism of an amphiphilic amido-amine in CO_2 saturated solution. Corrosion Science. 2011;**53**(12):4033–4043.

[16] Umeda J. and K. Kondoh: Process optimization to prepare high-purity amorphous silica from rice husks via citric acid leaching treatment. Transactions of JWRI. 2008;**37**(1):13–17.

[17] Thuadaij N. and A. Nuntiya: Preparation of nanosilica powder from rice husk ash by precipitation method. Chiang Mai Journal of Science. 2008;**35**(1):206–211.

[18] Al-Sabagh A.: Quaternary ammonium salts from hydrolyzed fatty oil based on novel tertiary amines used as corrosion inhibitors for pipelines carbon steel at acid job in petroleum industry. Journal of Dispersion Science and Technology. 2012;**33**(9):1307–1320.

[19] Li W.: Some new triazole derivatives as inhibitors for mild steel corrosion in acidic medium. Journal of Applied Electrochemistry. 2008;**38**(3):289–295.

[20] Kumar D. and N. Sharma: Study of compressive strength of concrete using nanosilica. Journal of Ceramics and Concrete Sciences. 2016;**10**(17); 38536–38542.

[21] Belkhaouda M.: Inedible avocado extract: an efficient inhibitor of carbon steel corrosion in hydrochloric acid. International Journal of Electrochemical Science. 2013;**8**:10987.

[22] Haryono G.: Ekstrak Bahan Alam sebagai inhibitor Korosi. Prosiding Seminar Nasional Teknik Kimia. 2010; D09; 1–6.

[23] Saji V.S. and J. Thomas: Nanomaterials for corrosion control. Current Science. 2007;**92** (1):51–55.

[24] Solmaz R.: Investigation of corrosion inhibition mechanism and stability of vitamin B1 on mild steel in 0.5 M HCl solution. Corrosion Science. 2014;**81**:75–84.

[25] Aljourani J., K. Raeissi and M. Golozar: Benzimidazole and its derivatives as corrosion inhibitors for mild steel in 1 M HCl solution. Corrosion Science. 2009;**51**(8):1836–1843.

[26] Bard A.J., M. Stratmann and E.J. Calvo: Encyclopedia of electrochemistry, interfacial kinetics and mass transport. 2003; **2**; 10–25.

[27] Khaled K. and M.A. Amin: Dry and wet lab studies for some benzotriazole derivatives as possible corrosion inhibitors for copper in 1.0 M HNO_3. Corrosion Science. 2009:**51** (9):2098–2106.

[28] Özcan, M.: Adsorption properties of barbiturates as green corrosion inhibitors on mild steel in phosphoric acid. Colloids and Surfaces A. Physicochemical and Engineering Aspects. 2008;**325**(1):57–63.

[29] Na K. and S.-I. Pyun: Effects of sulphate, nitrate and phosphate on pit initiation of pure aluminium in HCl-based solution. Corrosion Science. 2007;**49**(6):2663–2675.

[30] Umoren S.A. and U.M. Eduok: Application of carbohydrate polymers as corrosion inhibitors for metal substrates in different media: a review. Carbohydrate Polymers. 2016;**140**:314–341.

[31] Umoren S.: Effect of halide ions on the corrosion inhibition of aluminium in alkaline medium using polyvinyl alcohol. Journal of Applied Polymer Science. 2007;**103**(5):2810–2816.

[32] Hegazy M.: A novel Schiff base-based cationic gemini surfactants: synthesis and effect on corrosion inhibition of carbon steel in hydrochloric acid solution. Corrosion Science. 2009;**51**(11):2610–2618.

Chapter 5

Silica from Rice as New Drug Delivery Systems

Salazar-Hernández Carmen,
Salazar-Hernández Mercedes, Lona-Ramos Rocío,
Elorza-Rodríguez Enrique and
Rocha-Ramírez Agustín Hilario

Additional information is available at the end of the chapter

http://dx.doi.org/10.5772/66723

Abstract

The pharmaceutical industry has seen an increased need of carriers or excipients design that allows the controlled release of a drug in the human body. The main role of an excipient is to carry the drug for its administration under therapeutic index. Among the new generation of excipients, the ordered mesoporous silica (MS) presents several advantages, such as excellent biocompatibility, good adsorption capacity, and precise control in the drug delivery. However, the high cost of synthesis of mesoporous silica restricts its use to industrial applications; therefore, a low-cost procedure is necessary for widespread use. Biogenic silica from rice husk (SiO_2-rice) could be a new choice as a drug delivery system. This silica is obtained from an acid leaching of rice husk followed by calcinations processes at low temperatures; these conditions produce silica with good adsorption properties, similar to those of MS. In consequence, the excipient behavior of SiO_2-rice was assessed using folic acid as the model drug, displaying an 18.5% of absorption in the SiO_2-rice pores, while MS absorbed around 19%. The drug release profiles were similar for both the silicas, suggesting that SiO_2-rice could be a low-cost, similar yield excipient for drugs similar to folic acid.

Keywords: mesoporous silica, SiO_2-rice, drug delivery systems, adsorption capacity

1. Introduction

Tablets are solid dose containing an active substance or drug and an excipient. The purpose of the excipient is to provide the optimal concentration of the drug, as well as chemical, physical, and biological stability. **Figure 1a** illustrates the function of excipient in a tablet, which is to catch the drug and allow its release. However, according to **Figure 1b**, the excipient shows an uncontrolled fragmentation causing the release of the drug at differ-

ent speeds (J_1 and J_2), and even part of the drug remains trapped in the tablet, causing the decrease of drug bioavailability [1–3].

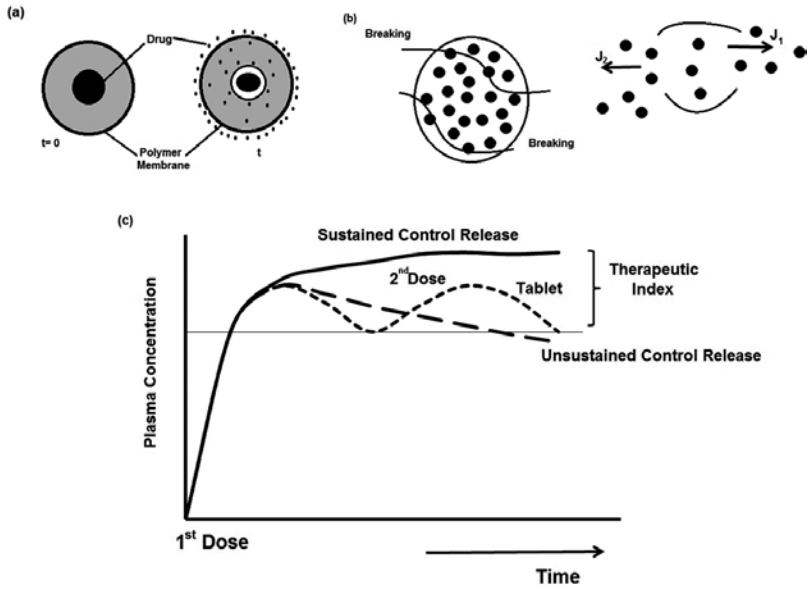

Figure 1. (a) Excipient function. (b) Fragmentation excipient. (c) Release profiles for pharmaceutical formulation.

Figure 1c shows the release profile of a tablet. A tablet rapidly releasing the drug and reaching its maximum concentration in short time subsequently loses its biological activity making necessary a second or third dosage to maintain biological activity. However, there are sustained release systems, which release initially the maximum drug concentration and continue to release this amount for sustained periods of time. Commonly, this substances are polymers and hydrogels. **Figure 2** shows the three main mechanisms of drug release through a polymeric matrix [2, 3]:

1. In diffusion from the polymer, the drug is released into the medium through a controlled diffusion process (**Figure 2a**).
2. **Figure 2b** shows a diffusion process through polymer swelling. In this system, the excipient (polymer) undergoes a swelling process due to the adsorption of water or pH change and the structural change of the polymer allows the diffusion of the drug through its structure at a controlled rate.
3. **Figure 2c** shows the polymer erosion and degradation release mechanism. This mechanism requires external factors such as moisture or pH, which will break the layers of the polymer, consequently carrying out a controlled drug release.

Although many substances have been proposed as controlled release systems, these are synthetic chemical substances that could be nonbiocompatible in some cases. Nowadays, new excipients have been proposed, one of them is the ordered MS [4, 5] and biogenic silica obtained from rice husk (SiO_2-rice) [6, 7]. The MS and SiO_2-rice have several chemical

properties, which provide an excellent biocompatibility that could be employed as a new generation of excipients employed to transport a variety of drugs.

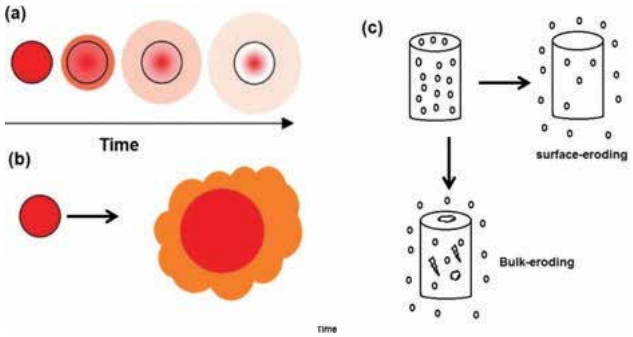

Figure 2. Pharmaco-release mechanism [3].

2. Mesoporous silica as drug delivery

The mesoporous materials are a group of inorganic solids with a system of gaps (pores), which may be arranged to form a hexagonal geometry (**Figure 3**), as well as present disordered pores into the bulk silica. However, in both states the inorganic solid has pore diameters ranging between 2 and 50 nm [8, 9]. **Table 1** shows the classification of porous materials according to the International Union of Pure and Applied Chemistry (IUPAC), which is based in the pore size, therefore, macroporous materials are those whose pore diameters are greater than 50 nm while microporous materials show diameters smaller than 2 nm.

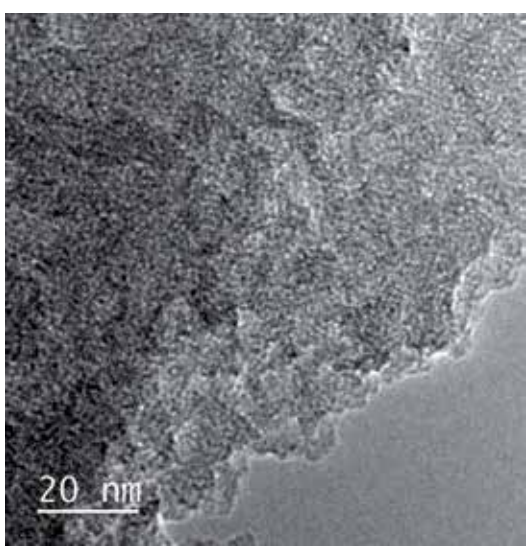

Figure 3. Ordered mesoporous materials structure view by TEM [11].

	Pore size (nm)
Microporous	<2
Mesoporous	2–50
Macroporous	>50

Table 1. IUPAC mesoporous materials classification.

Meso-porous materials have a pore network that can be disarranged or arranged; the latter is called an ordered mesoporous material whose main characteristic is to have a surface area between the ranges of 300 and 1200 m^2 [9]. According to the absorption capacity and chemical properties of MS, these materials could be used as new adsorption systems at different industrial applications, such as adsorption of pollutants [10, 11], catalyst supports [12], and sustained drug release systems [13–16].

Some drugs like ibuprofen [17], naproxen [18], carbamazepine [19], and fenofibrate [20], among others, have been adsorbed on ordered silica structures, such as MCM-41 and SBA-15. Ordered mesoporous silica can control the drugs kinetic release according to excipients of continuous and controlled release. Actually, biogenic silica such as the silica obtained from husk rice (SiO_2-rice) has been scarcely studied as a drug excipient, due to the limited order in the silica pores which could hinder the drug release [6, 7]. However, the good adsorption properties and the low cost of production may show advantages as a drug excipient.

Salazar-Hernandez and collaborators have performed research of SiO_2-rice as an excipient for folic acid [6]. In these works the high adsorptivity of drugs on the silica, and the drug release profiles at different pH values, were studied. This report will be discussed in this chapter.

3. Silica from rice husk as drug delivery

3.1. Obtained silica from rice husk

Silica is a compound found naturally in plants without playing an essential role for growth or development thereof. Similarly to phosphate ions, the silicate ions can be moved from the ground surface and delivered to the root, stem, and leaves of plants [21]. The role silica plays in plants is circumscribed to mechanical resistance of stems and leaves, and generating resistance to fungal diseases. **Figure 4** shows the mechanism employed by plants to fix the silica. Silicon oxide is transported throughout the plant as silicic acid ($Si(OH)_4$), which is concentrated as gel and depending on water evaporation, the silica is progressively deposited within the intercellular spaces.
Among plants containing a large percentage of silica we find rice husk. It contains between 13 and 29% of the total weight in cellulose and about 24.7% in silica [22–24]. To obtain SiO_2-rice it is necessary to remove all organic matter (cellulose) through prolonged calcinations. A pretreatment with nitric and hydrochloric acid allows the removal of inorganic ions, such as Ca^{2+}, Mg^{2+}, and Fe^{3+}; while the preoxidation of the organic material begins. This procedure favors

the removal of the organic material through calcinations at low temperatures (650°C) [22–24], with the concomitant benefit of avoiding the sintering of silica. **Figure 5** shows the sintering process, which involves the removal of hydroxyl groups distributed on the surface through condensation, causing the collapse of the pores in the material [25]. **Table 2** shows the textural properties observed in SiO_2-rice obtained with nitric/hydrochloric acid treatment and calcinations at different temperatures [6, 22–24].

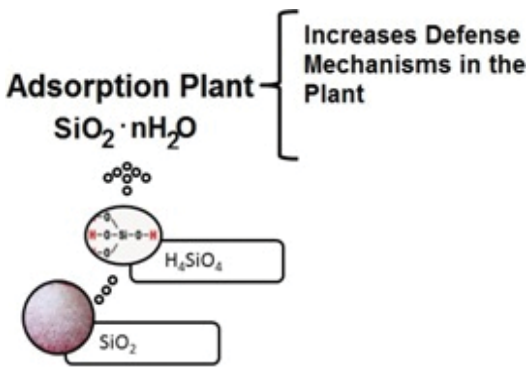

Figure 4. Setting mechanism silica in plants.

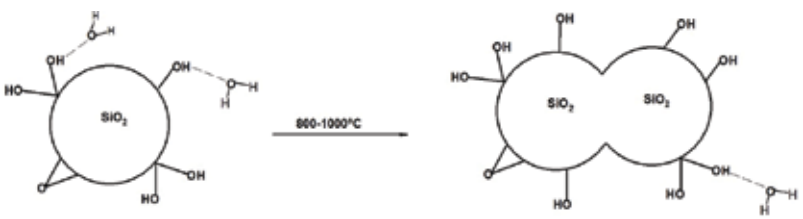

Figure 5. Sintering process of the silica [25].

	Calcination temperature (°C)	Surface area A_{BET} (m^2/g)	Volume pore (cm^3/g)	Size pore, D (nm)
SiO_2-rice	900	94.9	5.37	0.130
SiO_2-rice	500	291.8	4.25	0.320
SiO_2-gel	–	299.0	14.72	1.13

Table 2. Textural properties for SiO_2-rice.

According to **Table 2**, the Area surface calculated by Brunauer, Emmett and Teller Model (BET) surface area of the SiO_2-rice obtained at 500°C is similar to silica gel. The average pore diameter for SiO_2-rice is smaller than those of silica gel; however, this pore size suggests a

similar adsorption capacity to synthetic silicas (SBA-15, MCM-41). When the SiO_2-rice is extracted at high temperatures (900°C), the sintering process causes the elimination of porosity and the consequent loss of any adsorption capacity [6].

The adherence to such conditions (acid pretreatment and calcinations temperatures) is essential in order to control the textural properties and adsorption capacity in the silica. Thus, it is possible to obtain SiO_2-rice with similar adsorption properties than ordered mesoporous silica; opening the possibility to use this biogenic silica as a drug delivery system.

3.2. Silica from rice characterizations

IR analysis for both silicas, SiO_2-rice and MS, is shown in **Figure 6**. Broad signals of Si–O–Si [1027 cm^{-1} (ν_{as}) and 793 cm^{-1} (νs)], water adsorption [3456 cm^{-1} (ν) and 1638 cm^{-1} (δ)], Si–OH groups at 945 cm^{-1} were observed [6, 26]. A signal with smaller intensity at 2934 cm^{-1} was observed, corresponding to C–H of the nonhydrolyzed Si–OC_2H_5 groups on SBA (**Figure 6b**) and the organic material such as cellulose on SiO_2-rice (**Figure 6a**). Silanol groups were present in the MS as a signal at 945 cm^{-1}, while SiO_2-rice shows a shoulder at this wavenumber. These results could suggest a major amount of silanol on the surface of the mesoporous silica. The folic acid adsorption capacity on both silicas will be discussed later.

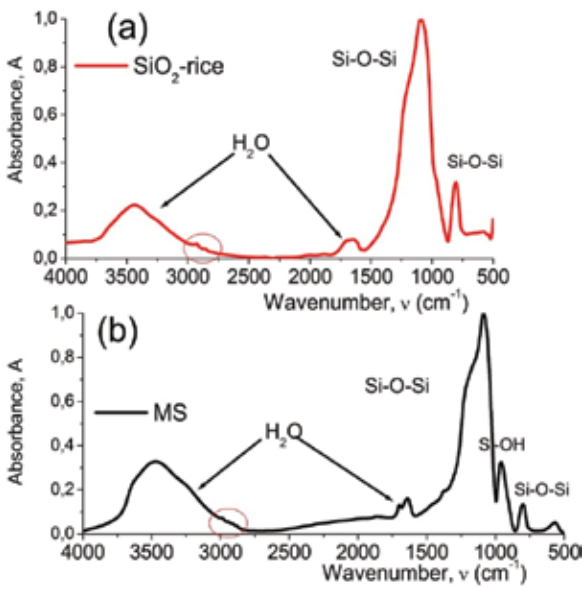

Figure 6. FT-IR analysis of (a) SiO_2-rice and (b) mesoporous silica (MS).

The results of the silica thermal analysis are shown in **Figure 7**; the total amount of SiO_2 formed was higher for SiO_2-rice, a value close to 96%, while 76% corresponded to SBA

(**Figure 7a**). Both silicas appeared around 120°C, represented by an endothermic peak (peak 1 on Differential Temperature Analysis (DTA), **Figure 7b**), corresponding to the complete loss of the water and solvent adsorbed in the structure; however, the intensity of this loss was higher on SBA. On the other hand, the organic material loss was observed for SBA as two exothermic peaks between 240 and 400°C (peaks 2 and 3 on DTA, **Figure 7b**). These reactions could be due to the loss of the remainder pluronic-123 and the unreacted ethoxy groups, $Si–OC_2H_5$, from TEOS (starting materials for mesoporous silica). Nevertheless, no organic material loss was observed for SiO_2-rice, which is established with the highest ceramic yield observed by the biogenic silica.

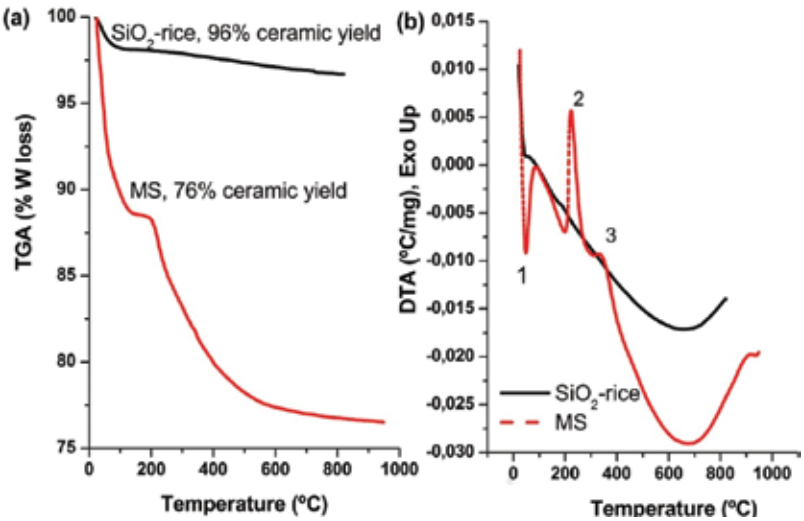

Figure 7. Thermal analysis. (a) TGA and (b) DTA.

3.3. Folic acid load on silica from rice husk

Figure 8a shows the percentage of adsorbed drug, which was calculated from Thermal Gravimetric Analysis (TGA) analysis for the silicas/folic acid adsorbed until 75 min. A large weight loss happened between 200 and 500°C, corresponding to the gradual loss of the organic material (drug adsorbed); the integration from TGA line on this range of temperature corresponding to the amount of drug adsorbed. **Figure 8b** indicates the percentage of drug adsorbed by the silicas at different adsorption times; these results suggest that both silicas have similar adsorption capacities, MS adsorbed 19.3% in weight of folic acid, while SiO_2-rice adsorbed around 18.5%.

Table 3 shows the change on silicas' textural properties after drug adsorption, a major modification on pore volume was observed for MS while the modification in SiO_2-rice was 12% higher. However, SiO_2-rice presented almost two times more modification on BET area in MS.

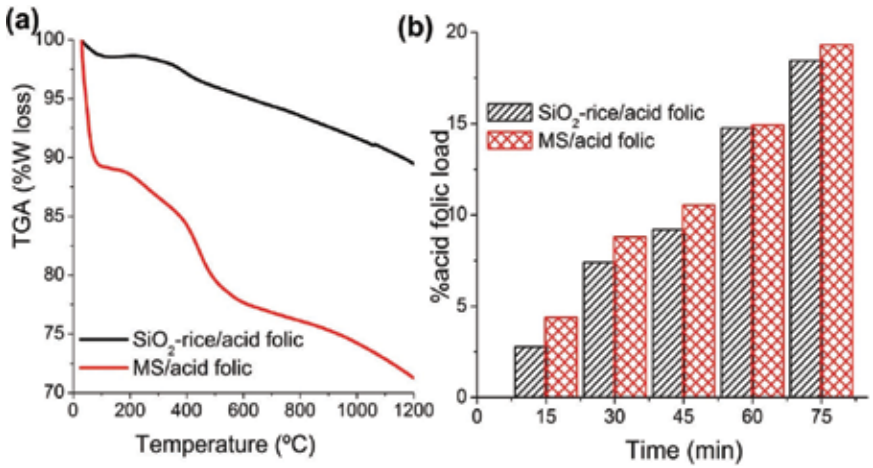

Figure 8. Folic acid adsorption on silica. (a) TGA analysis and (b) adsorption at different time.

	A_{BET} (m^2/g^{-1})			V_{pore} (cm^3/g^{-1})		
	Before adsorption	**After adsorption**	**% change**	**Before adsorption**	**After adsorption**	**% change**
SiO_2-rice	286.17	145.31	49.2(−)	0.3183	0.2531	20.5(−)
MS	600.04	461.37	23.1(−)	0.5922	0.4021	32.1(−)

Table 3. Silica textural properties before and after of the folic acid adsorption.

3.4. Folic acid releases using therapeutic concentration

Folic acid is a vitamin administered orally with a daily dose for adults of 400 μg. Then, the release profile of 400 μg of folic acid adsorbed on silicas was compared to a similar process with a commercial tablet and the same drug dosage (**Figure 9**). The obtained results indicated that the MS and biogenic silica allow a similar drug release profile as a commercial tablet. In gastric condition, pH 3, silicas and commercial tablet desorbed around 3% of the drug, reaching desorption equilibrium at 30 min (**Figure 9a**). However, desorption equilibrium was not observed at pH 5.5 and pH 7 for silicas and commercial excipient. At pH 5.5, around 90% of the drug was released by silica systems, while a commercial tablet desorbed around 80% (**Figure 9b**). **Figure 9c**, with a drug release profile at pH 7, shows an 80% release of folic acid for the commercial tablet and the biogenic silica, while MS shows only a 72% release.

These results suggest an important effect of pH on the desorption process of folic acid, an acid pH most probably increase attractive interactions between the silica surface and the drug. According to **Figure 10**, an acid pH could lead to a positive polarization of the silica surface due to the silanol groups' protonation, and a negative polarization of folic acid due to the deprotonation of acid groups. Therefore, a strong electrostatic attractive force will be generated, delaying the release process where the attractive interaction would decrease concur-

http://dx.doi.org/10.5772/66723

rently to a pH reduction in the system. On the other hand, a high amount of silanols on the MS surface were identified by FT-IR. This result suggests a strong interaction between this silica and the drug, because more silanols are able to interact with folic acid (**Figure 10**). However, the release profile indicated a similar desorption behavior for both silicas, which may be due to some molecules of folic acid being trapped in the pore and did not show interaction with the MS surface. These results make us think that drug size may affect the desorption process.

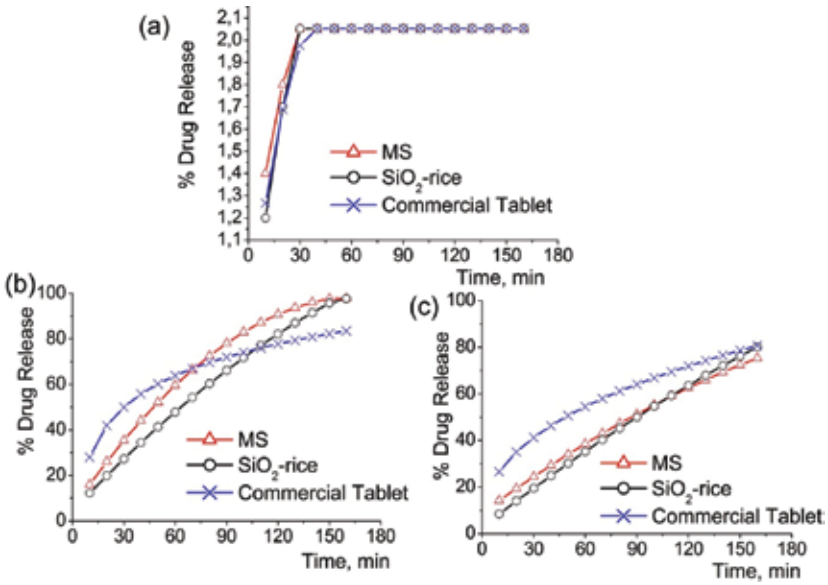

Figure 9. Folic acid release profile for 400 μg of drugs adsorbed.

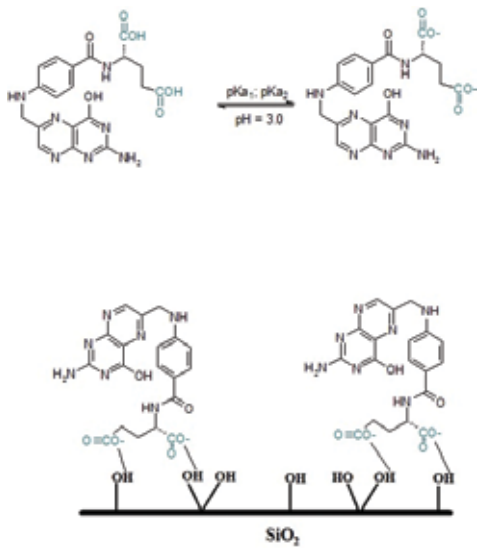

Figure 10. The pH effect on folic acid desorption process.

4. Conclusion

Biogenic silica, SiO_2-rice, presented a similar adsorption-desorption behavior to mesoporous silica. This silica adsorbed around 18% of the drug, while the MS adsorbed 19% of it; also, similar drugs release profile was observed for both silicas at different pH studies. The results obtained suggest that the size of the drug affects the adsorption/desorption process of folic acid on both silicas. On the other hand, pH shows an important effect on the drug desorption process, evidenced by the studied folic acid model. An acid pH could increase the attractive interaction between the surface silica and the drug, delaying the release of the folic acid, thus, pH 5.5 and 7 (pH for duodena after and before eating) would be the optimal condition for desorption of this drug. Additionally, the drug release profile observed for 400 μg adsorbed on silicas allow us to suggest that biogenic silica could be an excellent drug delivery system for folic acid and probably for other drugs. This silica, in comparison with MS, has a low-cost obtaining process.

Author details

Salazar-Hernández Carmen[1]*, Salazar-Hernández Mercedes[2], Lona-Ramos Rocío[1], Elorza-Rodríguez Enrique[2] and Rocha-Ramírez Agustín Hilario[1]

*Address all correspondence to: msalazarh@ipn.mx

1 Unidad Profesional Interdisciplinaria de Ingeniería Campus Guanajuato, Instituto Politécnico Nacional, Silao de la Victoria, México

2 Engineering Department from Mine, Metallurgy and Geology, Guanajuato University, Guanajuato, México

References

[1] Abrantes CG, Duarte D, Reis CP. An overview of pharmaceutical excipients: Safe or not safe? Journal of Pharmaceutical Sciences. 2016; **105** (7): 2019–2026. DOI: 10.1016/j.xphs.2016.03.019

[2] Park K. Controlled drug delivery systems: Past forward and future back. Journal of Control Release. 2014; **190**: 3–8. DOI:10.1016/j.jconrel.2014.03.054

[3] Ukmar T, Planinsek O. Ordered mesoporous silicates as matrices for controlled release of drugs. Acta Pharmaceutica. 2010; **60** (4): 373–385. DOI: 10.2478/v1007-010-0037-4

[4] DeMuth P, Hurley M, Wu CH, Galanie S, Zachariah M.R, Deshong P. Mesoscale porous silica as drug delivery vehicles: Synthesis, characterization and pH sensitive release profiles. Microporous and Mesoporous Materials. 2011; **141**(1–3): 128–134. DOI: 10.1016/j.micromeso.2010.10.035

[5] Tsai CH, Vivero-Escoto JL, Slowing II, Fang IJ, Trewyn BJ, Lin VSY. Surfactant assisted controlled release of hydrophobic drugs using anionic surfactant template mesoporous silica nanoparticles. Biomaterials. 2011; **32**(26): 6234–6244. DOI: 10.1016/j.biomaterials.2011.04.077

[6] Salazar-Hernández M, Salazar-Hernández C, Gutiérrez-Fuentes A, Elorza E, Carrera-Rodríguez M, Puy-Alquiza MJ. Silica from rice husks employed as drug delivery for folic acid. Journal of Sol-Gel Science and Technology. 2014; **71**(3): 514–521. DOI: 10.1007/s10971-014-3378-5

[7] Salazar-Hernández M, Salazar-Hernández C, Juarez-Ríos H, Caudillo-González M, Rocha AH. Estudio del control de crecimiento de C. albicans con sistemas de griseofulvina adsorbida en SiO_2-porosa obtenida de la cascara de arroz. Revista Iberoamericana de Ciencias. 2014; **1**(2): 223–232. DOI: ReIbCi – Julio 2014 – www.reibci.org

[8] ALOthman ZA. A review: Fundamental aspects of silicate mesoporous materials. Materials. 2012; **5**: 2874–2902. DOI: 10.3390/ma5122874

[9] Kresge CHT, Roth WJ. The discovery of mesoporous molecular sieves from the twenty year perspective. Chemical Society Reviews. 2013; **42**: 3663–3670. DOI: 10.1039/c3cs60016e

[10] Salazar-Hernández MM, Salazar-Hernández C, Elorza E, Juárez-Ríos H. The use of mesoporous silica in the removal of Cu (I) from the cyanidation process. Journal of Material Science. 2015; **50**(1): 439–446. DOI: 10.1007/s10853-014-8603-7

[11] Shukla P, Wang S, Sun H, Ang HM, Tadé M. Adsorption and heterogeneous advanced oxidation of phenolic contaminants using Fe loaded mesoporous SBA-15. Chemical Engineering Journal. 2010; **164**: 255–260. DOI: 10.1016/j.cej.2010.08.061

[12] Huirache-Acuña R, Nava R, Peza-Ledesma CL, Lara-Romero J, Alonso-Núñez J, Pawelec B, Rivera-Muñoz ER. SBA-15 mesoporous silica as catalytic support for hydrodesulfurization catalysts: Review. Materials. 2013; **6**(9): 4139–4167. DOI: 10.3390/ma6094139

[13] Steven CR, Busby GA, Mather C, Tariq B, Briuglia ML, Lamprou DA, Urquhart AJ, Grant MH, Patwardhan SV. Bioinspired silica as drug delivery systems and their biocompatibility. Journal of Materials Chemistry B. 2014; **2**: 5028–5042. DOI: 10.1039/c4tb00510d

[14] Barbé C, Bartlett J, Kong L, Finnie K, Lin HQ, Larkin M, Callejas S, Bush A, Callejas G. Silica particle: A novel drug-delivery system. Advance Materials. 2004; **16**(21): 1959–1966. DOI: 10.1002/adma.200400771

[15] Gurka MK, Pender D, Chuong P, Fouts BL, Sobelov A, McNally MA, Mezera M, Woo SY, McNally LR. Identification of pancreatic tumors in vivo with ligand-targeted, pH responsive mesoporous silica nanoparticles by multispectral optoacoustic tomography. Journal of Controlled Release. 2016; **231**: 60–67. DOI: 10.1016/j.jconrel.2015.12.055

[16] An N, Lin H, Yang C, Zhang T, Tong R, Chen Y, Qu F. Gated magnetic mesoporous silica nanoparticles for intracellular enzyme-triggered drug delivery. Materials Science and Engineering C. 2016; **69**: 292–300. DOI: 10.1016/j.msec.2016.06.086

[17] Charnay C, Bégu S, Tourné-Péteilh C, Nicole L, Lerner DA, Devoisselle JM. Inclusion of ibuprofen in mesoporous templated silica: Drug loading and release property. European Journal of Pharmaceutics and Biopharmaceutics. 2004; **57**(3): 533–540. DOI: 10.1016/j.ejpb.2003.12.007

[18] Halamová D, Badanicová M, Zelenák V, Gondová T, Vainio U. Naproxen drug delivery using periodic mesoporous silica SBA-15. Applied Surface Science. 2010; **256**(22): 6489–6494. DOI: 10.1016/j.apsusc.2010.04.044

[19] Miloví M, Djuris J, Djekí L, Vasiljeví D, Ibrí S. Characterization and evaluation of solid self-microemulsifying drug delivery systems with porous carriers as systems for improved carbamazepine release. International Journal of Pharmaceutics. 2012; **436**(1–2): 58–65. DOI: 10.1016/j.ijpharm.2012.06.032

[20] Speybroecka MV, Mellaertsb R, Molsa R, Thia TD, Martensb JD, Humbeeckc JV, Annaerta P, Van den Mootera G, Augustijns P. Enhanced adsorption of the poorly soluble drug fenofibrate by tuning its release rate from ordered mesoporous silica. European Journal of Pharmaceutical Sciences. 2010; **41**(5): 623–630. DOI: 10.1016/j.ejps.2010.09.002

[21] Tzong-Horng L. Preparation and characterization of nano-structured silica from rice husk. Materials Science and Engineering A. 2004; **364**(1–2): 313–323. DOI: 10.1016/j.msea.2003.08.045

[22] Gosh R, Bhattacherjee S. A review study on precipitated silica and activated carbon from rice husk. Journal Chemical Engineering & Process Technology. 2013; **4**(4): 156. DOI: 10.4172/2157-7048.1000156

[23] Shen Y, Zhao P, Shao Q. Porous silica and carbon derived from rice husk pyrolysis char. Microporus and Mesoporous Materials. 2014; **188**: 46–76. DOI: htttp://dx.doi.org/10.1016/j.micromeso.2014.01.005

[24] Ma X, Zhou B, Gao W, Qu Y, Wang L, Wang Z, Zhu Y. A recyclable method for production of pure silica from rice hull ash. Powder Technology. 2012; **217**: 497–501. DOI: 10.1016/j.powtec.2011.11.009

[25] Yalcin N, Sevin V. Studies on silica obtained from rice husk. Ceramics International. 2001; **27**(2): 219–224. DOI: 10.1016/S0272-8842(00)00068-7

[26] Battisha IK, Beyally AE, Mongy SE, Nahrawi AM. Development of the FTIR properties of nano-structure silica gel doped with different rare earth elements, prepared by sol-gel route. Journal of Sol–Gel Science and Technology. 2007; **41**(2): 129–137. DOI: 10.1007/s10971-006-0520-z

Chapter 6

Physical and Chemical Characterization of Rice Using Microwave and Laboratory Methods

Kok Yeow You, Li Ling You, Chen Son Yue,
Hou Kit Mun and Chia Yew Lee

Additional information is available at the end of the chapter

http://dx.doi.org/10.5772/66050

Abstract

Two main species of cultivated rice in the world are *Oryza sativa* (Asian rice) and *Oryza glaberrima* (African rice). The *Oryza sativa* species, which is grown worldwide, is far more widely utilized compared with the *Oryza glaberrima* species, which is grown in West Africa. Recently, the annual rice production has reached almost 480 million tonnes, and this demand is expected to rise to 550 million tonnes in 2035. Thus, this increases the need to characterize and maintain the quality of rice and hence to determine the price of rice appropriately. Obviously, modern technologies that can provide fast and accurate measurement are essential in the large-scale industrial rice processing. In this chapter, several technologies and instruments used for rice processing are reviewed. The principle of the measurement for each technology is briefly described. The strength of this chapter is to introduce the application of microwave technology during rice processing, such as rice dying process, rice moisture detection, broken rice measurement and rice insect control. The pros and cons of the microwave method will be discussed in detail. Hence, some standard test laboratory for monitoring of carbohydrate, protein, fat and trace elements content is also described in this chapter.

Keywords: rice, rice physical properties, rice chemical properties, moisture, broken rate, protein, fat, carbohydrate

1. Introduction

There are more than 40,000 different types of rice in the world. However, commonly, rice is categorized by its physical shape and sizes or length either long grain, medium grain or short grain. Rice consists of two main species, which are *Oryza sativa* known as Asian rice and *Oryza glaberrima* known as African rice. *Oryza glaberrima* is less common as compared to

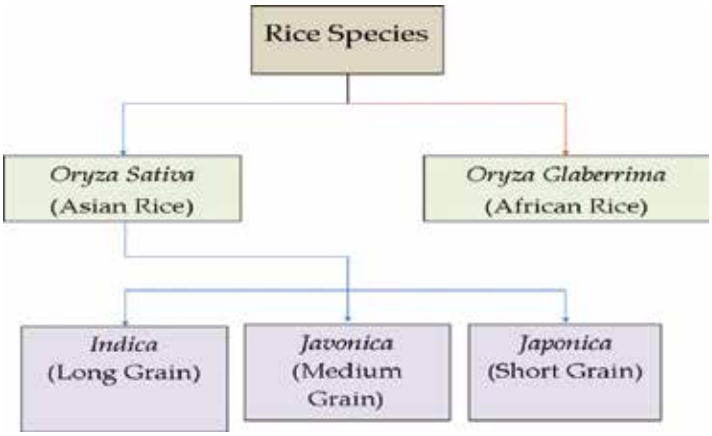

Figure 1. Categories of rice species.

Oryza sativa. *Oryza sativa* can be divided into *indica, javonica and japonica* subspecies as shown in **Figure 1**.

Oryza sativa Indica is known as long grain rice, which has a long and slender kernel. This type of rice is commonly grown in warm climate regions, such as at Thailand, India, Pakistan, Brazil and Southern USA. Furthermore, long grain rice is much fluffier and less sticky than short grain rice. On the other hand, medium grain rice has a size and length in between the other two subspecies grains that belong to *Javonica* group called *Oryza sativa Javonica*. It is shorter, plump and slightly wider than long grain rice but not round in shape and only found in Indonesia. Besides, the other type of grain rice, which is short and fat, that belongs to *Japonica* group is known as *Oryza sativa Japonica*. The short grain rice needs a cold weather environment to grow such as at Japan, Korea, Northern China and California. In particular, the short grain rice has high starch content, moist and viscous. The quality of milled rice is indicated by the combination of both physical and chemical characteristics. The physical characteristics of rice consist of milling degree, whiteness, grain shape, foreign matter, head rice, chalkiness and moisture content, *m.c.*, while the chemical characteristics are amylose content, gelatinization temperature and gel consistency [1]. However, the main characteristics used for milled rice grading are head rice, broken rice (BR) and brewer percentage, defectiveness, foreign matter, presence of paddy and *m.c.* [1].

2. Various manufactured brand of rice grain

There is existing variety of rice in the market, but most of the users are not experienced in distinguishing between the rice in terms of its physical and chemical properties. In this chapter, up to 10 types of commercial rice grain have been chosen to show the distinction between their properties, as well as the techniques used to characterize its properties. The basic physical properties (moisture content, *m.c.*, and size) of the 10 different brands of commercial rice are tabulated in **Table 1**.

Manufactured brand of rice	Weight before heat (g)	Weight after heat m_d (g)	Weight losses m_w (g)	Moisture content *m.c.* (%)	Average length l (mm)	Average width w (mm)
1. Sakura Super Thai Brown Rice	10.005	8.556	1.449	14.48	7.52	1.76
2. Jasmine Nutririce	10.003	8.524	1.479	14.79	7.29	2.04
3. Floral Glutinous	10.004	8.389	1.615	16.14	7.06	1.95
4. Maharaja Basmathi	10.009	8.377	1.632	16.30	6.79	1.52
5. SUMO Calrose	10.008	8.320	1.688	16.87	4.92	2.80
6. Bird of Paradise Thai Fragrant	10.010	8.303	1.707	17.05	7.18	1.86
7. Sakura Super Basmathi Pakistan	10.008	8.248	1.76	17.59	7.06	1.80
8. Giant Super Special White Rice	10.002	8.228	1.774	17.74	7.33	2.06
9. Sun Rise Australian Fragrant	10.005	8.203	1.802	18.01	7.22	1.90
10. Phkarkhnei Cambodi Organi	10.002	8.150	1.852	18.52	7.58	1.92

Table 1. Moisture content, *m.c.* and sizes of ten different brands of rice grain.

The actual *m.c.* of the rice grains in **Table 1** was obtained by the standard oven-drying method. Ten grams of each type of commercial rice grain was dried in a forced convection oven at 130°C for 24 h [2]. The *m.c.* was calculated in percent on the wet basis as:

$$m.c.(\%) = \frac{m_w}{m_w + m_d} \times 100 \tag{1}$$

where m_w and $m_d$are mass of water and dry grain, respectively. On the other hand, the average length, l, and width, w, for the 30 pieces rice grain from each type of bulk rice samples have been measured using digital vernier caliper. All the ten different types of rice samples showed the lowest moisture content, *m.c.* ranging from 14.48 to 18.52%. The length, l, and width, w, of the 10 samples are shown between 4.92–7.58 mm and 1.76–2.04 mm, respectively. More sophisticated ways to determine the physical properties of rice grain, as well as the rice processing using the latest technology, have been described in Sections 3.1–3.4. Meanwhile, the laboratory scientific methods used for testing the chemical properties have been described and discussed in detail in Section 3.5.

3. Applications of scientific methods and microwave equipments in rice processing

3.1. Rice drying and sterilization processing

The moisture content, *m.c.*, of the grain is the most important criteria for quality assessment and process control. The *m.c.* inside the rice grain is a crucial parameter for grain processing

such as harvesting, milling, storage, transporting and quality control. For instance, rice grain is usually harvested between moisture content, *m.c.* 19–25% for maximum grain yield and needed to be dried to 14% or less depend on the season and the weather for safe storage [3]. Besides, the ideal *m.c.* for milling is 14% in order to maximize the head rice and minimize the broken rate (BR) [1]. If the *m.c.* in rice grain is too low, the milled grain will become fragile. Thus, precise determination of the rice grain *m.c.* is important. In general, the hot-air drying oven is implemented in conventional rice grain drying process. However, this method is time-consuming and causes energy loss. Recently, most of microwave equipments and measurement techniques are used to dry or monitor the moisture content, *m.c.*, inside the agriculture products and foods under test. The reason is because of the tendency of water to absorb microwave energy and generate the heat within the agri-foods under test. When the moist rice grain is exposed to the microwave, the water molecules in the rice grain will be induced to rotate and produce heat as shown in **Figure 2**. Thus, the rate of water removal is higher than hot-air drying method. Besides, the microwave heating is capable of maintaining original texture structure and color of the rice gain compared to conventional oven-drying techniques.

In fact, the interaction between agri-foods materials containing water with microwave can be described by the complex relative permittivity, ε_r:

$$\varepsilon_r = \varepsilon_r' - j\varepsilon_r'' \tag{2}$$

where the real part, ε_r'', is the dielectric constant and imaginary part, ε_r', is the dielectric loss factor. The ε_r'' influences the electric field distribution and the phase of waves traveling through the material. In contrast, the $\varepsilon_r\varepsilon$ influences the energy absorption or attenuation by the material.

The water removal rate of the rice grain is increased with the microwave power. However, the higher microwave power will increase the percentage of the broken milled rice and higher rate of oxidation as well as nutritional losses of the milled rice. Typically, the microwave oven

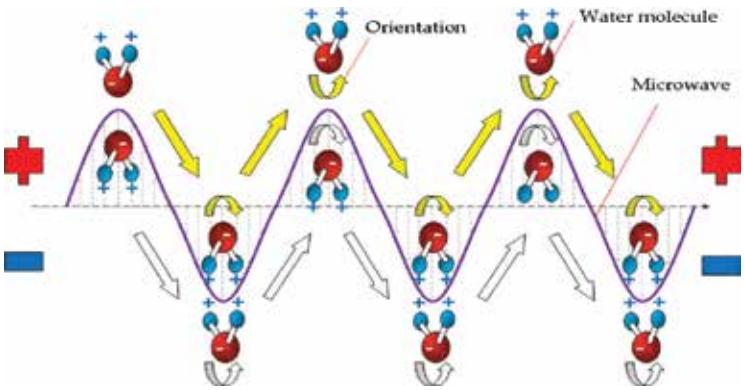

Figure 2. Microwave heating mechanisms: water molecules are oriented when exposed to microwave.

http://dx.doi.org/10.5772/66050

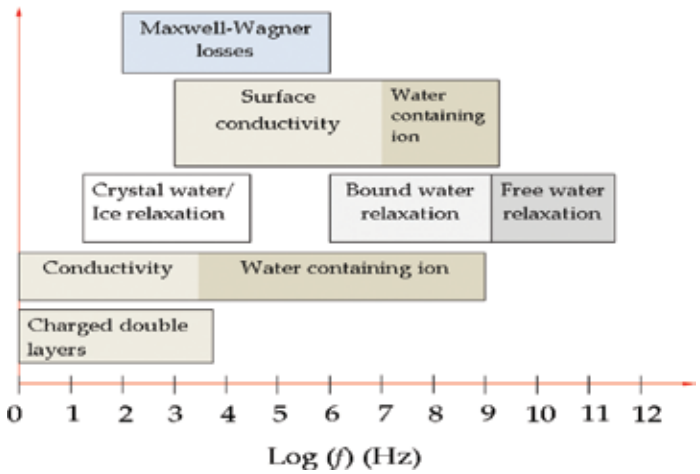

Figure 3. The mechanisms of water molecules when exposed to different range of operating frequency.

power will be adjusted to 55°C of heating temperature in order to reduce the *m.c.* of the rice grain from ~20 to 14% within 20 min [4]. The mechanisms of water molecules in agri-food specimens are different when exposed to different ranges of operating frequency, *f*, as shown in **Figure 3**.

There are two microwave frequencies allocated by the US Federal Communications Commission (FCC) for industrial, scientific and medical (ISM) use, which are 915 MHz and 2.45 GHz. Normally, most of the microwave heating applications are devoted to 2.45 GHz, since it provides a suitable compromise between power deposition and penetration depth, as well as it is an unlicensed operating frequency. For instance, the manufactured microwave heating system for agri-food products is shown in **Figure 4**.

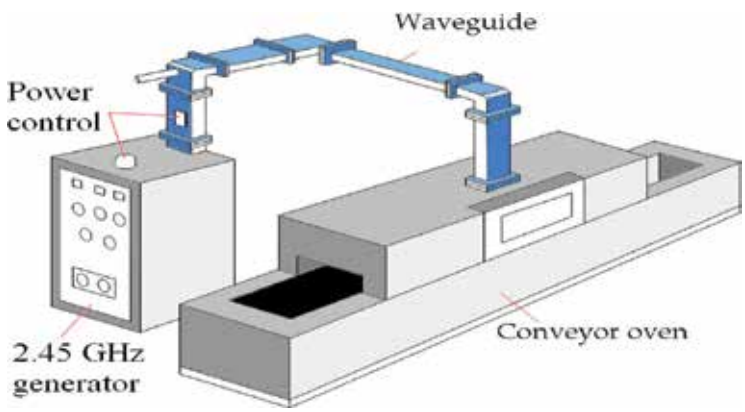

Figure 4. Microwave heating equipment.

3.2. Rice moisture sensing

There are two methods of determining moisture content, *m.c.*, of rice grain, which are the direct method and the indirect method. Direct method determines the *m.c.* by removing the *m.c.* of rice grain bulk using oven-drying method (130°C with 24 h) or chemical solvents as mentioned in Section 2. The direct method is the most accurate method to determine the grain *m.c.*, but it is time-consuming. For direct method, the water content in the rice grain is removed totally and *m.c.* is calculated from Eq. (**1**). The heating temperature must exceed the temperature of boiling water because water molecules in rice grain were bound with molecules of rice substance.

In contrast, the indirect method requires the measurement of the electrical property of the rice grain using fabricated instrument, so-called moisture meter. The change in electrical properties can be directly correlated with a change in the actual moisture content, *m.c.*, of the rice grain obtained from oven-drying method (direct method). Recently, the indirect methods become more popular than the direct method due to rapid test, high sensitivity and user-friendly features. In this section, only indirect methods that use high operating frequency for grain moisture determination are described.

As mentioned above, the polarization of water molecules contained in the rice grain is sensitive and showed a significant response when exposed to microwaves, and this will allow the microwave sensor to be used as a measuring technique to sense the moisture content, *m.c.*, in the moist rice grain. The volume of water in the total volume of moist rice grain heavily influences the relative permittivity of the moist rice grain due to the relative permittivity of pure water ($\varepsilon_r \approx 80$ at very low frequencies) being much greater than that of the other constituents in the rice grain bulk (rice substance: $\varepsilon_r \approx 2.5$, air: $\varepsilon_r = 1$). Thus, when the amount of moisture changes in the rice grain, the sensor will measure a change in reflection/transmission coefficient or resonant frequency (from the change in permittivity) that can be directly correlated with a change in *m.c.* of the rice grain, which was obtained from oven-drying method previously.

In this section, some of the microwave sensors related to the grain moisture measurement are presented. A microwave microstrip ring resonator as miniaturized and nondestructive sensor for single wheat grain microwave estimation were reported by Abegaonkar et al. [5] as shown in **Figure 5**. The ring resonator was designed on an alumina substrate with a h of 0.635 mm and $\varepsilon_{r,sub}$ of 9.98 to resonate at 10 GHz.

In this study, a wheat grain was overlaid on the ring resonator and its corresponding measured resonant frequency f_r, bandwidth BW and quality factor Q were obtained from a scalar

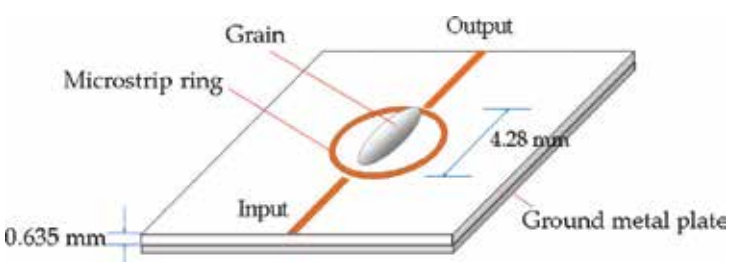

Figure 5. Microstrip ring resonator overlaid by grain [5].

http://dx.doi.org/10.5772/66050

network analyzer. Then, the calibration equations related to the moisture content, *m.c.* with f_r, *BW*and *Q*, respectively, were developed. Validation test showed that the average error for *m.c.* prediction was 2.12%. The major drawback of this ring resonator is that the grain orientation within the sensor significantly affects the accuracy and sensitivity of the measurement. Kim et al. [6] proposed a prototype microwave transceiver grain moisture meter based on free-space transmission method for rice grain *m.c.* prediction. The prototype grain moisture meter is mainly composed of oscillator, isolator, horn antenna, detector and rectangular grain holder. The schematic diagram of the prototype grain moisture meter is depicted in **Figure 6**. A generated microwave signal at 10.5 GHz from an oscillator is transmitted to the rice grain sample through an isolator and a transmitting horn antenna. The attenuated signal is then received by a receiving horn antenna and detected by a detector that converts the signal to voltage, *V*. A calibration equation, which relates the moisture content, *m.c.*, with moisture density, ε, voltage, *V*, and temperature, *T*, is developed and validated in this study. Validation result showed that the moisture meter can predict the *m.c.* with average error of 0.52%. However, the moisture meter is relatively large in size and operates at high frequency, which will increase its cost. In addition, the output voltage, *V*, of the meter needs to be substituted into the calibration equation manually for *m.c.* calculation.

A multilayer microstrip moisture sensor was developed by Jafari et al. [7] for measuring the *m.c.* of rice grain. The sensor was designed on a laminated RT/Duroid substrate with a *h* of 1.575 mm and $\varepsilon_{r,sub}$ of 2.2 to operate at 9 GHz. The sensor consists of two main parts: the stripline section, which is covered by aluminum plate, and the semi-infinite layer microstrip line, which is the

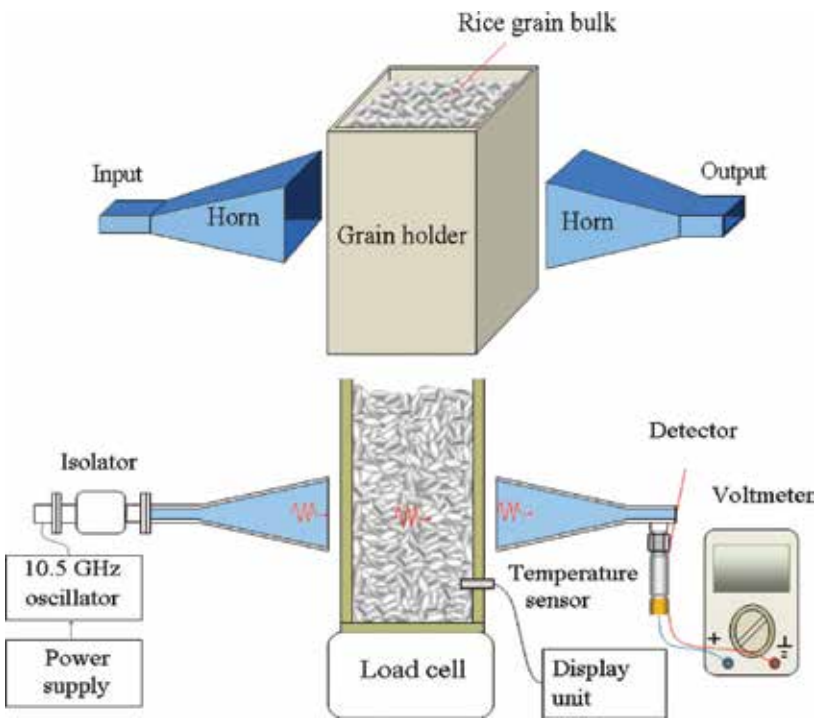

Figure 6. The prototype microwave transceiver grain moisture meter [6].

sensing region as shown in **Figure 7**. The attenuation as a function of complex permittivity of three dielectric layers (substrate, protective and grain layers) and effective dielectric constant was derived from complex propagation constant. Besides that, the relationship between the complex permittivity of rice grain and *m.c.* was also established based on mixture theory. To predict the *m.c.* of rice grain, the rice grain was loaded on the sensor and the corresponding attenuation signal was obtained from the vector network analyzer. Then, the *m.c.* was calculated from the measured attenuation through both derived attenuation and mixture equations based on numerical method. Thus, this method is complex as compared to aforementioned studies [5–6].

You et al. [8] proposed cylindrical slot antennas as sensors for rice quality (*m.c.* and percentage of BR) determination. A single slot antenna sensor and a coupling slots antenna sensor were fabricated by using SMA stub panel with a radius of 0.65 mm and length of 1.436 cm. For coupling slots antenna, the separation distance of the slots is 1 cm in which one of the slot was terminated. Both sensors were positioned on an aluminum ground plane with an acrylic holder. The configuration of the single slot antenna and coupling slot antenna sensors is illustrated in **Figure 8(a)** and **Figure 8(b)**, respectively.

Both sensors were designed to operate at 1 GHz for *m.c.* measurement based on the measured magnitude of reflection coefficient from a vector network analyzer. Calibration equations based on the relationship between the measured magnitude of reflection coefficient and *m.c.* were also developed for both sensors. The coupling slots sensor was more sensitive to

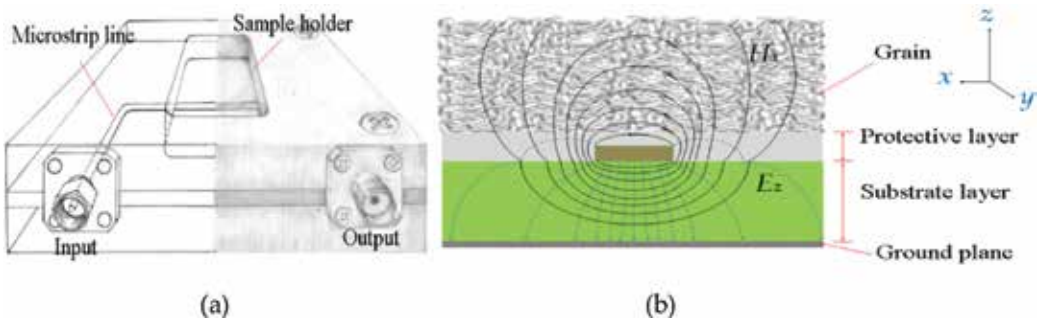

Figure 7. (a) Multi-layer microstrip moisture sensor. (b) Cross section of microstrip sensing region [7].

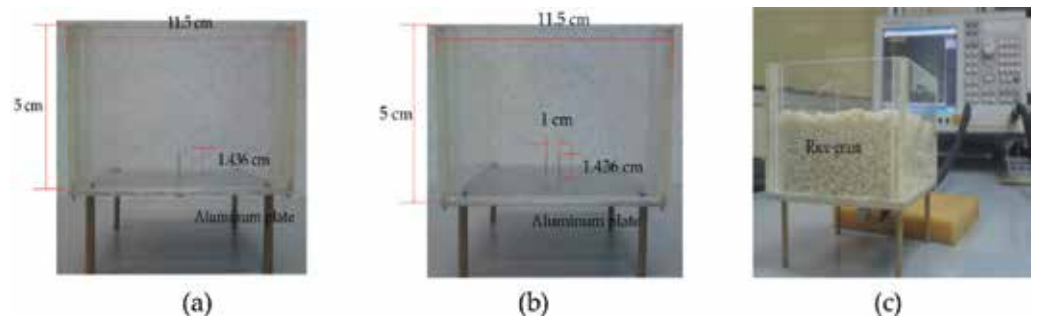

Figure 8. Configuration of the (a) single slot sensor and (b) ccoupling slots sensor [8]; (c) Eexperiment- set-up.

http://dx.doi.org/10.5772/66050

the *m.c.* of the rice grain than single slot sensor. The coupling effects between the two slots will increase the density of the sensing fields for the sensor. Recently, microstrip wide-ring, microstrip coupled-line [9] and small coaxial probe [10], as shown in **Figure 9**, have been used for rice moisture measurements. By using wide-ring and coupled-line sensors, the bulk rice grain samples with different levels of *m.c.* were placed into the sample holder of the sensor as shown in **Figure 10**. On the other hand, the small and slim coaxial probe has a small sensing area, which is able to cover the size of single rice grain and provides a single grain moisture measurement. Moreover, the single grain measurement does not depend on the bulk density of the rice grains, and thus, the uncertainty of bulk density in the rice measurement (due to a different rate of broken rice in the bulk grain) can be ignored.

The comparison of the measured ε_r' and ε_r'' for rice grain with various *m.c.* at 2.45 GHz by using the wide-ring sensor, coupled-line sensor, literature data [11] and small coaxial probe is shown in **Figure 11**. Obviously, the value of ε_r' for single rice grain measurement is much higher than the bulk rice measurements. This is because the bulk rice is composed of a mixture of air and rice grains. The measured ε_r' will affect by the volume of air gap in the total volume of the bulk rice grain since the value of ε_r' for the air is approximately unity which is being much lower than the constituents in the rice grain.

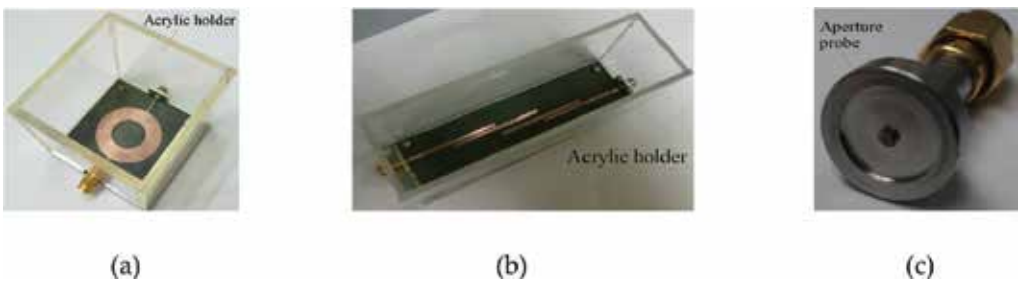

Figure 9. (a) Microstrip wide-ring sensor [9]; (b) microstrip coupled-line sensor [9]; (c) customized small coaxial probe with outer conductor radius b = 0.33 mm and inner conductor radius a = 0.1 mm [10].

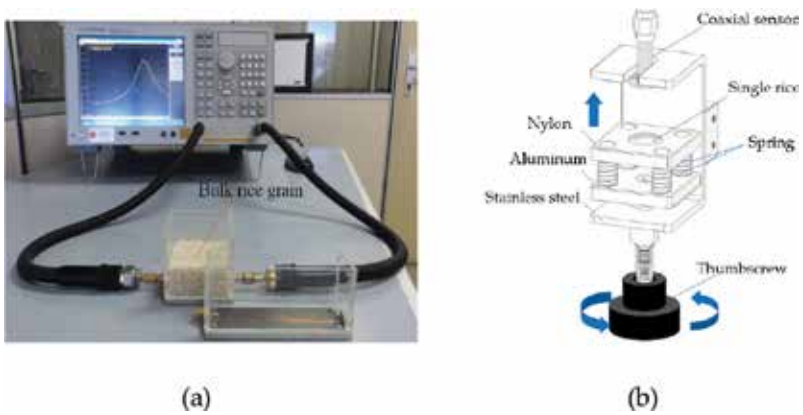

Figure 10. Measurement set-up for (a) bulk rice grain moisture measurement [9] and (b) single rice grain measurement [10].

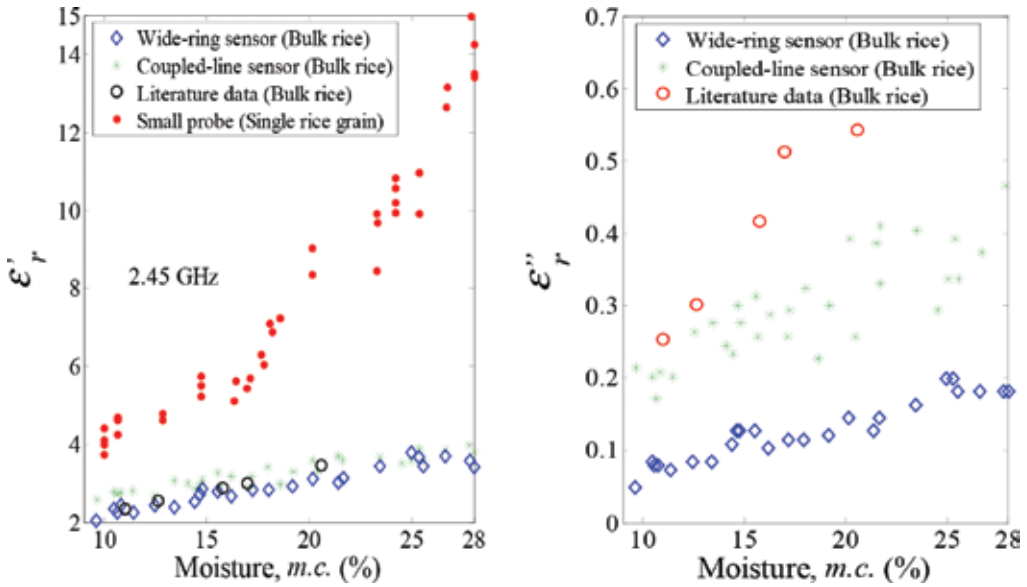

Figure 11. The variations in ε_r' and ε_r'' of single rice grain and rice grain bulk with its moisture content, *m.c.* at 2.45 GHz [10, 11].

3.3. Broken rice detection

The rice grain has a length <3/4 but more than 1/4 of the average head grain length are categorized as a broken rice as shown in **Figure 12**. Normally, the bulk rice, which contains broken grain for 0–5, 5–20, 20–35 and 35–50%, is classified as a premium grade, grade 1, grade 2 and grade 3, respectively. Using conventional broken rice sorting machine, the mechanical filter techniques are implemented. Since broken rice has a size smaller than head rice, the broken rice can be filtered by the wire net with small size of mesh in the machine. Recently, the image processing technique is popularly used for grading and classification of rice, in which the optical scanning is used to differentiate the size and color of the rice grain [12–14].

The optical techniques are able to recognize the ratio of broken rice and the impurities in bulk rice sample based on the pixel image area and pixel intensity for each rice grain. By using

Figure 12. The rice grain with (a) 0%, (b) 50% and (c) 100% broken rate.

http://dx.doi.org/10.5772/66050

the developed image processing software, the dimensional features of the rice kernels such as length, perimeter and projected area were extracted from the captured images. Empirical equations that relate the BR percentage and characteristic dimension ratio, which is computed from the dimensional features, were developed for percentage of BR estimation. The result showed that the BR percentage can be estimated with average error of 2%. For instance, in the work done by Lloyd et al. [13], a commercial GrainCheck machine vision system was evaluated to determine its performance in BR percentage measurement as shown in **Figure 13**. Most of the optical systems need to be controlled with various adjustments to acquire reproducible dimensional features from the capture images. Consequently, a trained operator is required to set up the system. Besides that, the rice kernels also need to be arranged manually to avoid any touching prior to the image capturing process. In addition, the machine is also large in size, expensive and affected by external light conditions.

In this section, an alternative broken rice measurement using microwave techniques is introduced. The measurement technique is based on the change in air gap density in the bulk rice, since the air gap between broken grains is smaller than the normal rice grains. The electromagnetic wave is generated from microwave sensor and radiated into the bulk grain sample. In fact, the air gap density in the grain sample is inversely proportional to the density of radiated field, which is covering inside the grain sample [15].

Besides moisture measurement, the cylindrical slot sensors in **Figure 8(a)** and **Figure 8(b)** (Section 3.2) can also be implemented for percentage of BR determination. In this BR percentage measurement, the sensors were operated at 13.5 GHz based on the measured magnitude of reflection coefficient $|\gamma|$ from a vector network analyzer. The short wavelength or high-frequency signal is required to enhance the air gap sensitivity for broken rice measurement and reduce the penetration of energy into the rice grains [8]. **Figure 14** shows the variation in measured reflection coefficient $|\gamma|$ of the rice grain with the percentage of broken rice in the samples at 13.5 GHz.

3.4. Rice insect detection and control

In addition to the above applications, microwave method can also be used to control and eliminate the rice weevils (in **Figure 16**) without affecting the texture of the rice grain. It is because each agri-food or biological specimen has unique energy absorption properties,

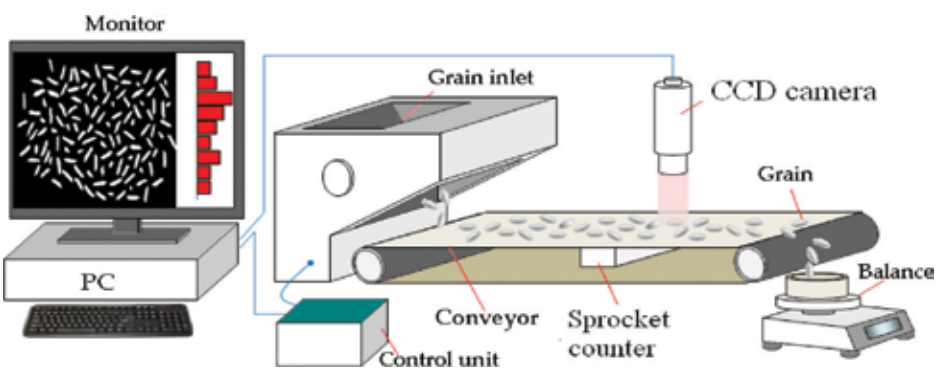

Figure 13. The GrainCheck machine vision system [13].

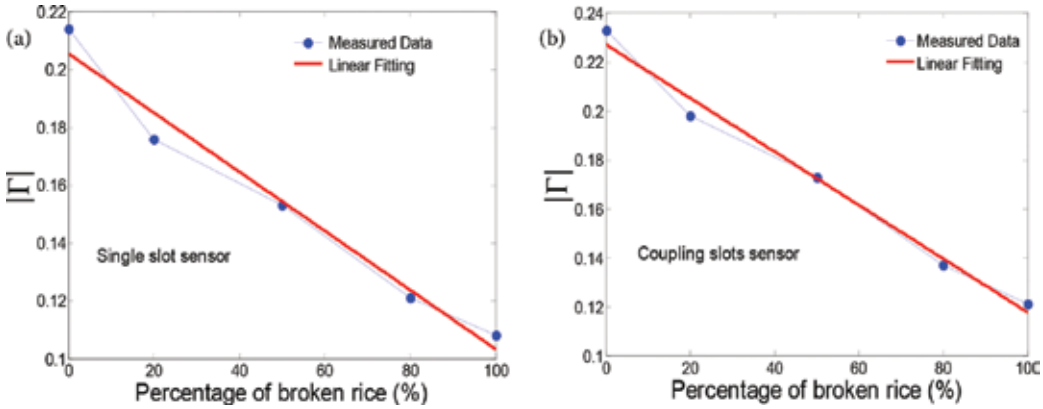

Figure 14. Variation in magnitude reflection coefficient |γ| with the percentage of broken grain in the bulk rice sample at 13.5 GHz using the (a) single slots sensor and (b) coupling slots sensor, respectively [8].

which is mainly influenced by its loss factor ε_r''. The value of ε_r'' for the material is frequency dependent. The typical relationship between the loss factor ε_r'', mechanism of water molecules and operating frequency is shown in **Figure 15**.

For instance, the values of ε_r' and ε_r'' of the rice weevils versus frequency *f* are shown in **Figure 16** [16] By comparing **Figure 15** and **Figure 16**, it was found that the water content in the rice weevils is in a state of bonding at a few MHz. This means that the internal response of the rice weevils is sensitive to the external wave at few MHz. Thus, Nelson et al. [16] found that the complete mortality of the rice weevils can be obtained with 40°C of grain temperature when infested grain was exposed to microwave at 39 MHz and then it was treated at 2.45 GHz (ISM band).

3.5. Rice nutrition test

3.5.1. Determination of total carbohydrate content by using phenol-sulfuric acid method

Hundred milligrams of each rice sample was weighed and hydrolyzed with 5 mL of 2N hydrochloric acid in a boiling water bath (80°C) for 1 h. The sample was left to cool at room

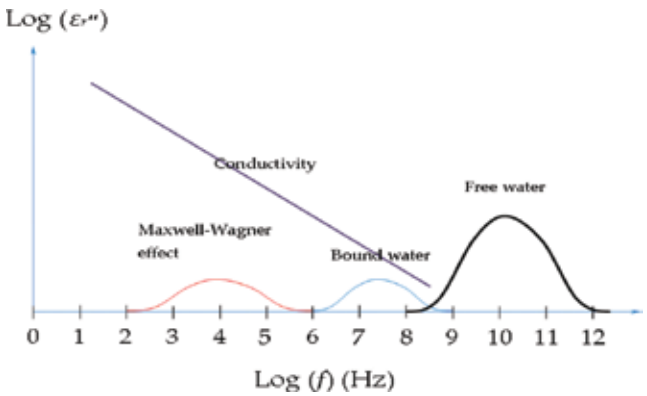

Figure 15. Relationship between ε_r'', mechanism of water molecules and frequency, *f*.

http://dx.doi.org/10.5772/66050

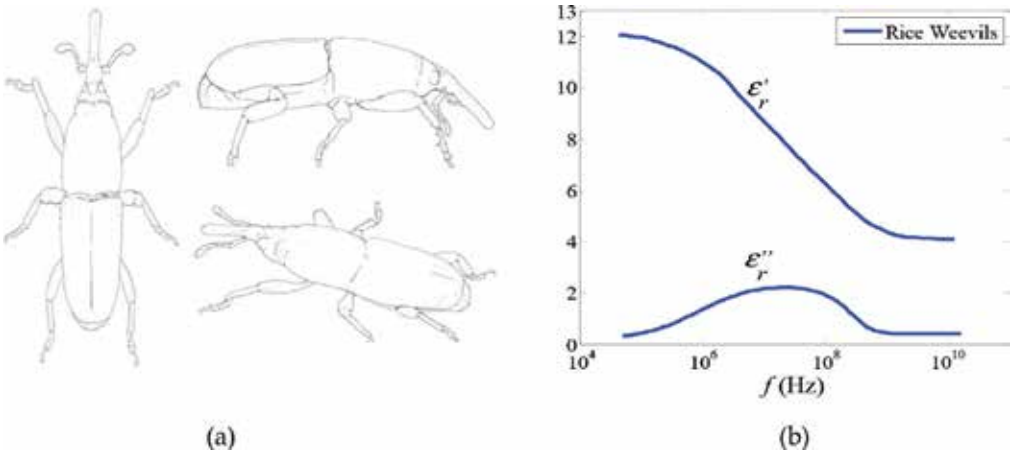

Figure 16. (a) Rice weevils (*Sitophilus oryzae*); (b) variation in ε_r' and ε_r'' of the rice weevils with frequency, f at 24°C [16].

temperature and neutralized with solid sodium carbonate, and then, distilled water was added to top the sample up to 100 mL. Meanwhile, the standard glucose solution was prepared by dissolving 100 mg of D-glucose with distilled water in a 100-mL volumetric flask. Ten milliliter of the standard glucose solution was further diluted to 100 mL, and the standard solution was used as working standard. A series of working standard of glucose solution was prepared by transferring 0.2, 0.4, 0.6, 0.8 and 1 mL of the working standard solution into five different volumetric flasks and topped up with distilled water (except the 1 mL sample) until the mark of 1 mL. On the other hands, 0.1 mL of the digested rice samples was pipetted and added with distilled water to bring the digests to 1 mL. Then, 1 mL of phenol solution (5%) and 5 mL of sulfuric acid (96%) were added to each digest, working standard and blank solution. All the digests, working standards and a blank solution were placed on a shaker and shook for 20 min to obtain homogeneous solutions. The amount of total carbohydrate content for all the digests, working standards and the blank was measured using an ultraviolet-visible spectrophotometer at 490 nm, and the absorbances were recorded as tabulated in **Table 2**.

As given in **Table 2**, the carbohydrate contents for the ten different rice samples were ranged from 43 to 88%. Floral rice sample gave the highest carbohydrate content (88%), while Phkarkhrrel rice sample had the lowest carbohydrate content (43%). The average carbohydrate content for the 10 different rice samples was 70.2%. This result was similar to the finding that obtained by Deepa and coworkers [17] on various Indian rice samples. The carbohydrate content of their analysis was ranged from 61.7 to 91.7% with the average value of 73.5%.

3.5.2. Determination of protein content by using Kjeldahl method

To determine the protein content in rice samples, 0.15 g of each sample was refluxed with 1 mL of mixed catalyst (96% sodium sulfate anhydrous and 3.5% copper sulfate) and 3 mL of concentrated sulfuric acid. When the sample solution was turned into green-blue, 30 mL of distilled water, 10 mL of 45% sodium hydroxide, 10 mL of 0.5 N hydrochloric acid and a few drops of methyl red indicator were added into the mixture. The ammonia solution produced

No.	Manufactured rice grain	Concentration of rice sample (mg/mL)	Total carbohydrate content (%)
1	Maharaja Basmathi	0.085	85
2	SUMO Calrose	0.072	72
3	Jasmine Nutririce	0.066	66
4	Floral Glutinous	0.088	88
5	Sun Rise Australian Fragrant	0.083	83
6	Bird of Paradise	0.055	55
7	Phkarkhrrel Cambodi Organi	0.043	43
8	Sakura Super Thai	0.086	86
9	Sakura Super Pakistan	0.073	73
10	Giant Super Special Rice	0.051	51

Table 2. Total carbohydrate content in rice samples from various brands.

from the reaction was distilled and collected in a conical flask. The distillate was titrated with 0.5 N sodium hydroxide solution in order to determine the protein content.

The results of the protein content analysis for the 10 different types of rice sample were ranged from 1.40 to 11.11% as shown in **Table 3**. The highest protein content was found in Jasmine rice (11.11%), and the lowest was the Sun rice (1.40%). The average protein content for the 10 different types of rice sample was 6.25%. This result is similar to the results obtained by Kenedy and Burlingame [18] who had done a comprehensive protein analyses on thousands of rice varieties from different regions of the world. The protein content for the rice samples ranged from 4.50 to 15.90%, with the mean value of 8.8%.

No	Manufactured rice	Volume of NaOH to titrate blank (mL)	Volume of NaOH to titrate HCl (mL)	% Nitrogen	% Protein (% nitrogen ×5.95)
1	Maharaja Basmathi	8.75	8.95	0.9333	5.55
2	SUMO Calrose	8.75	8.90	0.7000	4.17
3	Jasmine Nutririce	8.75	9.15	1.8667	1.11
4	Floral Glutinous	8.75	9.00	1.1667	6.94
5	Sun Rise Australian Fragrant	8.75	8.80	0.2333	1.40
6	Bird of Paradise	8.75	8.90	0.7000	4.17
7	Phkarkhrrel Cambodi Organi	8.75	8.90	0.7000	4.17
8	Sakura Super Thai	8.75	9.00	1.1667	6.94
9	Sakura Super Pakistan	8.75	9.05	1.6333	8.33
10	Giant Super Special Rice	8.75	9.10	1.6333	9.72

Table 3. Protein content in rice samples from various brands.

3.5.3. Determination of fat content by using Soxhlet method

For analyzing the fat content, 1 g of each sample was placed in a porous thimble and the extracting solvent (150 mL of hexane) was placed in a dried, weighed distillation flask. The extraction was repeated continuously for a period of 1 h. The extracted fat presented in the distillation flask was dried in an oven at 100°C for 30 min. The flask was reweighted, and the increase in weight of the flask was taken as the weight of the fat present in the rice sample. **Table 4** lists the fat content for the ten different types of rice sample. The highest fat content was found in the Bird of Paradise rice (4.79%), and the lowest was Jasmine rice (3.0%). The average fat content for the 10 different types of rice samples was 3.65%. However, the fat content obtained in this analysis is slightly higher compared to the results obtained by Oko et al. [19] with the average fat content of 2.5 and 1.5%, respectively.

3.6. Rice trace element test

3.6.1. Chemicals and reagents

All chemicals and solvents were of analytical-reagent grade. Nickel(II) sulfate and chromium(III) chloride-6-hydrate were purchased from Hamburg Chemicals. Copper standard solution and calcium standard solution, magnesium sulfate heptahydrate and lead nitrate were purchased from Merck. Zinc chloride and cadmium nitrat-4-hydrate were purchased from Riedel-de Haen Chemicals. Nitric acid, perchloric acid and sulfuric acid were purchased from R & M chemicals.

3.6.2. Preparation of acid digested rice samples

One gram of each rice sample was accurately weighed in a sample container and transferred into a 250-mL conical flask. A mixture of concentrated acids containing nitric acid (67 mL),

Manufactured rice grain	Weight of round bottom flask (g)	Weight of round bottom flask and extracted fat (g)	Weight of sample (g)	Extracted fat (g)	Fat (%)
1. Maharaja Basmathi	95.2746	95.3135	1.0306	0.0377	3.77
2. SUMO Calrose	94.8465	94.8798	1.0001	0.0333	3.33
3. Jasmine Nutririce	94.8440	94.8747	1.0383	0.0307	3.00
4. Floral Glutinous	94.8337	94.8760	1.0004	0.0423	4.23
5. Sun Rise Australian Fragrant	95.2816	95.3184	1.0312	0.0368	3.57
6. Bird of Paradise	95.2751	95.3239	1.0185	0.0488	4.79
7. Phkarkhrrel Cambodi Organi	94.8476	94.8786	1.0235	0.0310	3.01
8. Sakura Super Thai	95.2832	95.3253	1.0150	0.0421	4.15
9. Sakura Super Pakistan	95.2675	95.3015	1.0002	0.0340	3.40
10. Giant Super Special Rice	95.2782	95.310	1.0225	0.0328	3.21

Table 4. Fat content in rice samples from various brands.

perchloric acid (22 mL) and sulfuric acid (13 mL) was added to each of the rice sample. The mixture was digested according to the wet digestion method [20] for 20 min at room temperature until a clear yellow solution was obtained. The digested rice samples were further digested with a reflux system for 40 min. The digested rice samples were allowed to cool down at room temperature for about 20 min until all the nitric fumes were evaporated. The digested rice samples were then boiled using a hot plate by increasing the temperature gradually until all perchloric fumes were evolved. The boiling process was stopped when a final volume of about 10 mL of clear liquid solution was obtained. The clear liquid solutions were then transferred into a 100-mL volumetric flask and topped up with deionized water. The concentration of trace elements in the rice samples was measured by using Shimadzu AA-6200 flame-AAS. Each analysis was conducted in triplicate, and the uncertainty in measurements was <10%.

3.6.3. Preparation of standard solutions

Stock solution (100 ppm) of a metal salt was prepared by dissolving appropriate amount of the metal salt with 20 mL of deionized water in 100-mL volumetric flasks. A mixture of acids containing nitric acid (5 mL), per chloric acid (1.7 mL) and sulfuric acid (0.8 mL) was added to the metal salt and topped up with deionized water to 100 mL. A series of standard solutions (2, 4, 6, 8, 10, 12, 14, and 16 ppm) were prepared by diluting from this stock solution and used to obtain the standard calibration curves. A blank standard solution containing same amount of concentrated acids but without rice sample was prepared as control.

3.6.4. Results and discussion

The results of trace element contents for 10 different types of rice sample are summarized in **Table 5**. These results indicated that the average content of Mg, Ca, Zn and Cu in the rice

Manufactured rice	**Trace element levels (mg kg^{-1})**							
	Mg	**Ca**	**Zn**	**Cu**	**Cr**	**Cd**	**Ni**	**Pb**
1. Maharaja Basmathi	23.0	9.0	10.0	9.0	nd	nd	nd	nd
2. SUMO Calrose	287.0	3.0	12.0	3.0	nd	nd	nd	nd
3. Jasmine Nutririce	42.0	14.0	18.0	14	nd	nd	nd	nd
4. Floral Glutinous	33.0	1.0	14.0	1.0	nd	nd	nd	nd
5. Sun Rise Australian Fragrant	31.0	6.0	14.0	6.0	nd	nd	nd	nd
6. Bird of Paradise Thai Fragrant	22.0	nd	9.0	nd	nd	nd	nd	nd
7. Phkarkhnei Cambodia Organi	35.0	13.0	13.0	13.0	nd	nd	nd	nd
8. Sakura Super Thai Brown Rice	29.0	10.0	11.0	10.0	nd	nd	nd	nd
9. Sakura Super Basmathi Pakistan	34.0	11.0	11.0	11.0	nd	nd	nd	nd
10. Giant Super Special White	91.0	8.0	11.0	8.0	nd	nd	nd	nd
Average value nd	62.7	8.3	12.3	7.5	nd	nd	nd	nd

nd = not detected

Table 5. Trace element levels for different types of rice sample.

samples was 62.7, 8.3, 12.3, 7.5 mg kg^{-1}, respectively, while the Cr, Cd, Ni and Pb were not detected. All the 10 different types of rice sample showed the highest average Mg content ranging from 22 to 287 mg kg^{-1}, followed by Zn (9–18 mg kg^{-1}), Ca (0–14 mg kg^{-1}) and Cu (0–14 mg kg^{-1}). Comparing the results in **Table 5** with the heavy metal content of rice samples from foreign countries, we found that there was not much difference in the heavy metal content between the two different sources. For example, the average Cd, Cr, Cu, Ni, Pb and Zn content in the rice samples from Taiwan was 0.02, 0.07, 2.20, 0.26, 0.01 and 14.6 mg kg^{-1}, respectively [21].

4. Conclusion

In this chapter, the emerging microwave and laboratory measurement techniques for rice processing and rice testing were presented. Up to 10 brands of manufactured rice grain in the market were analyzed in terms of physical and chemical properties. A wide range of microwave applications can be implemented in the rice industry. Besides microwave heating, the microwave technique used for rice insert control is considered new and attractive since this method leaves no chemical residues on the rice grain product. Microwave technology has provided a rapid and accurate measurement to test the quality of the rice in order to increase the rice production.

Author details

Kok Yeow You[1,*], Li Ling You[2], Chen Son Yue[3], Hou Kit Mun[4] and Chia Yew Lee[5]

*Address all correspondence to: kyyou@fke.utm.my

1 Department of Communication Engineering, Faculty of Electrical Engineering, Universiti Teknologi Malaysia, Johor, Malaysia

2 Faculty of Pharmacy, Mahsa University, Selangor, Malaysia

3 Department of Physical Science, Faculty of Applied Science and Computing, Tunku Abdul Rahman University College, Kuala Lumpur, Malaysia

4 Department of Electrical and Electronic Engineering, Faculty of Engineering and Information Technology, Southern University College, Johor, Malaysia

5 Department of Biotechnology and Medical Engineering, Universiti Teknologi Malaysia, Johor, Malaysia

References

[1] International Rice Research Institute (IRRI). Rice Quality. 2009. [Report]. Retrieved on November 24, 2012. Available from http://www.betuco.be/rijst/Rice%20Quality.pdf

[2] American Society of Agricultural and Biological Engineers (ASABE). ASAE S352.2 Moisture measurement – unground grain and seeds. 1998; St Joseph, MI, USA.

[3] Bhattacharya K R: Rice Quality: A Guide to Rice Properties and Analysis. New Delhi, India: Woodhead Publishing; 2011. ISBN: 9781845694852

[4] Yu X R, Su Y, Wang Y, Zheng T S, Zhao S M, Huang S Z: Study on microwave drying of grain. Proceedings of the 7th International Working Conference on Stored-product Protection.14-19 October. Beijing, China. 1998: 1096-1101.

[5] Abegaonkar M P, Karekar R N, Aiyer R C: A microwave microstrip ring resonator as a moisture sensor for biomaterials: application to wheat grains. Measurement Science Technology. 1999; **10(3)**: 195–200. doi:10.1088/0957-0233/10/3/014

[6] Kim K B, Kim J H, Lee S S, Noh S H: Measurement of grain moisture content using microwave attenuation at 10.5 GHz and moisture density. IEEE Transactions on Instrumentation and Measurement. 2002; **51(1)**: 72–77. doi:10.1109/19.989904

[7] Jafari F, Khalid K, Yusoff W M D W, Hassan J: The analysis and design of multi-layer microstrip moisture sensor for rice grain. Biosystem Engineering. 2010; **106(3)**: 324–331. doi:10.1016/j.biosystemseng.2010.04.005

[8] You K Y, Salleh J, Abbas Z, You L L: Cylindrical slot antennas for monitoring the quality of milled rice. Progress in Electromagnetics Research Symposium Proceedings. 12–16 September. Suzhou, China. 2011: 1370–1373.

[9] Mun H K, You K Y, Dimon M N: Rice grain moisture determination using microstrip wide-ring and microstrip coupled-line sensors. American Journal of Applied Sciences. 2015; **12(3)**: 112–120. doi:10.3844/ajassp.2015.112.120

[10] You K Y, Mun H K, You L L, Jamaliah S, Abbas Z: Small and slim coaxial probe for single rice grain moisture sensing. Sensors. 2013; **13(3)**: 3652–3663. doi:10.3390/s130303652

[11] Nelson S O: Dielectric properties of agricultural products – measurements and applications. IEEE Transactions on Electrical Insulation. 1991; **26(5)**: 845–869. doi:10.1109/14.99097

[12] Yadav B K, Jindal V K: Monitoring milling quality of rice by image analysis. *Computers* and Electronics in Agriculture. 2001; **33(1)**: 19–33. doi:10.1016/S0168-1699(01)00169-7

[13] Lloyd B J, Cnossen A G, Siebenmorgen T J: Evaluation of two methods for separating head rice from brokens for head rice yield determination. Applied Engineering in Agriculture. 2001; **17(5)**: 643–648. doi:10.13031/2013.6902

[14] Courtois F, Faessel M, Bonazzi C: Assessing breakage and cracks of parboiled rice kernels by image analysis techniques. Food Control. 2010; **21(4)**: 567–572. doi:10.1016/j.foodcont.2009.08.006

[15] Mun H K, You K Y, Dimon M N: Broken rice detection based on microwave measurement technique using microstrip wide-ring sensor and microstrip coupled-line sensor. Australian Journal of Crop Science. 2013; **7(13)**: 2079–2090. ISSN: 1835-2707[CE7]

[16] Nelson S O: Dielectric Properties of Agricultural Materials and Their Applications. U.S.: Elsevier; 2015. ISBN: 9780128023051.

[17] Deepa G, Singh V, Naidu K A: Nutrient composition and physiochemical properties of Indian medicinal rice–Njavara. Food Chemistry. 2008; **106**: 165–171.

[18] Kennedy G, Burlingame B: Analysis of food composition data on rice from a plant generic resources perspective. Food Chemistry. 2003; **80**: 589–596.

[19] Oko A O, Onyekwere S C: Studies on the proximate chemical composition, and mineral element contents of five new lowland rice varieties planed in Ebonyi State. International Journal of Biotechnology. 2010; **6**: 949–955.

[20] American Society for Testing and Materials (ASTM). Standard Guide for Preparation of Biological Samples for Inorganic Chemical Analysis, Water and Environmental Technology. Annual Book of ASTM standards. 2000; **11.01**, D 4638-95a. doi:10.1520/D4638-11

[21] Haw T L, Sue S W, Gwo C L: Heavy metal content of rice and shellfish in Taiwan. Journal of Food and Drug Analysis. 2004; **12(2)**: 167–174.

Edited by Amanullah and Shah Fahad

Rice is life, for most people living in Asia. Rice has shaped the cultures, diets, and economies of thousands of millions of people. Growing, selling, and eating rice are integral to the culture of many countries. Products of the rice plant are used for a number of different purposes, such as fuel, thatching, industrial starch, and artwork. Rice is the staple food of more than half of the world's population - more than 3.5 billion people depend on rice for more than 20% of their daily calories. Asia accounts for 90% of global rice consumption, exceeding 100 kg per capita annually in many countries. Keeping in view the importance of rice, the United Nations declared 2004 as the International Year of Rice. Food security, which is the condition of having enough food to provide adequate nutrition for a healthy life, is a critical issue. Sustainable rice production is important for food self-sufficiency and food security in changing climates. Sustainable rice production practices are those which (1) increase rice productivity and its quality, (2) improve soil fertility and health, (3) increase water use efficiency and conservation, and (4) increase diversification of rice fields, growers' income, and climate resilience.

ISBN 978-953-51-5480-8

Photo by sittipong_srikanya / iStock

IntechOpen